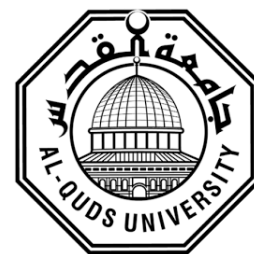


**Deanship of Graduate Studies
Al-Quds University**



**Design, Synthesis and Cytotoxic Activity of Novel 2,3-
Disubstituted Pyrazine Derivatives**

Ala' Mahmoud Rabie Faroun

MSc. Thesis

Jerusalem-Palestine

1439-2017

**Design, Synthesis and Cytotoxic Activity of Novel 2,3-
Disubstituted Pyrazine Derivatives**

Prepared by:

Ala' Mahmoud Rabie Faroun

BSc. Pharmacy Al-Quds University/palestine

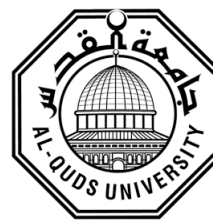
Supervisor:

Dr. Yousef Najajreh

**A thesis submitted in partial fulfillment of the requirements
for the degree of Master of Postgraduate Studies in
Pharmaceutical Sciences
Faculty of Pharmacy- Al-Quds University**

1439/2017

Al-Quds University
Deanship of Graduate Studies
Pharmaceutical Sciences



Thesis Approval

Design, Synthesis and Cytotoxic Activity of Novel 2, 3-Disubstituted Pyrazine Derivatives

Prepared By: Ala' Mahmoud Rabie Faroun

Registration No: 21213201

Supervisor: Dr. Yousef Najajreh

Master thesis submitted and accepted, Date: 6-12-2017

The names and signatures of the examining committee members are as follows:

1-Head of Committee: Dr. Yousef Najajreh

Signature:

2-Internal Examiner: Dr. Imad Odeh

Signature:

3-External Examiner: Dr. Michel Hanania

Signature:

Jerusalem – Palestine

1439/2017

Dedication:

To my dear husband, Mohammed, who has been a source of unwavering support and encouragement during my stressful times. Thank you for your patience, endless love, and most of all for believing in me.

To my beloved family especially my parents whose contribution in my life is immeasurable, I am grateful for your unconditional love and support.

Declaration:

I certify that this thesis submitted for the degree of Master in Postgraduate Studies in Pharmaceutical Sciences is the result of my own research, except where otherwise acknowledged, and this (or any part of the same) has not been submitted for a higher degree to any other university or institution.

Signed:

Ala' Mahmoud Faroun

Date: 6/12/2017

Acknowledgments:

First and foremost, praises and thanks to God for the wisdom and perseverance that he has been bestowed upon me during this research project, and indeed, throughout my life.

A guide is the pivot to the wheel of process. I would like to express my sincere gratitude to my supervisor Dr. Yousef Najajreh whose expertise, understanding, insightful comments and patience, added considerably to my experience during this work and throughout my academic life. I am deeply honored to be one of your students.

I am highly indebted to AQU/ Faculty of Pharmacy for their relevant support and for providing me the excellent laboratory facilities to accomplish this work.

I am extremely thankful to my research colleagues and friends at the Anticancer Drugs Research Lab for their fruitful discussion, help, and experimental assistance at various stages. Working with you has been a real pleasure to me.

Last but not least, I am very delighted and enraptured to thank everyone who helped and encouraged me throughout this research.

Abstract

Pyrazine derivatives possess numerous pharmacological effects including but not limited to antiviral, antibiotic, antifungal, diuretic, anticonvulsant, antidiabetic, analgesic and anti proliferative effect. Consequently, interest has been shown by researchers in the field of pyrazine-based drug synthesis and many of the synthesized derivatives succeeded to reach the clinical field. A promising research discipline was concerned in utilizing the antiproliferative and cytotoxic activity of pyrazine derivatives -that is attributed to various mechanisms one of which is protein kinase inhibition- in designing new anti-cancer agents.

In this study a set of disubstituted pyrazine derivatives has been designed and synthesized through a sequential nucleophilic substitution of chlorine atoms of 2,3-dichloropyrazine with amines or other nucleophiles. The synthesized derivatives were purified using several chromatographic techniques, and characterized by (¹H-NMR, ¹³C-NMR, FT-IR, and MS (ESI)) spectroscopy.

The mono-substituted pyrazine derivative A-7 (7) and three of its disubstituted analogues (YAN-1(18), YAN-2 (19), and YAN-3(20)) were *in vitro* screened for their biological activity against two forms of acute myeloid leukemia cells (Molm-13). The viability of the cells was determined using WST-1 assay. Initial results of the tested derivatives showed that A-7 (7) was more potent than its analogues with IC₅₀ of 18 and 39 μM against Molm-13 (sh-p53) and Molm-13 (empty vector) respectively.

The biological activity of mono and disubstituted pyrazine derivatives was predicted using PASS software. Initial results demonstrated that A13 (13), A14 (14), YAN-7 (24), and YAN-8 (25) exhibited predicted activities as antineoplastic agents and signal transduction pathway inhibitors with relatively high Pa values. The previously mentioned compounds shared also the same mechanism of action “protein kinase inhibitor” with Pa values larger than 0.8.

SAR derived from PASS and initial biological activity screening results proved that the activity of the synthesized derivative is highly affected by the site and type of the substituent on the pyrazine ring. 2,3-disubstituted derivatives showed better Pa values when compared to the corresponding 2,5-disubstituted ones. In addition, amine substituents at positions 2 and 3 of pyrazine ring were preferred over alkoxide substituents in terms of antineoplastic activity. It was noticed that 1-(5-trifluoromethylpyridin-2-yl)-piperazine and 2-aminopyridine pharmacophores were the most active amine substituents.

In order to gain an insight into the binding mode of pyrazine derivatives with CDK-2, a series of sixteen derivatives were docked with inactive monomeric cyclin dependent kinase-2 using SwissDock software. Results were compared with 'Aloisine B', a well-known CDK-2 inhibitor.

In terms of binding mode, pyrazine derivatives occupied the CDK-2 ATP binding site and made hydrogen bonds to the kinase backbone within the hinge sequence that links the two lobes of the kinase. The docked derivatives exhibited different binding affinities to the target, YAN-8 (25) showed the highest full fitness value (-1422.14 kcal/mol) among the synthesized derivatives. Moreover, both the full fitness and energy values indicated that YAN-8 (25) has higher affinity to the target in comparison to the known inhibitor Aloisine B (-1406.92 kcal/mol).

Finally, the concept of drug likeness of the synthesized derivatives was investigated using the rule of five. Results revealed that all of the tested derivatives successfully met the rule of 5 requirements except YAN-9 (26) and YAN-10 (27) which possessed molecular weights larger than 500 Daltons.

Table of contents:

List of abbreviations.....	viii
List of figures.....	xi
List of schemes.....	xiii
List of tables.....	xv
Chapter one: Introduction.....	1
1.1. Background.....	2
1.2. Chemistry of pyrazine.....	3
1.3. Prevalence of pyrazine.....	5
1.3.1. Natural pyrazines and pyrazine derivatives.....	5
1.3.2. Synthetic pyrazines.....	6
1.4. Importance of pyrazine derivatives.....	8
1.5. Therapeutic potential of pyrazine derivatives: literature review.....	9
1.6. Anticancer activity.....	11
1.6.1. Cytotoxic substituted pyrazine derivatives.....	11
1.6.2. Cytotoxic fused pyrazine derivatives.....	14
1.7. Cyclin dependent kinase structure and function.....	18
1.7.1. Summary.....	18
1.7.2. Kinase structure and binding.....	18
1.7.3. Cyclin dependent kinase activation.....	20
1.7.4. Cyclin dependent kinase inhibition.....	21
1.7.5. Mode of action.....	21

1.8. Pyrrolopyrazines as kinase inhibitor.....	22
1.8.1. Binding and structure activity relationship.....	22
1.8.2. Designing selective CDK inhibitors.....	24
1.9. Pyrazine containing drugs in clinical use.....	26
Aims and objectives of the study.....	29
Chapter two: Experiments and methods.....	30
2.1. Synthetic chemistry.....	30
2.2. Initial <i>in-vitro</i> biological activity.....	47
2.3. Computational chemistry of the synthesized compounds.....	48
2.3.1. Computer-aided prediction of biological activity spectra of the synthesized compounds.....	48
2.3.2. Lipinski's rule of five: computational approach to predict drug-likeness of the synthesized compounds.....	50
2.3.3. Docking of the synthesized compounds using SwissDock.....	51
Chapter three: results and discussion.....	52
3.1. Chemical synthesis of compounds.....	53
3.2. Initial <i>in-vitro</i> biological activity.....	66
3.3. Computational chemistry of the synthesized compounds.....	70
3.3.1. Computer-aided prediction of biological activity spectra of the synthesized compounds.....	70
3.3.2. Lipinski's rule of five: computational approach to predict drug-likeness of the synthesized compounds.....	78
3.3.3. Docking of the synthesized compounds using SwissDock.....	82
Chapter four: Conclusion.....	86
Chapter five: References.....	89

List of Abbreviations:

Abbreviation	Full form
ADME	Absorption, distribution, metabolism, excretion
ATP	Adenosine tri phosphate
ATR kinase	Ataxia telangiectasia and Rad3 related protein kinase
B-RAF	V-raf murine sarcoma viral oncogene homolog B1
CaCl₂	Calcium chloride
CAK	CDK-activating kinase
CDCl₃	Chloroform-d
CDK	Cyclin dependent kinase
CHCl₃	Chloroform
ChK₁	Check Point Kinase inhibitor
DCM	Dichloromethane
DIEA	Diisopropylethylamine
DCC	N,N'-Dicyclohexylcarbodiimide
DCU	1,3-Dicyclohexyl-urea
DMF	N,N-Dimethylformamide
DMSO	Dimethyl sulfoxide
DMSO-d₆	Deuterated dimethyl sulfoxide
EA	Ethyl acetate

ERK	Extracellular signal –regulated kinase
EtOH	Ethanol
FTIR	Fourier transform infrared spectroscopy
GSK	Glycogen synthase kinase
HCl	Hydrochloric acid
Hsp90	Heat shock protein 90
IC₅₀	Inhibitory concentration
K₂CO₃	Potassium carbonate
KBr	Potassium bromide
MAP kinase	Mitogen activated protein kinase
MeOH	Methanol
MS (ESI)	Electrospray ionization mass spectrometry
MWT	Molecular weight
Na₂SO₄	Sodium sulfate
NBS	N-bromosuccinimide
NH₃	Ammonia
NHS	N-hydroxysuccinimide
NIMA	Never in mitosis A-related kinase
NMP	N-methylpyrrolidone
NSCLC	Non-small-cell lung cancer cell
PASS	Prediction of Activity Spectra for Substances
PDB	Protein data bank

PI₃K	Phosphatidylinositol-3-kinase
Q-SAR	Quantitative structure activity relationship
RF	Retention factor
RO₅	Rule of five
RT	Room temperature
SAR	Structure activity relationship
S_NAr	Nucleophilic aromatic substitution reaction
TEA	Triethylamine
TFA	Trifluoroacetic acid

List of Figures:

Figure No.	Details	Page
Figure 1.1	Structures of diazine monocyclic compounds (1) 1, 2-diazine (pyridazine), (2) 1, 3-diazine (pyrimidine), (3) 1,4-diazine (pyrazine).	3
Figure 1.2	Naturally occurring pyrazine derivatives responsible for aroma and flavor: 2-Methyl-6-vinyl-pyrazine (4) found in beans and wine, 2-Butyl-3-methoxy-pyrazine (5) found in coffee, 2-Ethoxy-6-methyl-pyrazine (6) gives pineapple flavor, botryllazine (7) anti-cancer pyrazine alkaloid.	5
Figure 1.3	Important pyrazine derivatives: eurhodines (8), safranines (9), indulenes (10), quinoxalines (11), phenazines (12), pteridines (13), flavins (14).	8
Figure 1.4	Pyrazine derivatives with different biological activities: Antimicrobial activity Pyrazinamide (15) and pyrazinamidrazone (16), herbicide activity (17, 18, 19), cardiovascular activity (20, 21), anti-inflammatory (22), analgesic mirfentanil (23)	10
Figure 1.5	Pyrazine derivatives with cytotoxic activities: [(1 <i>R</i>)-3-methyl-1-((2 <i>S</i>)-3-phenyl-2-[(pyrazin-2-ylcarbonyl)amino]propanoyl) amino)butyl] boronic acid (Bortezomib) (24). Comparison between 2,6-diphenylpyrazines (25) and the corresponding pyridine analogues in terms of DNA binding and cytotoxic properties. Series of 3,6-bis(3'-indolyl) pyrazine derivatives (26).	12
Figure 1.6	Pyrazine based inhibitors of different protein kinases: Di substituted pyrazine derivatives as potent B-RAF inhibitors (27) and (28). 3-(6-hydroxyindol-2-yl)-5-(Phenyl) pyrazine as CDK5 inhibitor (29). 1-[3-Amino-6-(3,4,5-trimethoxy-phenyl)-pyrazin-2-yl]-2,3-dimethyl-piperidine-4-carboxylic acid as (NIMA) kinase inhibitor (30). 1-(5-chloro-2-alkoxyphenyl)-3-(5-cyanopyrazin-2-yl) ureas as Chk1 inhibitor (31) and (32). 3-(2-{5-tert-Butyl-3-[(4-methyl-furazan-3-ylmethyl)-amino]-2-oxo-2H-pyrazin-1-yl}-butyrylamino)-5-(hexyl-methyl-amino)-4-oxo-pentanoic acid as caspase 3 inhibitor (33)	14
Figure 1.7	Fused pyrazines as anticancer agents: imidazo [1,2-a]pyrazines (34) (35) (36). pyrido[2,3-b]pyrazines (37) (38) (39).	16
Figure 1.8	Fused pyrazines as anticancer agents (42) diaminopteridine-benzenesulfonamide, (43) phenazine, (44) quinoxaline N-oxide.	16

Figure 1.9	Pyrrrolopyrazine derivatives as kinase inhibitors	17
Figure 1.10	a) The CDKs responsible for progression through the various phases of the cell division cycle are indicated. b) Tertiary structure of human CDK2, determined by X-ray crystallography.	19
Figure 1.11	Schematic structure of CDK2 in various states of activity.	20
Figure 1.12	View of CDK2/ATP (1HCK coordinates taken from PDB database) complex is shown in tube representation.	21
Figure 1.13	structures of Aloisine A (47): (4-(7-Butyl-5H-pyrrolo[2,3-b]pyrazin-6-yl)-phenol) and Aloisine B (48): (6-(4-Chloro-phenyl)-7-isopropyl-5H-pyrrolo[2,3-b]pyrazine	22
Figure 1.14	The binding of Aloisine B to CDK2.	23
Figure 1.15	Pharmacophore maps of CDK5, GSK3 β and ERK2 (a-c). Binding of pyrrolopyrazine to CDK5, GSK3 β and ERK2 (d-f).	25
Figure 2.1	Chemical structure of A7 (7).	34
Figure 3.1	Concentration-response effect of A-7 (7), YAN-1 (18), YAN-2 (19), and YAN-3 (20) on Molm-13 cancer cell lines. Cell viability was measured using WST-1 assay and the data expressed as the mean \pm SD of two independent experiments.	68
Figure 3.2	Viability chart of molm-13 empty vector and molm-13 sh-p53 cells at different concentration (1, 3.16, 10, 31.6, and 100 μ M) of A-7 (7), YAN-1 (18), YAN-2 (19), and YAN-3 (20).	69
Figure 3.3	CDK2 (1-HCL.PDB) structure in ribbon representation. The N-terminal lobe is dominated by a five-stranded antiparallel β -sheet, and the C-terminal lobe is predominantly α -helical. Picture was taken from chimera software.	82
Figure 3.4	Docking of CDK2 (1-HCL.PDB) with Aloisine B (A), YAN-8 (25) (B) and A14 (14) (C). The compounds soak into the CDK-2 ATP binding site. Crystallographic structure was taken from chimera software.	83

List of Schemes:

Scheme No.	Details	Page
Scheme 1.1	The resonance hybrid of pyrazine.	3
Scheme 1.2	The resonance stabilization of pyrazine during nucleophilic aromatic substitution.	4
Scheme 1.3	Synthetic methods for the preparation of pyrazine derivatives: (a) Staedel-Rugheimer method, (b) Gutknecht method, (c) Gastaldi method.	6
Scheme 1.4	Synthetic routes for the preparation of pyrazine derivatives: (a) de-amino cyclisation of ethylenediamine, (b) condensation reaction of 1,2-diketones with 1,2-diamine.	7
Scheme 3.1	Sequential substitution of 2,3-dichloropyrazine by various nucleophiles. Typical method for preparation of monosubstituted and disubstituted pyrazines.	54
Scheme 3.2	Representative procedure for the synthesis of (2-amino-3-chloropyrazine) derivatives using acyclic amines under basic conditions. (a) dioxane or THF, TEA or DIPEA, stirring at reflux, R= aliphatic linear amine.	55
Scheme 3.3	Representative procedure for the synthesis of (2-amino-3-chloropyrazine) derivatives using cyclic amines under basic conditions (a) dioxane or THF, TEA or DIPEA, stirring at reflux, R= aliphatic cyclic amines.	56
Scheme 3.4	Representative procedure for the synthesis of (2-amino-3-chloropyrazine) derivatives using aromatic amines under acidic conditions (a) dioxane or THF, HCL, stirring at reflux, R= aromatic amines.	57
Scheme 3.5	Synthesis of (2-alkoxy-3-chloropyrazine) derivative A17 (17) . (a) dioxane, K ₂ CO ₃ , reflux.	57
Scheme 3.6	De-protonation and resonance stabilization of the phenolic hydroxyl group in acetaminophen using potassium carbonate.	58
Scheme 3.7	Synthesis of 2-amino-3-alkoxy pyrazine derivatives using A7 (7) and different aliphatic or aromatic alcohols, (a) sodium, reflux 12h under calcium chloride for YAN-1 (18), and YAN-2 (19). (a) Sodium, dry THF, reflux 18h under calcium chloride for YAN-3 (20).	59

Scheme 3.8	Synthesis of 2,3-diaminopyrazine derivatives using A7 (7) and different aromatic amines under acidic conditions (a) HCl, dioxane, reflux.	60
Scheme 3.9	Synthesis of 2,3-diaminopyrazine symmetrical derivatives YAN-8 (25) and YAN-9 (26) using 2,3-dichloropyrazine and different amines, (a) HCl, dioxane and DMF, reflux (b) K ₂ CO ₃ , DMSO, reflux.	61
Scheme 3.10	Detailed mechanism showing the coupling of carboxylic acid terminus with amine using DCC and NHS coupling system.	62
Scheme 3.11	Synthesis of YAN-10 (27) and YAN-11(28) by extending the carboxylic acid terminus of YAN-5 (22) via amide bond formation using different amines, (a) DCC, NHS, dioxane, TEA, room temperature overnight	63
Scheme 3.12	Detailed mechanism showing C-H activation of A1 (1) using NBS. (a) NBS, acetonitrile, stirring at room temperature overnight. R= ethanolamine.	64
Scheme 3.13	Synthesis of 2-amino-3-chloro-5-alkoxy pyrazine derivatives YAN-13 (30) and YAN-14 (31), (a) Sodium, reflux, synthesis of YAN-15 (32): (b) K ₂ CO ₃ , dioxane, reflux.	65

List of Tables:

Table No.	Details	Page
Table 1.1	List of pyrazine containing drugs in clinical use along with their biological activities.	26
Table 2.1	¹ H-NMR and ¹³ C-NMR data for A7 (7).	34
Table 2.2	FTIR data for A7 (7).	34
Table 2.3	List of synthesized compounds and their chemical and structural formulas.	43
Table 3.1	Structure activity relationship and IC ₅₀ values of (7 , 18 , 19 , and 20).	67
Table 3.2	Computer-aided prediction of biological activity spectra (PASS) results of the synthesized compounds.	70
Table 3.3	Drug likeness prediction results of the synthesized compounds using Lipinski's rule of five.	78
Table 3.4	Docking outcomes of (14 , 18 , 20 , 21 , 22 , 23 , 24 , 25 , 26 , 27 , 28 , 30 , 31 , 32) and Aloisine B with monomeric CDK-2 . Results include estimated binding energies and full fitness values as seen in Swiss-dock and chimera software.	84

Chapter One

Introduction

1. Introduction

1.1. Background

The burden of cancer is noticeably increasing worldwide especially in developing countries such as Palestine. According to recent statistics published by the Palestinian Ministry of Health in October 2016, the total reported cancer cases in west bank were 2536 with higher incidence percentage in women (52.4%, 1330 case) than men (47.6%, 1206 case) and a total incidence rate of 86.4 per 100,000 of the population. Cancer is considered the second leading cause of death proceeded only by cardio and cerebra vascular diseases with approximately 14% of the total population deaths. With significant improvement in treatment and prevention of cardio and cerebra vascular diseases, cancer will soon become the number one killer in many parts of the world. It is predicted that there will be more than 15 million new cancer cases and 12 million deaths due to cancer in 2020 all around the globe^[1].

Discovery of new drugs for the treatment of cancer has been gaining a great deal of interest mainly due to resistance toward conventional chemotherapeutic agents. Furthermore, multidrug resistance^[2, 3] characterized by resistance not only to drugs that are similar structurally and functionally but also cross-resistance to unrelated drugs has also been emerged. Hence, search for novel anticancer agents with diverse chemical structures was the need of the hour.

In the last decade, uncountable efforts were made to synthesize different (five, six and seven membered, condensed) heterocyclic compounds and their derivatives relying on the fact that they possess promising antitumor activities^[4]. Nitrogen containing cyclic structures has maintained the interest of researchers through the development of organic chemistry. For instance, substitution of two carbon atoms of the benzene ring by trivalent nitrogen occupying different positions of the ring gives rise to “diazines”, with the molecular formula of $C_4H_4N_2$, which are odorous, colorless compounds possessing solubility in organic solvents and relative stability^[5]. The diazine family was considered a promising lead in the field of drugs development because of the diverse biological activities endowed by the heterocyclic core itself and by its derivatives as well^[4, 6].

1.2. Chemistry of pyrazine

One of the naturally occurring diazines is pyrazine (also known as *p*-diazine or 1,4-diazine) (**Figure 1.1 (3)**), a 6π -electron-deficient aromatic heterocyclic ring with two nitrogen atoms located in the 1 and 4 position of the heterocycle ^[7, 8]. This ring is isomeric with two other forms of diazine, pyridazine and pyrimidine (**Figure 1.1 (1, 2)**).

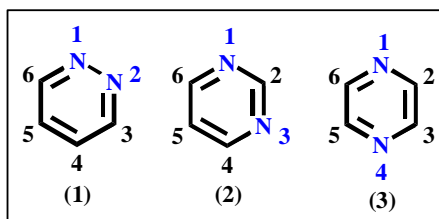
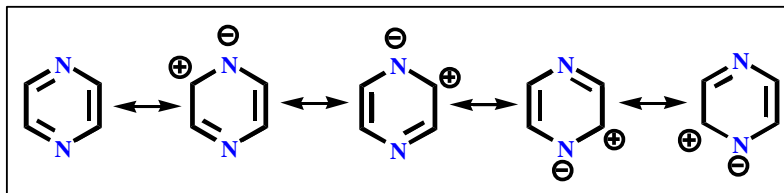


Figure 1.1: Structures of diazines, (1) 1, 2-diazine (pyridazine), (2) 1, 3-diazine (pyrimidine), (3) 1, 4-diazine (pyrazine).

Pyrazine is considered a stable, colorless tertiary amine with a boiling point of 116°C and a melting point of 54°C . The additional pyridine-like nitrogen highly decreases the basicity of pyrazine ($\text{pK}_b = 13.49$) in comparison to pyridine ($\text{pK}_b = 8.7$), while the symmetrical Para position of the electron-attracting nitrogen atoms makes pyrazine a weaker base than its isomeric analogous pyrimidine ($\text{pK}_b = 12.77$), or pyridazine ($\text{pK}_b = 10.76$).^[9] In general, pyrazine behaves as monoacidic bases protonated at N-1. N, N-diprotonation of pyrazine is difficult and has only been observed in very strong acidic media. Pyrazine forms monoquaternary salts with alkyl halides which are unstable and are best prepared at temperature below 40°C . Pyrazine also reacts with halogenated acids to form pyrazinium salt.

According to an x-ray study, it was shown that the pyrazine ring is planar hexagon. The carbon-carbon bond length is 1.39\AA which is longer than that of benzene, while the carbon-nitrogen bond length is 1.34\AA . The bond angle (N-C-C) is 121.8° whereas the bond angle (C-N-C) is 116.3° ^[10].

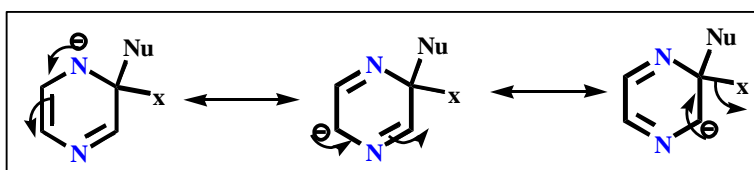
One of the very distinct characteristics of pyrazines is that they are electron deficient aromatic heterocycles. The nitrogen atoms present in the aromatic ring possess lone pairs which are not involved in the aromatic ring π system. Both nitrogens are sp^2 hybridized and their lone pairs reside in one of the hybridized orbitals.



Scheme 1.1: The resonance hybrid of pyrazine.

sp^2 orbitals are perpendicular to the un-hybridized p orbitals that form the π system; therefore the electrons are unable to participate in the ring's π network. This characteristic leads to an inductive effect caused by these nitrogens. Instead of increasing ring electron density, they decrease it. Nitrogen is more electronegative than carbon, therefore the electron density in the ring σ -bonds is unevenly distributed, with partially negative nitrogens and partially positive carbons^[11, 12]. The resonance hybrid of pyrazine is depicted in **Scheme 1.1**.

Since pyrazine is an aromatic heterocycle, therefore it should undergo aromatic substitution reaction. From the forms shown in **Scheme 1.1**, it can be seen that the electron deficiencies are at 2, 3, 5 and 6 positions. Therefore, nucleophilic reagents could attack at these positions. However, studies have shown that the nucleophiles attacked the ring only if there is at least one powerful electron releasing group such as NH_2 , OH , SH in another position^[13-15]. During (S_NAr) of halogenated pyrazine, the nitrogen participates in resonance stabilization of the negatively charged anion as shown in **Scheme 1.2**.



Scheme 1.2: The resonance stabilization of pyrazine during nucleophilic aromatic substitution.

Pyrazine demonstrates unique physicochemical properties that are caused by a low-lying unoccupied p -molecular orbital and by the ability to act as bridging ligand or building blocks for the construction of multinuclear transition metal complexes, metal-organic frameworks, highly luminescent complexes, and catalysts. The inherent bi functionality and the low-lying unoccupied molecular orbital permit pyrazine to form coordination polymers having unusual electrical and magnetic properties^[16].

1.3. Prevalence of pyrazine

1.3.1. Natural pyrazines and pyrazine derivatives

There are various natural substituted pyrazines. They may carry substituents on one or more of the four pyrazine ring carbon atoms including alkoxy, acyl, thiols, or sulfide. Alkylated pyrazines are the most abundant form of pyrazine in nature. ^[17, 18]

Some of the naturally occurring pyrazines are found in plants or animals in which pyrazines play the roles of attractants, pheromones, signal substances, repellents and site markers especially in insects and bees (**Figure 1.2 (4,5,6)**).

One of the naturally occurring and biologically active pyrazine alkaloids is Botryllazine b (**Figure 1.2 (7)**) which was first isolated from the red ascidian *Botryllus leachi* by Duran *et al*, Botryllazine is now synthesized and used as cytotoxic agent. ^[19] Pyrazines are also biosynthesized by a number of fungi and bacteria, examples include the antibiotic aspergillilic acid and the fungicidal pigment pulcherrimin. ^[20]

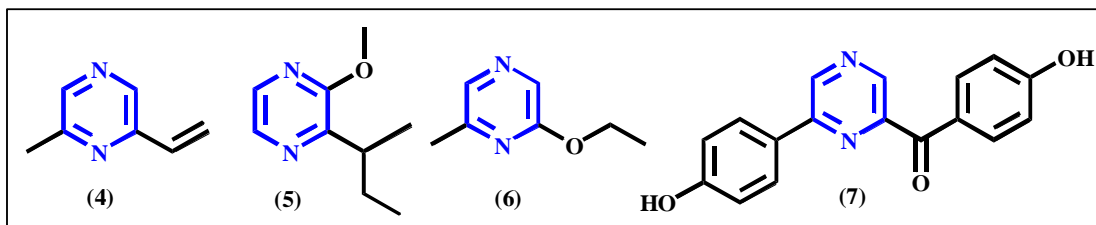


Figure1.2: Naturally occurring pyrazine derivatives:

(4) 2-methyl-6-vinyl-pyrazine found in beans and wine, (5) 2-isobutyl-3-methoxy-pyrazine found in coffee, (6) 2-ethoxy-6-methyl-pyrazine gives pineapple flavor, (7) Botryllazine “b” anticancer pyrazine alkaloid.

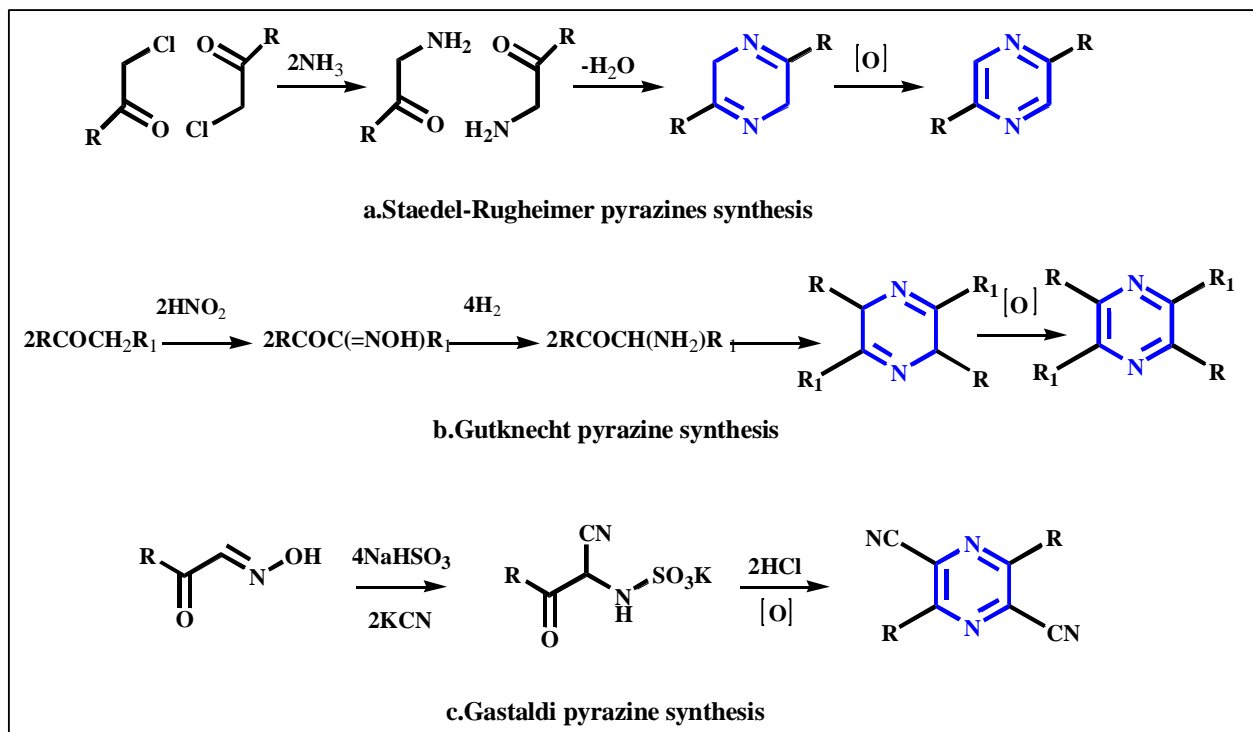
Moreover, several approaches for extracting pyrazine out of its natural sources were documented in the literature, one of them is the so-called ‘Maillard reaction’ which mainly depends on heating food to produce pyrazines ^[21]. This reaction was first discovered by Louis Camille Maillard in 1912 while attempting to reproduce biological Protein synthesis.

1.3.2. Synthetic pyrazines

Although pyrazines occur ubiquitously in nature, they can be synthesized chemically by different methods, and are then used as industrial flavoring additives or biologically active substances. In general, pyrazine is prepared by the catalytic reaction of diamines with diols in a vapor phase, dehydrogenation of piperazine or dealkylation of methyl pyrazine.

Several synthetic methods for pyrazine nucleus have been reported in the literature. In fact one of the oldest methods was reported by Staedel-Rugheimer in 1876. In this method, 2-chloroacetophenone is reacted with ammonia to form the amino ketone which is then condensed and oxidized to form pyrazine (**Scheme 1.3 (a)**)^[22].

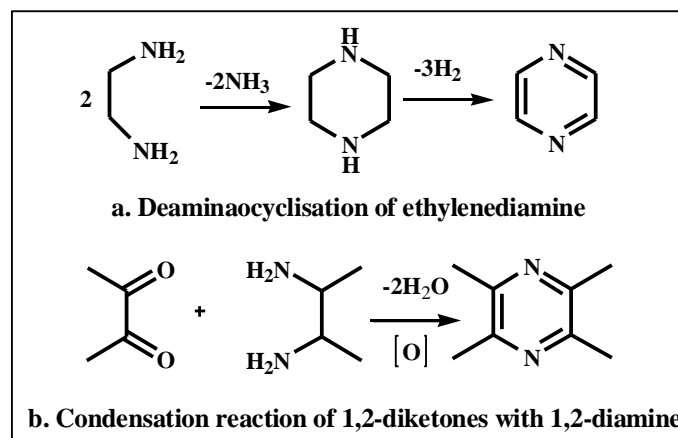
Gutknecht extended the field of pyrazine synthesis in 1879, applying self-condensation of 2-aminoketone, with a slight difference in the way that the alpha-ketoamine is synthesized. The ketone was reacted with nitrous acid to form an oximino ketone followed by reduction to an α -amino ketone^[23]. Nevertheless the two methods described above result in the formation of symmetrical pyrazines (**Scheme 1.3 (b)**).



Scheme 1.3: Synthetic methods for the preparation of pyrazine derivatives: (a) Staedel-Rugheimer method, (b) Gutknecht method, (c) Gastaldi method.

The Gastaldi reaction (1921) is another variation that provides alternate use of alpha-oximino-ketones to afford dicyanopyrazines by cyclization of two molecules of an aminocyanomethyl ketone, produced by treatment of an isonitrosomethyl ketone bisulfite with potassium cyanide, heating in hydrochloric acid, and oxidation^[24] (Scheme 1.3 (c)). As synthetic organic methods evolved, simple and efficient pyrazine synthesis pathways emerged, including the preparation of pyrazine through the condensation of 1,2-diketones with 1,2-diamine^[25], this method can be used for both symmetrical and non-symmetrical pyrazine synthesis in good yields (**Scheme 1.4 (b)**).

Moreover, synthetic methods can vary depending on the planned pyrazine derivatives and they have prominently been cited in the literature using different catalytic techniques. For instance, the synthesis of pyrazine derivatives by direct conversion of α -hydroxy ketones and α -keto oximes in the presence of a catalytic amount of ceric ammonium nitrate was reported by A. Shaabani *et al*^[26]. While M. Latha *et al.* synthesized pyrazine from ethylene diamine using copper oxide/copper chromite catalysts. The procedure depends on the deaminocyclisation (deamination reaction leading to the cyclisation process) of ethylenediamine followed by dehydrogenation over copper chromite catalysts which results in the formation of pyrazine with greater selectivity (**Scheme 1.4 (a)**). In this method, ethylenediamine vapor was passed over a series of copper oxide/copper chromite catalysts in the temperature range of 340°C-440°C. Two molecules of ethylenediamine condensed to form piperazine by releasing two molecules of ammonia, which further dehydrogenated to form pyrazine as a major product.



Scheme 1.4: Synthetic routes for the preparation of pyrazine derivatives: **(a)** deaminaocyclisation of ethylenediamine, **(b)** condensation reaction of 1,2-diketones with 1,2-diamine.

The formation of pyrazine as the major component suggests the high activity of the copper based catalysts to effect spontaneous dehydrogenation of piperazine^[27]. Another approach was the Synthesis of 2-methyl pyrazine from zinc-modified ferrierite catalysts as documented by R. Anand *et al*^[28]. In addition the application of microwaves in promoting organic reactions has received intense attention recently. Microwave-assisted synthesis of pyrazine derivatives from α -halo ketone in 7% NH_3 solution was reported by T. Utsukihara *et al*^[29]. While Y.J. Cheng has developed an ancillary method for acceleration of nucleophilic aromatic substitution reactions under microwave irradiation^[30]. In this method, the formation of substituted pyrazines were obtained by the interaction of 2-chloropyrazine with the nucleophiles of PhSNa , MeSNa , EtONa and PhONa in (NMP) which gave the desired substitution products in a good yield of 69 – 96%.

1.4. Importance of pyrazine derivatives

Pyrazine ring is considered among the important diazines; it is believed that the cytotoxic activity of several natural and synthetic heterocyclic compounds is attributed to the presence of pyrazine heterocycles. On the other hand, pyrazine occupies an essential part of the systems including azine dyes eurhodines (8), safranines (9) and indulenes (10).^[31-34] In addition, this heterocyclic ring is part of various compounds that are relevant to biological and industrial use. Examples include quinoxalines (11), phenazines (12), bio-luminescent natural products pteridines (13), flavins (14) and their derivatives (Figure 1.3).

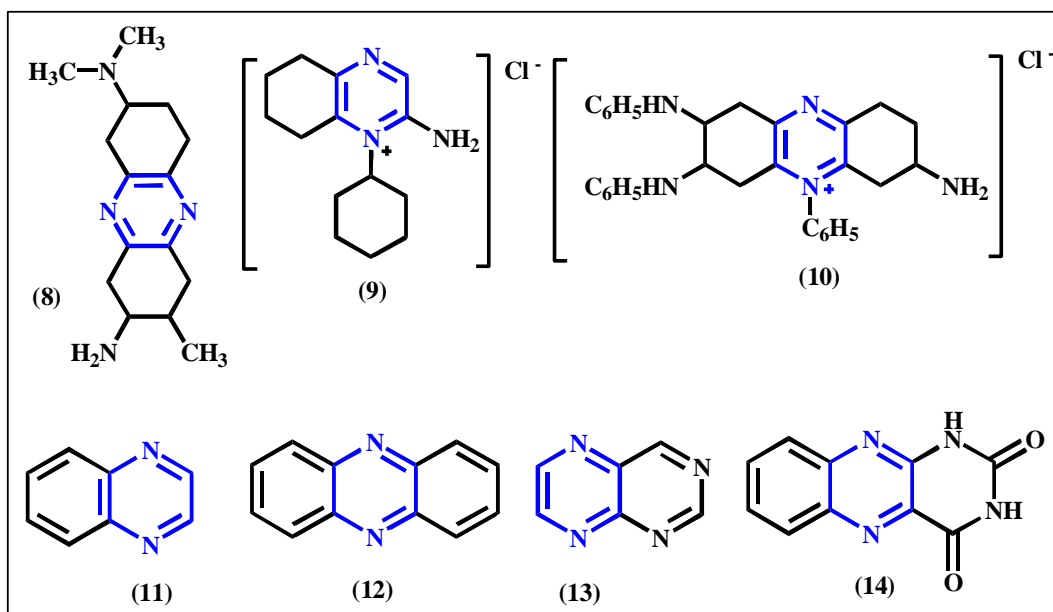


Figure 1.3: Important pyrazine derivatives: (8) eurhodines, (9) safranines, (10) indulenes, (11) quinoxalines, (12) phenazines, (13) pteridines, and (14) flavins.

1.5. Therapeutic potential of pyrazine derivatives: literature review

This section demonstrates some of the substituted pyrazine derivatives along with their diverse biological activities including antimicrobial, herbicide, cardiovascular, anti-inflammatory, analgesic, and anticancer activities.

1.5.1. Antimicrobial activity

Some pyrazine derivatives act as antimicrobial agents and exhibit different activities against bacteria, fungi, and mycobacterium species. A well-known derivative of pyrazine is the pyrazinamide (**Figure 1.4 (15)**). It is used as first line drug in tuberculosis treatment. The synthesis of pyrazinamide was first described in 1936 and the discovered molecule was implied for therapeutic use in 1952.^[35] Since then many of pyrazinamide analogs have been synthesized and evaluated as tuberculostatic agents by introducing structural modifications to the pyrazine ring.^[36] Foks and his coworkers reported the synthesis of pyrazinamidrazones (**Figure 1.4 (16)**).^[37] The synthesized compounds exhibited prominent antifungal activity.

1.5.2. Herbicide activity

It has been reported that compounds containing the pyrazine fragment as Diquat (**Figure 1.4 (17)**), Propaquizafop and Quizalofop-ethyl are very useful herbicides. Other synthetic compounds such as substituted N-phenylpyrazine-2-carboxamides and diazachalcones also showed remarkable herbicide activity. Some examples are the derivative of 6-chloro-N-(5-chloro-2-hydroxyphenyl)-pyrazine-2-carboxamide (**Figure 1.4 (18)**) and the ortho-hydroxyl substituted derivatives of chalcones and diazachalcones (**Figure 1.4 (19)**).^[38]

1.5.3. Cardiovascular activity

Stilbene derivatives containing ligustrazinyll moiety (**Figure 1.4 (20)**) are among the most important cardiovascular protective agents. They were synthesized by Deng and his coworkers. Most of the derivatives exhibited good protective effects on the oxidatively damaged endothelial cells and showed higher potency than Ligustrazine itself. Other pyrazine derivatives showed both antioxidative and thrombolytic effects (**Figure 1.4 (21)**).^[39]

1.5.4. Anti-inflammatory activity

A series of pyrazine N-acylhydrazone derivatives were found to have antinociceptive and anti-inflammatory activities by Da Silva *et al.* mainly compound (2-N-[(*E*)-(3,4,5-trimethoxyphenyl)methylidene]-2-pyrazinecarbohydrazide (**Figure 1.4 (22)**) that presented a good pharmacological profile and was also active in a murine model of chronic inflammation (adjuvant-induced arthritis test in rats).^[40]

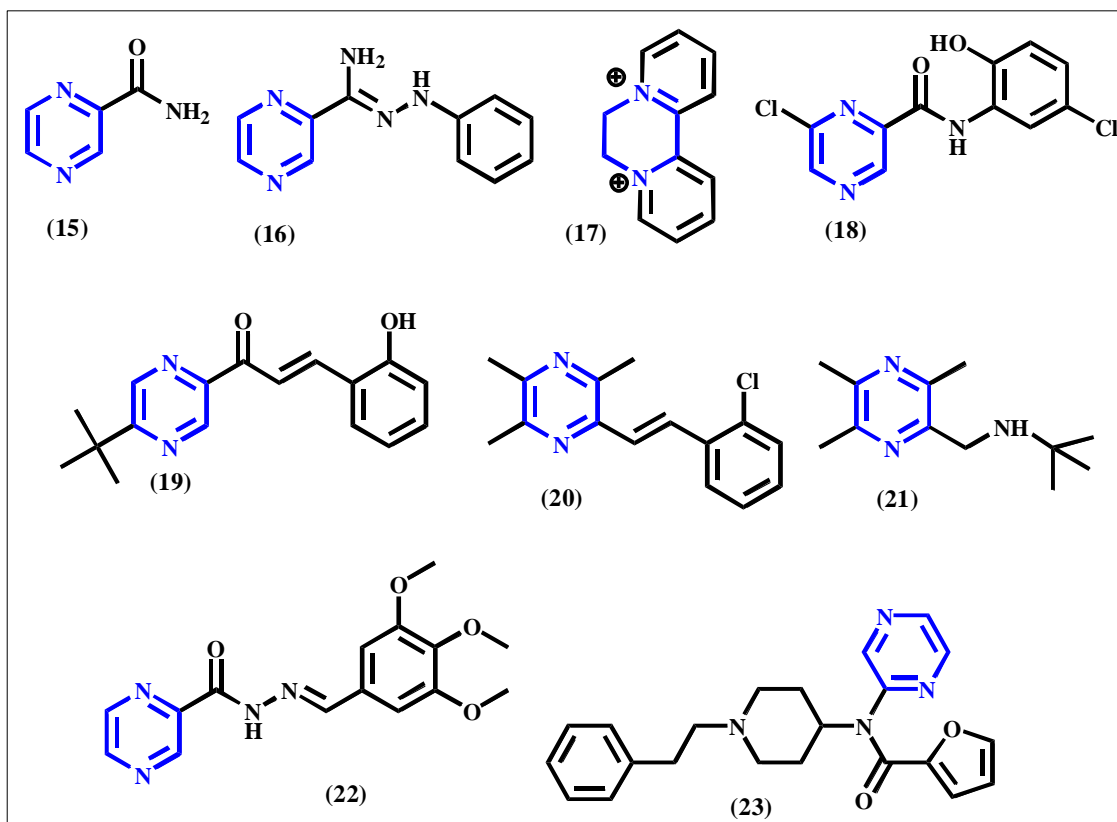


Figure 1.4: Pyrazine derivatives with different biological activities:

Antimicrobial activity (15) Pyrazinamide and (16) pyrazinamidrazone, (17, 18, 19) herbicide activity, (20, 21) cardiovascular activity, (22) antinflammatory, (23) analgesic mirfentanil.

1.5.5. Analgesic activity

Mirfentanil (**Figure 1.4 (23)**) is a pyrazine derivative with strong selectivity for the opioid receptor. This compound could be produced through many synthetic methods. One of the most widely used synthetic route is the use of 4-amino-1-phenethylpiperidine as a starting material to obtain 1-phenethyl-4-[N-(pyrazinyl)amino]piperidine followed by acylation with 2-furoyl chloride in 1,2-dichloroethane to yield mirfentanil.^[41]

1.6. Anticancer activity

Many pyrazine derivatives were synthesized and evaluated as potential anticancer agents working against various enzyme targets including protein kinase inhibitors, aurora kinase inhibitors, mitotic kinase inhibitors, B-RAF inhibitors, check point kinase inhibitors, A549 lung cancer cell inhibitors, mammalian target of rapamycin (mTORC1 and mTORC2) inhibitors, caspase-3 inhibitors and activated Cdc42-associated kinase inhibitors, this section illustrates some of the main anticancer derivatives along with their targets ^[42, 43].

1.6.1. Cytotoxic substituted pyrazine derivatives

1.6.1.1. Proteasome inhibitor Bortezomib:

Proteasomes are key regulators of protein degradation, during multiple myeloma it is likely that the malignant cells have altered or defective cell cycle proteins leading to an increased proliferation rate, increased accumulation of damaged proteins and therefore higher dependency on the proteasomal degradation processes^[44]. As a result inhibition of the proteasome has emerged as a clinically effective anti-cancer therapeutic approach over the past decade. The first-in-class Bortezomib (**Figure 1.5 (24)**) is a proteasome inhibitor that shows in preclinical studies good pleiotropic effects, disrupting multiple cellular signaling pathways and inducing tumor cell death. ^[45]

1.6.1.2. DNA binding 2,6-diphenylpyrazine derivatives:

DNA remains an attractive target for the design of antitumor agents. Series of bis-phenylpyridine derivatives substituted with different side chains, neutral or cationic showed little cytotoxicity but their anti-proliferative activity did not correlate with DNA binding. In an extension of this work, a new series of molecules for which the pyridine central ring has been replaced with a pyrazine ring were synthesized and the DNA binding and cytotoxic properties were investigated and directly compared to their pyridine analogs. In all cases the incorporation of the pyrazine ring promoted the cytotoxicity of the molecules compared to the corresponding pyridine analogues, previously synthesized (**Figure 1.5 (25)**).^[46]

1.6.1.3. Cytotoxic Bis (indolyl) pyrazine:

Series of 3,6-bis(3'-indolyl)pyrazine (**Figure 1.5 (26)**) were synthesized and evaluated for cytotoxic activity against diverse human cancer cell lines by the National Cancer Institute. These

compounds demonstrated significant inhibitory effects on the growth of a range of cancer cell lines. However the mechanism of action remained unknown. [47]

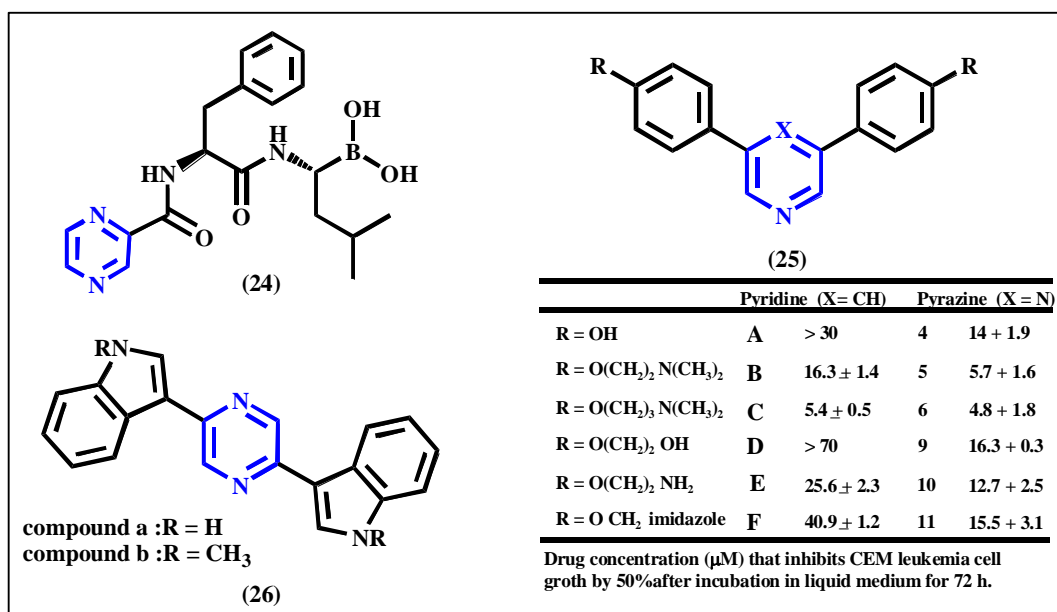


Figure 1.5: Pyrazine derivatives with cytotoxic activities: [(1*R*)-3-methyl-1-((2*S*)-3-phenyl-2-[(pyrazin-2-ylcarbonyl)amino]propanoyl) amino)butyl] boronic acid (Bortezomib) (24). Comparison between 2,6-diphenylpyrazines (25) and the corresponding pyridine analogues in terms of DNA binding and cytotoxic properties. Series of 3,6-bis(3-indolyl) pyrazine derivatives (26).

1.6.1.4. B-RAF inhibitors Di-substituted Pyrazine Scaffold:

The protein kinase B-RAF, is a member of RAF family proteins which are a serine/threonine kinases, it plays an important role in the development of certain classes of cancer, especially melanoma (50-70%), ovarian (~35%), thyroid (~30%) and colorectal (~10%) cancers. As a result of high-throughput screening, the lead compound 2-(3, 4, 5-trimethoxyphenylamino)-6-(3-acetamidophenyl) pyrazine was identified as a B-RAF inhibitor and was chosen as the starting point for producing potent inhibitors of B-RAF. A series of novel compounds, which involved extensive modifications to the 2-(3, 4, 5-trimethoxyphenylamino) moiety and their biological profiles against isolated B-RAF and mutated B-RAF in a cellular assay have been determined. These efforts led to the identification of two compounds exhibiting remarkably enhanced activities against B-RAF with IC₅₀ values of 0.79 μM and 0.74 μM, respectively (Figure 1.6 (27) and (28)). [48]

1.6.1.5. Kinase inhibitors V-shaped pyrazine derivatives:

Most 3-[(2-indolyl)]-5-phenyl-2,6-pyrazine derivatives are well known potential CDK inhibitors. New derivatives were synthesized using several Indoles and phenyls in aim to diversify substitutions of the pyrazine ring. Kinase assay was conducted for the synthesized derivatives and showed that compound (**Figure 1.6 (29)**) was the most potent inhibitor of CDK5. ^[49]

1.6.1.6. Mitotic Kinase Inhibitor

Nek2 which is also called as never in mitosis A-related (NIMA) kinase is a serine/threonine kinase which plays crucial role in division of cells. Over expression of Nek2 contributes to chromosome instability. This makes Nek2 a promising therapeutic target in cancer treatment. Whelligan *et al.*^[50] reported a series of aminopyrazine derivatives that inhibits Nek2 using structure based drug design. It was noticed that substitution on piperidine ring of the aminopyrazine led to the development of the most active compound (**Figure 1.6 (30)**) having IC₅₀ of 0.23 μM.

1.6.1.7. Check Point Kinase (Chk1) Inhibitor

Chk1 is a human serine/threonine protein kinase of cell nucleus. During DNA damage process, Chk1 is getting activated. Inhibition of Chk1 results in abrogation of arrest in the S and G2 phases in mitotic apoptosis. Hence, Chk1 inhibitors are considered as important therapeutic targets in the treatment of cancer^[51]. Wang *et al.* have reported a series of compound containing 1-(5-chloro-2-alkoxyphenyl)-3-(5-cyanopyrazin-2-yl) urea as Chk1 inhibitor. Among the series, (**Figure 1.6 (31)**) has been reported to cause S and G2/M phase check point arrest with IC₅₀ of 7 nM. The modified aromatic urea (**Figure 1.6 (32)**) carries a hydrophilic moiety i.e. tertiary aliphatic amine and showed the best enzymatic activity with IC₅₀ of 3 nM ^[52, 53].

1.6.1.8. Caspase-3 inhibitors

Caspases are cysteine proteases with an aspartate residue at the target cleavage site. These enzymes are grouped into 3 subclasses via group I, II and III on the basis of sequence homology and substrate specificity. Group III caspases are required for apoptotic cell death. Han *et al.* reported the development of potent and selective caspase-3 inhibitors. Compound (**Figure 1.6 (33)**) showed excellent anti apoptotic activities in vitro and in vivo models by inhibiting caspase-3 with a small IC₅₀ value of 0.006 μM ^[54].

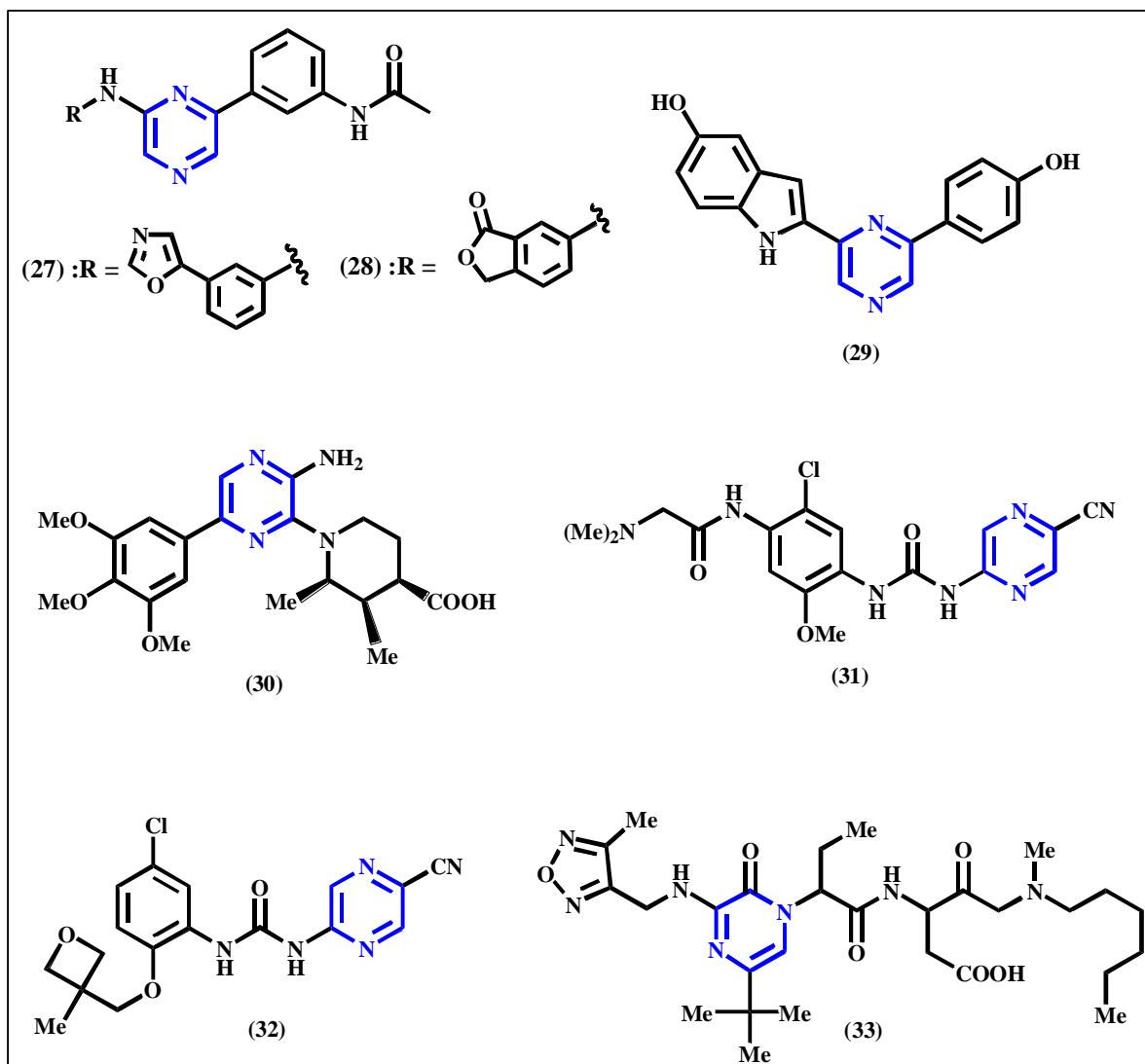


Figure 1.6: Pyrazine based inhibitors of different protein kinases: Disubstituted pyrazine derivatives as potent B-RAF inhibitors (27), (28). 3-(6-hydroxyindol-2-yl)-5-(phenyl)pyrazine as CDK5 inhibitor (29). 1-[3-Amino-6-(3,4,5-trimethoxy-phenyl)-pyrazin-2-yl]-2,3-dimethyl-piperidine-4-carboxylic acid as (NIMA) kinase inhibitor (30). 1-(5-chloro-2-alkoxyphenyl)-3-(5-cyanopyrazin-2-yl)ureas as Chk1 inhibitor (31), (32). 3-(2-{5-tert-butyl-3-[(4-methyl-furazan-3-yl)methyl]-amino}-2-oxo-2H-pyrazin-1-yl)-butyrylamino-5-(hexyl-methyl-amino)-4-oxo-pentanoic acid as caspase 3 inhibitor (33).

1.6.2. Cytotoxic fused pyrazine derivatives

Pyrazine ring has importance in exhibiting various biological activities in association with other scaffolds like pyrrole, pyrazole, imidazole, triazole, tetrazole, thiophene, oxazole, pyridine, piperidine and piperazine. This section highlights the most prominent cytotoxic fused pyrazine systems along with their targets.

1.6.2.1. Imidazo[1,2-a]pyrazine derivatives as Aurora kinase inhibitor:

Aurora kinases are cell cycle regulated serine/threonine kinases that play a key role in regulating mitosis. Aurora A and B are frequently overexpressed in various human tumors, including carcinomas of the breast, head, neck, ovary and colon. Hence inhibition of aurora is expected to impair tumor growth as a result of cell cycle disruption and cell death. The family of imidazo [1,2-a]pyrazines (**Figure 1.7 (34)**) have been gaining attention in drug discovery especially as structural analogues of purines. Kerekes^[55] and Belanger^[56] reported a series of compounds with imidazo [1,2-a]pyrazine core as potential aurora kinase inhibitors. Compound (**Figure 1.7 (35)**) has been reported as a lead compound with a promising activity as aurora A and B inhibitor with IC₅₀ 4 and 13 nM, respectively. Because of the importance of imidazo[1,2-a]pyrazines which stems especially from their remarkable anticancer activity and as an extension of the previous works on imidazo[1,2-a]pyrazine some novel 1,3-diarylpyrazino[1,2-a]benzimidazole and 2,3,6,8-tetraarylimidazo[1,2-a]pyrazine derivatives were synthesized by Kayagil and Demirayak. The cytotoxic effects of the compounds were evaluated in vitro against approximately 66 human tumor cell lines derived from 9 neoplastic diseases. Compound (**Figure 1.7 (36)**) provided a notable activity.^[57] Other imidazo[1,2-a]pyrazine derivatives like 8-heteroaryl-6-phenyl-imidazo[1,2-a]pyrazines were used as modulators of Hsp90 complex activity for treating a variety of diseases and disorders such as cancer^[58]. In addition, 6-aryl-imidazo[1,2-a]pyrazin-8-ylamines was patented as possible treatment of kinase implicated disorders.^[59]

1.6.2.2. Pyrido[2,3-b]pyrazine derivatives:

A series of 2,3,6-trisubstituted pyrido[2,3-b]pyrazines showed higher activity than 2,3,6-trisubstituted quinoxaline as potential small-molecule inhibitors of the Wnt/ β -catenin signal pathway in non-small-cell lung cancer cell (NSCLC) lines. one of the most potent derivatives was (**Figure 1.7 (37)**).^[60] Some derivatives of pyrido[2,3-b]pyrazine (**Figure 1.7 (38)**) were active for modulation of misdirected cellular signal transduction processes such as tyrosine kinases, serine/threonine kinases and/or lipid kinases, especially for the treatment of malignant disorders and other disorders based on pathological cell proliferations. Other pyrido[2,3-b]pyrazine derivatives (**Figure 1.7 (39)**) were used mainly as inhibitors of TGF- β receptor kinases, which can be used for the treatment of kinase-induced diseases, in particular tumors^[61].

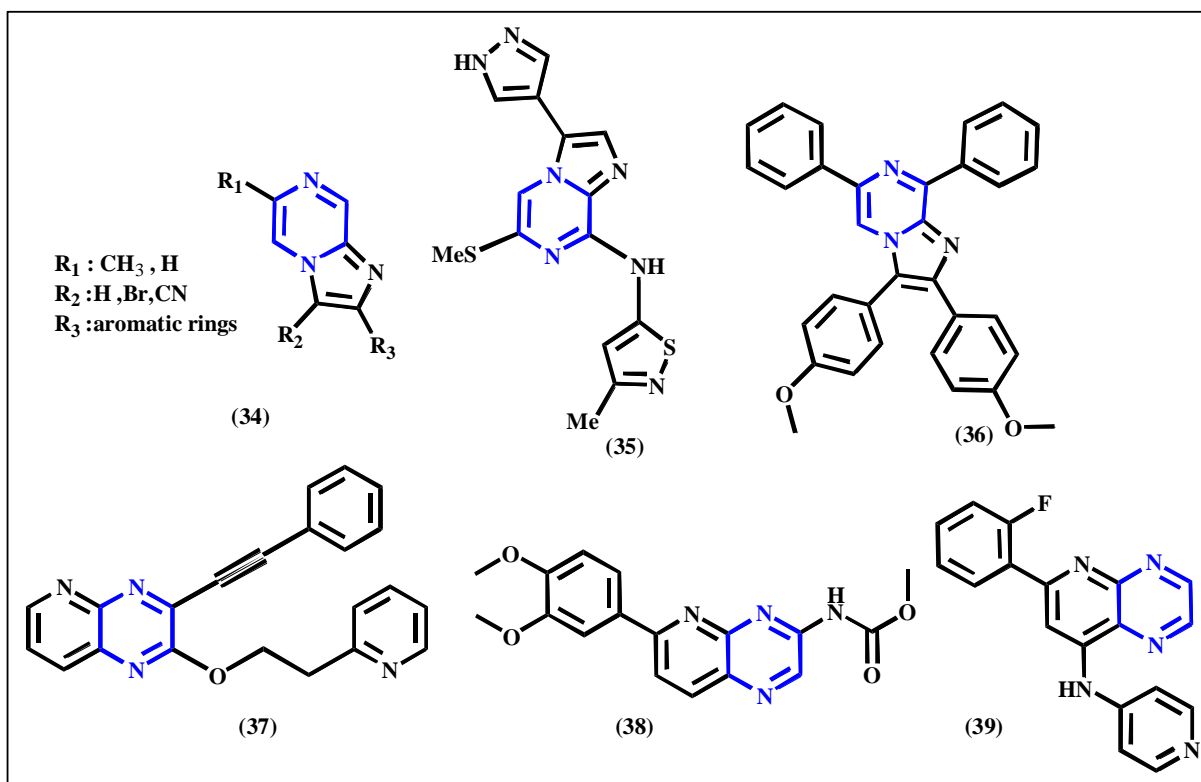


Figure 1.7: Fused pyrazines as anticancer agents: imidazo [1,2-a]pyrazines (34), (35), (36). pyrido[2,3-b]pyrazines (37), (38), (39).

1.6.2.3. Fused pyrazines as anticancer agents

Other fused pyrazine-based skeletons that were patented as potent anticancer agents include diaminopteridine-benzenesulfonamide (**Figure 1.8 (40)**) an inhibitor of carbonic anhydrase and dihydrofolate reductase, and phenazine (**Figure 1.8 (42)**) an inhibitor of quinone reductases 1 and 2, and inducible nitric oxide synthase. In addition, a number of quinoxaline N-oxide derivatives were also recognized as potent anticancer agents (**Figure 1.8 (41)**).^[3]

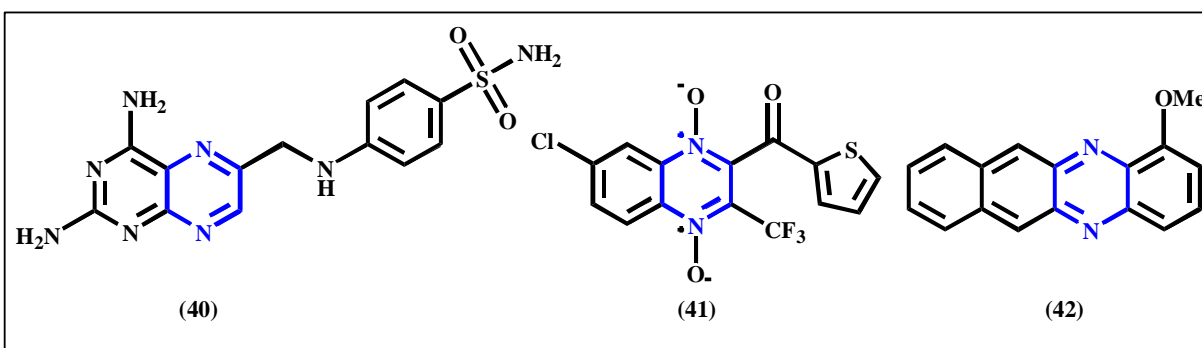


Figure 1.8: Fused pyrazines as anticancer agents (40) diaminopteridine-benzenesulfonamide, (42) phenazine, (41) quinoxaline N-oxide.

1.6.2.4. Pyrrolo-pyrazine derivatives as protein kinase inhibitors:

Protein kinase enzyme plays a vital role in the control of cell cycle progression, apoptosis, growth and metabolism. It is a well-known potential target for intervention in a number of diseases including cancer. The derivatives of pyrrolo[2,3-b]pyrazine are known to be biologically active. In addition to having antibronchospastic effect and the ability to inhibit the activity of p38 MAP Kinase, the compounds of this class could also inhibit cyclin dependent kinases (CDKs) and glycogen synthase kinase-3 (GSK-3), thereby exerting an antiproliferative effect. The most known pyrrolo[2,3-b]pyrazine derivatives are aloisines (**Figure 1.9 (43)**)^[62].

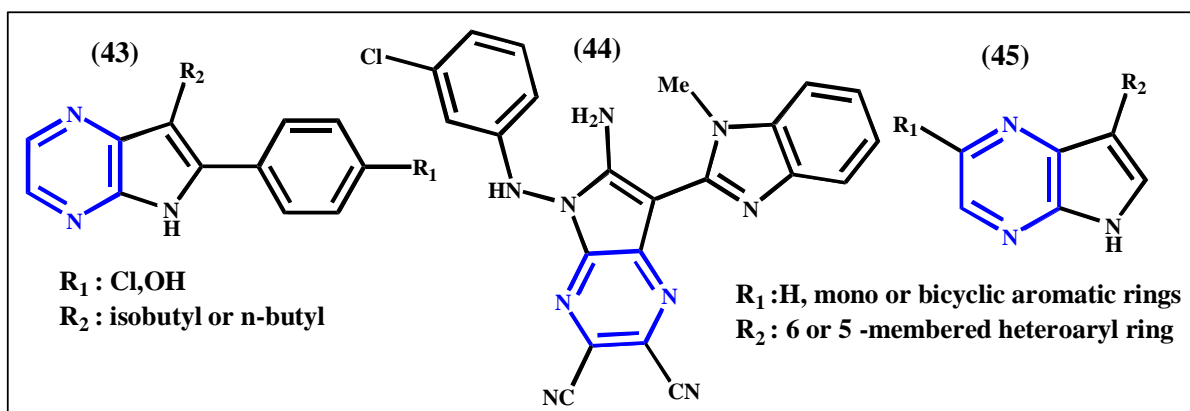


Figure 1.9: Pyrrolopyrazine derivatives as kinase inhibitors.

Dubinina *et al.* reported a series of compounds containing 5,7-disubstituted 6-amino-5H-pyrrolo[3,2-b]pyrazine-2,3-dicarbonitrile core as protein kinase inhibitors with anti-proliferative activity. Compound (**Figure 1.9 (44)**) exhibited a significant anti-proliferative activity against RXF 393 (renal cancer) and BT-549 (breast cancer) cell lines^[63]. Some pyrrolopyrazine derivatives were patented as useful inhibitors of ATR protein kinase^[64] and showed unexpected ability to treat cancer as single agents and exhibited surprising synergistic effect with other cancer agents, such as cisplatin (**Figure 1.9 (45)**).

At the end of this literature review, our main subject of focus was the aloisines as it exerts numerous inhibitory activities against different types of protein kinase systems especially the cyclin dependent kinase, along with its toxicity against wide panel of cancer cell lines. The next section will provide better understanding for the inhibitory activity and selectivity of this class of compounds in aim to prepare new pyrazinyl analogues that mimic the binding mode of aloisines with good selectivity toward cyclin dependent kinase (CDK).

1.7. Cyclin dependent kinase structure and function:

1.7.1. Summary

Cyclin-dependent kinases (CDKs) are a family of serine/threonine protein kinases whose members get activated by binding to their respective cyclin subunits. In most cases, full activation also requires phosphorylation of a threonine residue near the kinase active site. To date, 13 CDKs and 25 cyclins have been discovered and their biological functions remain incompletely understood. CDKs were originally studied for their direct role in cell cycle regulation (**Figure 1.10 (a)**). Cell-cycle events in multicellular eukaryotes are mainly controlled by two Cdk, known as Cdk1 and Cdk2, which operate primarily in M phase and S phase, respectively. In normal cells, progression from one phase of the cycle to the next can be initiated only after passage through checkpoints, where correct completion of the preceding steps, e.g. faithful DNA replication at the end of S phase, is verified. If the steps have not been properly executed, the cell undergoes apoptosis (programmed cell death). Tumor cells possess faulty checkpoints and can proliferate despite a compromised genome. Very often the mechanisms by which transformed cells can override checkpoints are closely related to CDK function. For this reason, restoration of cell cycle control through pharmacological inhibition of CDKs has been actively pursued over the last decade as a new strategy for the treatment of cancer. More recently, however, it has become clear that CDKs are involved in many other cellular processes, including regulation of transcription, differentiation and cell death. ^[65]

1.7.2. Kinase structure and binding

Cyclin dependent kinases (CDKs) are considered small proteins with a size of (~34–40 kDa), they are mainly composed of two subunits: The first subunit is the regulatory cyclin subunit which is the essential activator of CDKs, it is composed of about 100 amino acids rolled into a five-helix bundle, including a highly conserved box. The second subunit is the protein kinase catalytic domain, which contains ~250–300 amino acid residues. All CDKs share a common tertiary structure comprising two terminal lobes which differ in size: an upper, small amino terminal lobe (N lobe) characterized by a β -sheet structure, and a lower, larger carboxy-terminal lobe (C lobe) which is commonly α -helical in shape. The variation in the orientation of the two lobes yields open and closed conformations. The importance of closed conformation is

represented in forming of the ATP binding pocket. The ATP-binding pocket and the active site are located between the two lobes of the cleft; ATP fits snugly in that cleft, in such a way that the phosphates are oriented outwards toward the cleft mouth. The protein substrate attaches at the cleft's entrance and interacts with the surface of the C lobe. Subsequently adjacent residues catalyze the transfer of the terminal phosphate of ATP to a hydroxyl oxygen in the protein substrate.^[66]

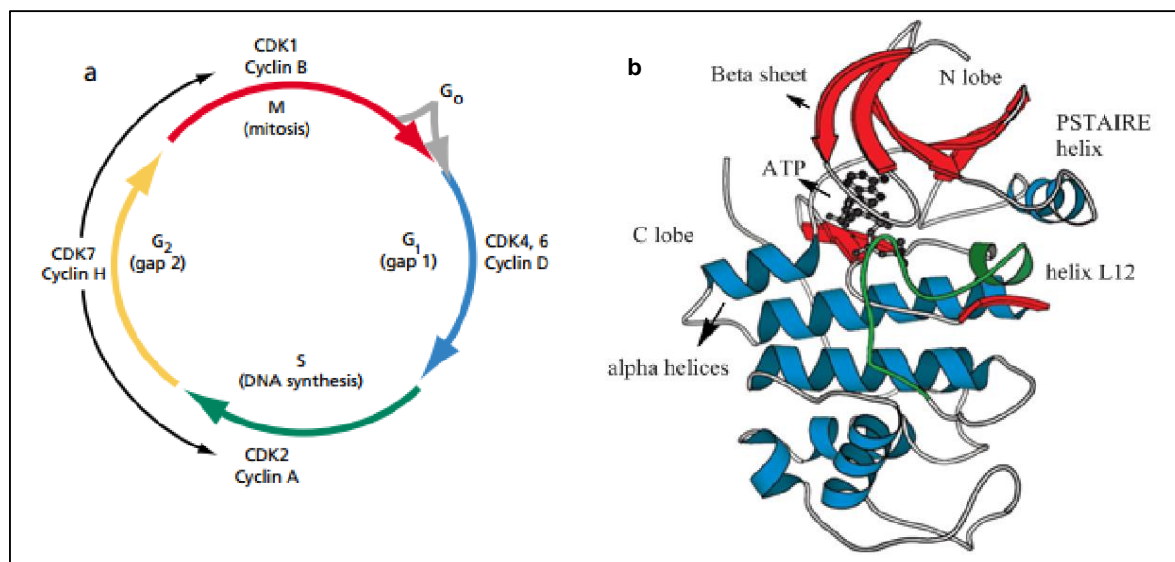


Figure 1.10: a) The CDKs responsible for progression through the various phases of the cell division cycle are indicated. CDK7 (CDK-activating kinase, CAK) is involved in activation through phosphorylation of both CDKs 1 and 2. b) Tertiary structure of human CDK2, determined by X-ray crystallography. The structure of CDK2 is composed of two parts: first part is the amino-terminal lobe which is composed of beta sheet structure (red color) and the PSTAIRE helix, second part is the carboxy-terminal lobe which is mainly composed of alpha helices (blue color). The ATP binding pocket and active site are located within the two lobes. The Helix L12 and T-loop are shown in green color.

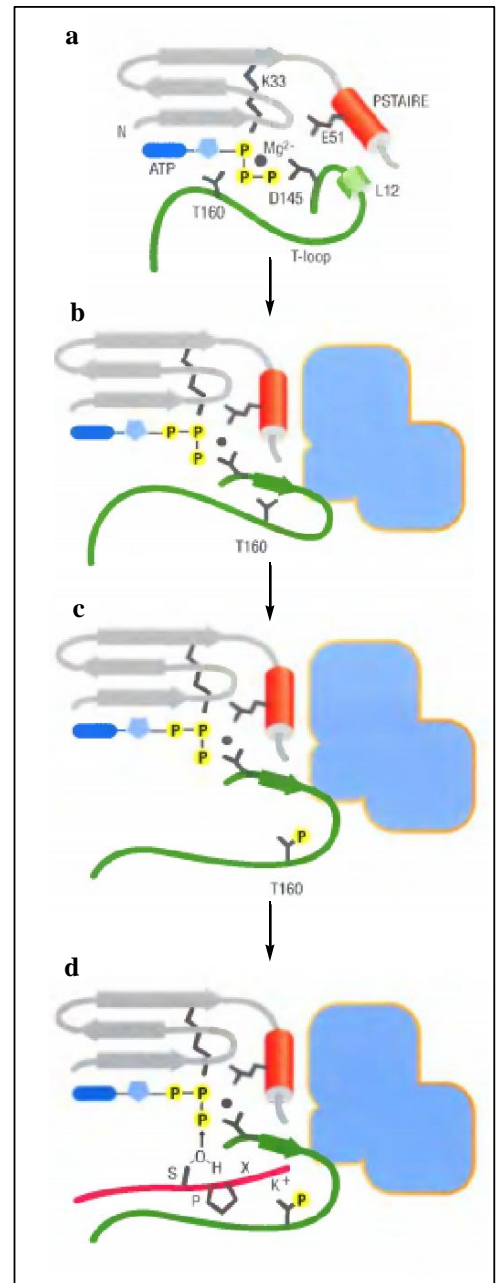
The structure of the two lobes of the CDKs is the same as other protein kinases, but with some structural differences that render them inactive in the absence of cyclin. One of the structural differences is that CDKs have a large flexible threonine loop (T loop), also known as the activation loop, which is located next to the active site and rises from the carboxy-terminal lobe to block the binding of protein substrate at the entrance of the active-site cleft. As a result the phosphorylation of this lobe is required to maximize kinase activation. Another structural difference is that in the case of inactive CDKs the active site residues (amino acid side chains) are not positioned properly, preventing ATP phosphate group from getting ideally oriented. Correspondingly proper enzyme activation requires massive structural changes in the active site

of CDK. The activity of CDK is mainly controlled by the contribution of two alpha helices; the first one is the PSTAIRE helix (an alpha helix close to the N lobe of CDK) which interacts with cyclin subunit. The movement of PSTAIRE helix reorients the residues that interact with the phosphate group of ATP in a way resulting in kinase activation, the second helix is the L12 helix (small alpha helix close to T-loop) changes its structure upon cyclin binding to become a beta strand, and contributes to the reconfiguration of the active site and T-loop. **(Figure 1.10 (b))** shows the structure of a protein kinase 2 catalytic domain. ^[66]

1.7.3. Cyclin-dependent kinase activation:

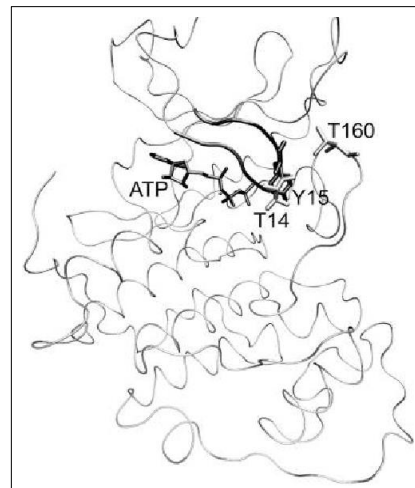
The activation of CDKs is achieved by two steps. The first step is triggered by the binding of the cell synthesized protein cyclin with its corresponding CDK **(Figure 1.11)**. ^{[59] [58]} The second step is phosphorylation of threonine160 on the CDKT-loop. This step is mediated by CDK activating kinase (CAK). Therefore, the phosphorylation step leads to a change in the CDK's active site conformation. Afterwards the T-loop moves from the entrance point of the active site reducing the steric hindrance that blocks the binding site. CDK2 activation transfers the cell into the next phase of the cell cycle. ^[66]

Figure 1.11: schematic structure of CDK2 in various states of activity. **a)** The inactive CDK2 monomer, the small L12 helix next to T loop pushes out the large PSATAIRE helix which contains glutamate 51, the T-loop blocks the active site cleft. **b)** When cyclin A binds to CDK2 the PSATAIRE helix moves inward and the L12 changes structure to form a small beta strand, E51 moves inward to interact with lysine33 while aspartate 145 also shifts position. These changes lead to the correct orientation of the ATP phosphate. The T loop also shifts out of the active site entrance. **c)** The phosphorylation of threonine 160 causes the T loop to flatten and interact more extensively with cyclin A. **d)** phosphorylation allows T loop to interact effectively with a protein substrate containing SPXK sequence (pink), a number of interactions occurs so the substrate is positioned in a correct way for nucleophilic attack on the phosphate of the ATP.



Once the cell has moved into the next phase, the CDK is deactivated by adding phosphate group to the two sites in G-loop, which are threonine (T14) and tyrosine (Y15) as shown in (Figure 1.12).^[66, 68]

Figure 1.12: View of CDK2/ATP (1HCK coordinates taken from PDB database) complex is shown in tube representation. The T160 (shown in gray-colored licorice representation) activation site is located on the T-loop. The G-loop (black-colored tube representation) includes two possible inhibitory sites, T14 (gray-colored licorice representation) and Y15 (black-colored licorice representation).



1.7.4. Cyclin-dependent kinase inhibition

Regulation of CDK activation and inhibition is a key component in controlling the cell cycle. Any changes in CDK activity would create errors in the cell cycle. This can lead to the uncontrolled cell growth and division, giving rise to cancerous cells. Scientist propose that inhibition of abnormal cell proliferation might be possible through the inhibition of CDKs. CDK inhibitors, therefore, are biologically interesting targets to design, synthesize and study as potential anti-cancer agents. Because of the clear connection between pharmacological CDK inhibition and cell cycle regulation, the potential use of CDK inhibitors in oncology was appreciated some time ago and the first molecules are now undergoing clinical evaluation.^[69, 70]

1.7.5. Mode of action

The inhibition of CDK can be done using different inhibitors that bind to the cyclin-CDK complex and inactivates it. These molecules result in promoting cell cycle arrest in G1 phase. The great majority of known CDK inhibitors are ATP-competitive type, interacting with cyclin-dependent kinases within their catalytic ATP-site. Until now, this strategy has been the most successful in designing inhibitors of CDKs. On the other hand, ATP Non-Competitive Inhibitors are a new inhibitors-generation which does not enter in competition with ATP, therefore exhibiting an action mode different from the other type of inhibitors. Nowadays two classes of ATP non-competitive CDKs inhibitors have been identified: Small Molecules Inhibitors and Small Peptide Inhibitors which are peptides designed based on their similarity with endogenous CDKs inhibitors. Moreover, Allosteric Inhibitors bind CDKs away from their ATP-binding site. Resulting in a conformational change to the CDKs, thus modifying their activity.^[71]

1.8. Pyrrolopyrazines as kinase inhibitor:

1.8.1. Binding and structure activity relationship

As mentioned earlier, the most recently reported pharmacophore with high CDK potency and selectivity encompasses compounds containing the 6-phenyl[5H]pyrrolo[2,3-b]pyrazine core structure (Aloisines), the conserved substructure of these compounds is shown in **(Figure 1.13)**. Aloisines are selective inhibitors of CDK1, CDK2, CDK5 and GSK3. The most potent aloisine so far is aloisine A, with reported IC_{50} values of 0.15 μM (CDK1), 0.12 μM (CDK2/cyclin A), 0.16 μM (CDK5) and 1.5 μM (GSK3 β) in functional kinase assays, on the other hand Aloisine A is less potent against ERK1 (IC_{50} = 18 μM) and ERK2 (IC_{50} = 22 μM). This concludes that aloisines are less potent towards ERKs; however the understanding of SARs suggests that this pharmacophore might lend itself to the design of inhibitors with differential selectivity profiles.^[72]

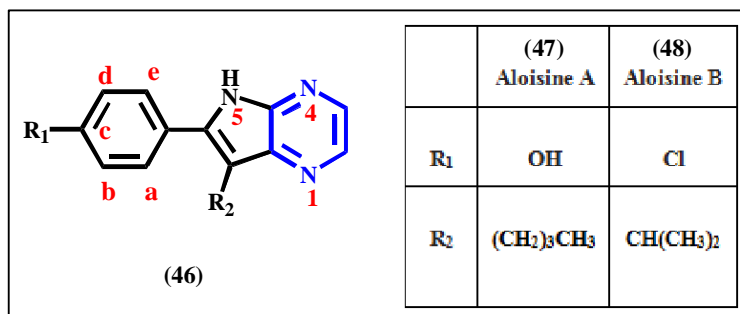


Figure 1.13: structures of Aloisine A **(47)**: (4-(7-Butyl-5H-pyrrolo[2,3-b]pyrazin-6-yl)-phenol) and Aloisine B **(48)**: (6-(4-Chloro-phenyl)-7-isopropyl-5H-pyrrolo[2,3-b]pyrazine

First, to investigate the mechanism of aloisine's action, kinetic studies were performed by varying both ATP levels and aloisine A concentrations. These experiments were performed with CDK1/cyclin B, CDK5/p25, and GSK-3 β . The data demonstrates that aloisine act by competitive inhibition of ATP binding to the catalytic subunit of the kinase. The resolution of a CDK2-aloisineB cocrystal structure was in agreement with these findings. **(Figure 1.14)** illustrates the interactions between aloisine B and the CDK2 ATP-binding site. As observed, aloisine occupies the ATP-binding pocket and makes two hydrogen bonds with nitrogen and oxygen atoms of Leu 83 amino acid which lies within the hinge region sequence that links the two lobes of the kinase.^[72]

An examination of the key features responsible for the potency and selectivity of known inhibitors of CDK, GSK3 β and ERK2 can be used as a guide in the design of new inhibitors. Pharmacophore maps of the ATP-binding sites show that there are two main criteria that need to

be met in order to yield compounds that have affinity for the ATP-binding pocket: the compounds need to bind effectively to the hinge region, through two or three H-bond donor or acceptor groups, and there must be sufficient hydrophobic interactions within the adenine-binding domain through two or more aromatic ring systems.

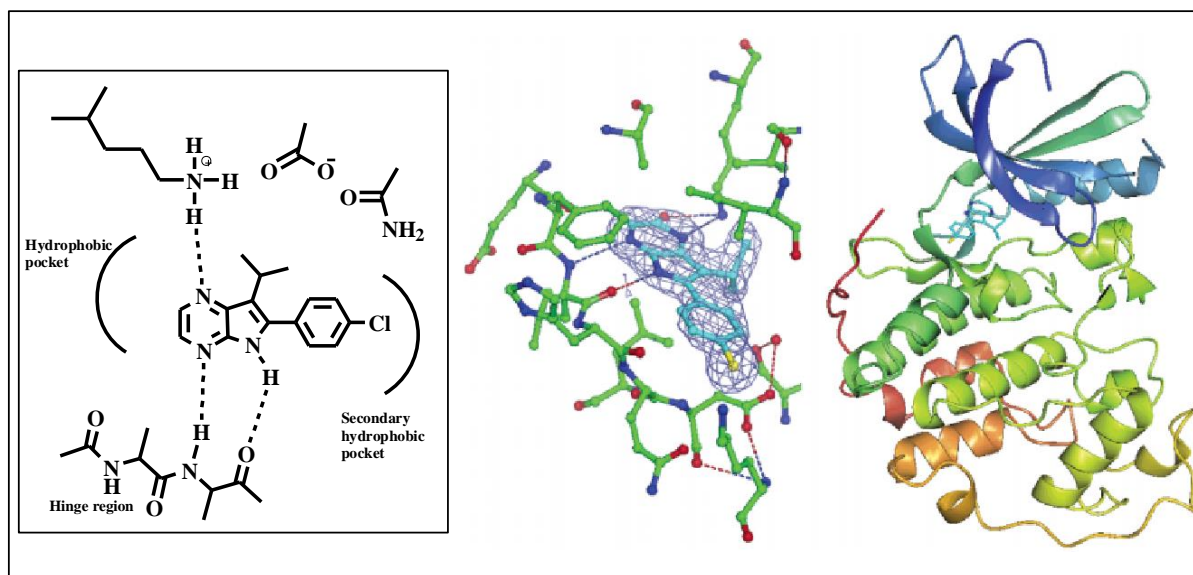


Figure 1.14: The binding of aloisine B to CDK2. a) Schematic representation of the interaction between aloisine B and the amino acids in the ATP binding site (hydrogen bonds are represented by dotted line). b) Stereoview showing the interactions between aloisine B and the CDK2 ATP-binding site. Residues that lie within 4 Å of the bound aloisine B molecule are drawn in ball-and-stick mode. Aloisine B carbon atoms are drawn in cyan and those of CDK2 in green. Oxygen atoms are colored red, nitrogen atoms blue, and the chlorine atom yellow. Dotted lines represent hydrogen bonds between aloisine B and the backbone nitrogen and oxygen atoms of Leu83. c) CDK2 is drawn in ribbon representation and color-ramped from blue to red, starting at the N-terminus. The N-terminal lobe is dominated by a five-stranded antiparallel β -sheet, and the C-terminal lobe is predominantly α -helical. Aloisine B is drawn in ball-and-stick mode bound at the ATP-binding site, which lies in the cleft between the two domains. Aloisine B carbon atoms are colored cyan, nitrogen atoms blue, and the chlorine atom yellow.

as the three nitrogen atoms of the phenylpyrrolo[2,3-b]pyrazine skeleton are engaged in hydrogen bonds with the Leu83 and Lys33 residues of CDK2, substitutions on these three positions are to be excluded. Furthermore, replacement of any of the nitrogen atoms in this skeleton by a carbon diminishes the inhibitory activity of the resulted compound. As a result, substitutions on other positions were undertaken to orientate the synthesis of derivatives toward improved CDK and GSK-3 inhibitory activity.

1.8.2. Designing selective CDK inhibitors

Many small-molecule CDK inhibitors have also been found to inhibit certain other kinases. Considering the fact that the human genome encodes around 800 protein kinases, these observations are hardly surprising. Many ATP antagonist kinase inhibitors previously thought to be selective were, in fact, later found to be less than selective when assayed against a large panel of functionally diverse kinases. CDKs are phylogenetically closely related to extracellular signal-regulated kinases (ERK-1 and ERK-2), as well as to glycogen synthase kinase-3 (GSK-3). These latter enzymes are frequently also affected by CDK inhibitors. In particular, many CDK2 inhibitors, including aloisines, are practically equipotent against GSK-3. The structural basis for rationalizing inhibitor selectivity for individual CDKs is still comparatively weak, since only CDK2-inhibitor complex X-ray co-crystal structures have so far been obtained, whereas other CDKs have not so far proven amenable to crystallization.^[73]

Assuming that aloisine A (a) binds to ERK2 in a similar fashion as to CDK5, the observed hydrogen bonds (H-bonds) with the kinase hinge region involve N4 and N5-H of the pyrrolopyrazine system for aloisine A (H-bonds indicated by broken lines). The n-butyl chain is not well resolved in the crystal structure, which suggests that there is a high degree of freedom of movement associated with this alkyl chain. The phenol hydroxyl is directed out of the binding pocket and makes suboptimal interactions with surface-specific residues. Whereas substitution at both positions b and d (panel a) with either chloro or methoxy resulted in loss of activity, monosubstitution at position a, b or c with OH and OMe was productive. Selectivity can apparently be controlled through the choice of substituents at position c on the aryl ring. Thus, large hydrophobic groups favor GSK3 and CDK1 versus CDK5, whereas small groups such as fluoro, methyl and cyano improve potency towards CDK5 without a significant gain in selectivity. The reduced potency of aloisine A with respect to ERK1 and ERK2 can be rationalized in terms of the less favorable interaction between the polar gate-keeper residue (Q103ERK2) and the pyrazine system of the ligand (panel d) as compared to hydrophobic interactions for CDK5 and GSK3 β (F80CDK5, L132GSK3 β). Moreover linear planar ligands are poorly tolerated by ERK2 as the length of the binding pocket is about 2 Å shorter than that of CDK5, as measured from the gate-keeper residue (F80CDK5, Q103ERK2) to the surface-specific Lys residue (K89CDK5, K112ERK2) (**Figure 1.15 (a-c)**).^[65]

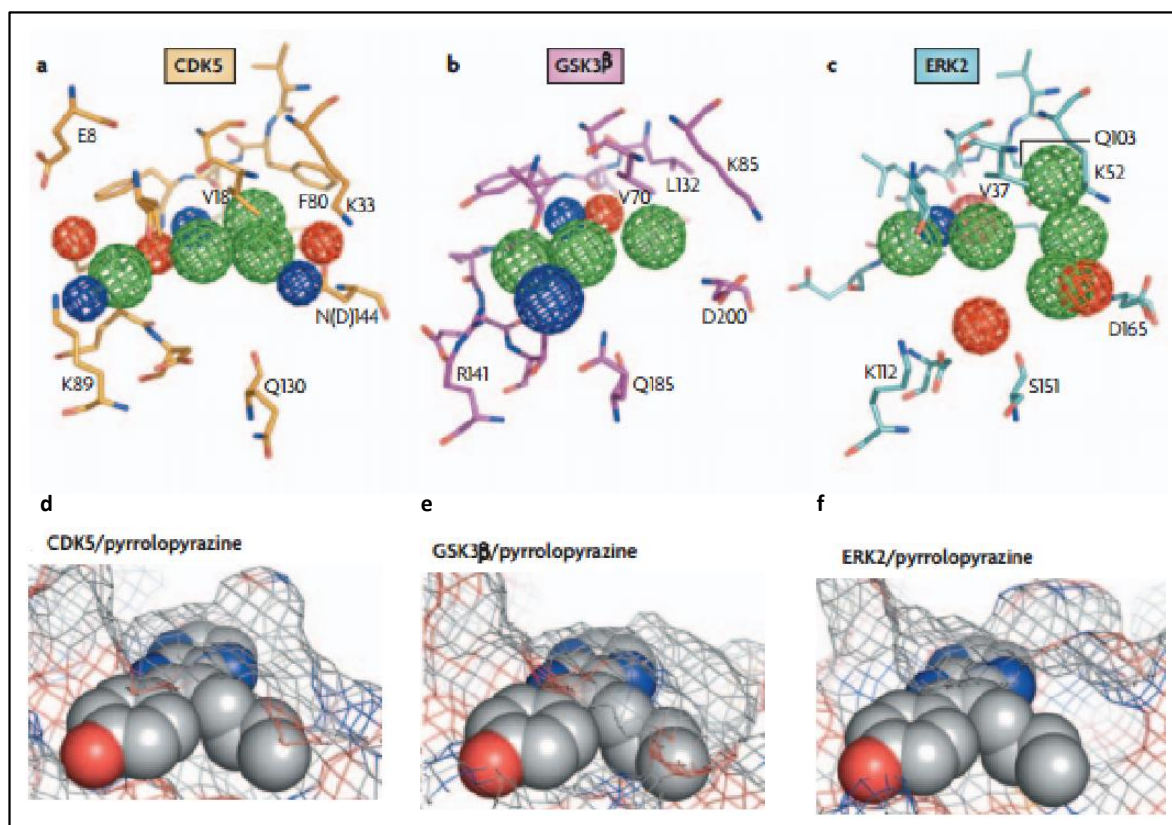


Figure 1.15: Pharmacophore maps of CDK5, GSK3 β and ERK2 (a-c). The main residues lining the ATP-binding pocket of the three kinases are shown as stick models and the prominent pharmacophore features that have yielded potent inhibitors of each kinase are indicated with mesh spheres. Regions that are occupied by hydrophobic and aromatic portions of these inhibitors are depicted as green spheres and those where inhibitors commonly display H-bond donor and acceptor functions are in red and blue, respectively.

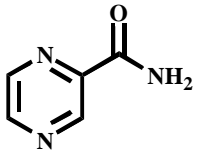
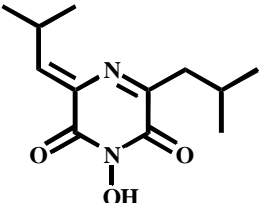
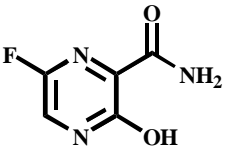
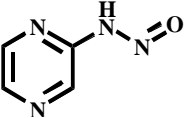
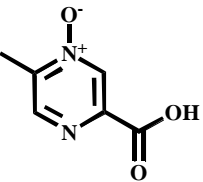
Binding of pyrrolopyrazine to CDK5, GSK3 β and ERK2 (d-f). Inhibitors and proteins shown as grey CPK space-filling models and mesh surfaces, respectively). Structures are modelled from PDB (Protein Data Bank).

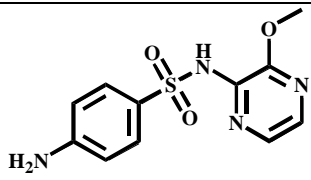
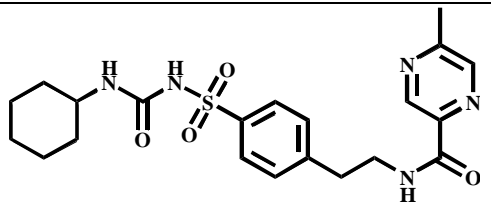
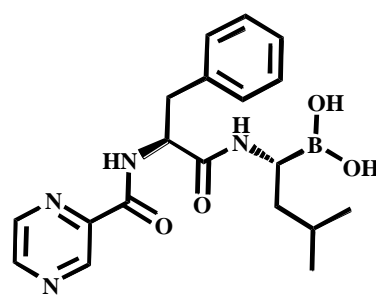
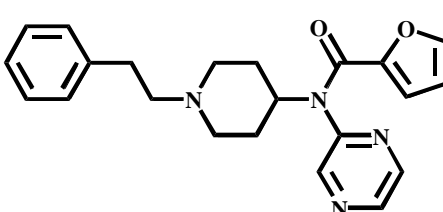
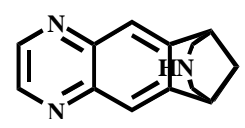
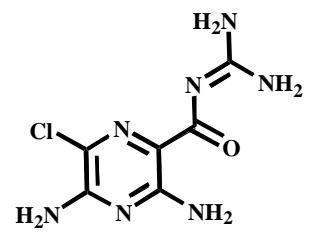
Despite the chemical similarity, between aloisines and ERK2- selective inhibitors, the binding pose of these compounds in the kinase ATP-binding site does not seem to be related to that of the aloisines. Unlike practically all other known CDK–GSK3 β –ERK inhibitors, which tend to be flat molecules, ERK2- selective inhibitors contains fused mutli heterocyclic systems that allows the formation of a highly complementary interaction with the unique features of the ERK2 ATP-binding pocket. In addition, unsubstituted phenyl group optimally occupies a small hydrophobic pocket adjacent to the gate-keeper residue in ERK2; this pocket is smaller in CDK5 and practically absent from GSK3 β (**Figure 1.15 (d-f)**).^[65]

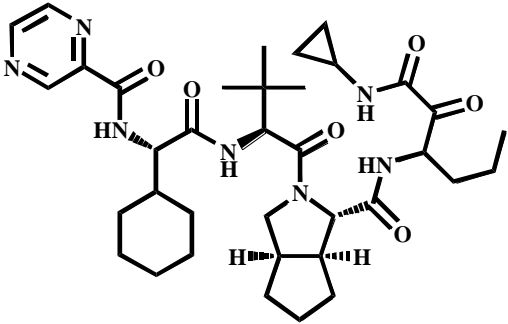
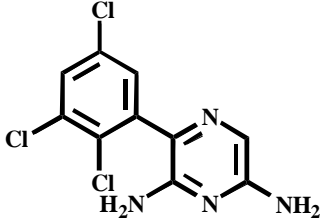
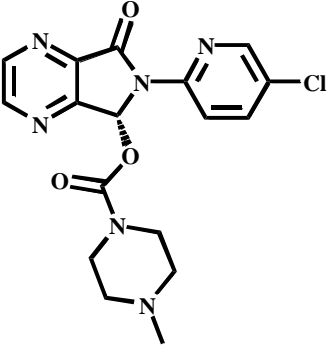
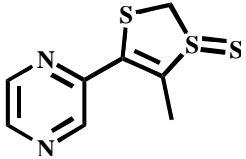
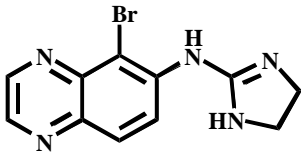
1.9. Pyrazine containing drugs in clinical use

Substituted pyrazines have been successfully introduced to clinical application with wide range of activities. The table below summarizes the structures of these drugs along with their pharmacological activities. ^[42]

Table 1.1: List of marketed pyrazine containing drugs along with their biological activity.

<u>number</u>	<u>Compound name</u>	<u>structure</u>	<u>Pharmacological activity</u>
(15)	Pyrazinamide		Antitubercular ^[74]
(49)	Flutimide		Antiviral ^[75]
(50)	Favipiravir		Antiviral ^[76]
(51)	Pyrazine diazohydroxide		Antineoplastic ^[77]
(52)	Acipimox		Hypolipidemic agent ^[78]

(53)	Sulfalene		Antibacterial sulfonamide ^[79]
(54)	Glipizide		Hypoglycemic agent ^[80] ,Angiogenesis inhibitor ^[81]
(55)	Bortezomib		Proteasome inhibitor ^[82] (multiple myeloma)
(23)	Mirfentanil		opioid receptor ^[41]
(56)	Varenicline		Smoking cessation ^[83]
(57)	Amiloride		Diuretic ^[84]

(58)	Telaprevir	 <p>The structure of Telaprevir is a complex molecule featuring a central bicyclic core (a decalin derivative). It is substituted with a cyclohexane ring, a pyridine ring, a cyclopropyl group, and several amide and ester functional groups.</p>	Protease inhibitor (hepatitis c) ^[85]
(59)	Elpetrigine	 <p>The structure of Elpetrigine consists of a pyrimidine ring system fused to a benzene ring. The benzene ring has two chlorine atoms at the 3 and 4 positions. The pyrimidine ring has an amino group at the 2 position and another amino group at the 6 position.</p>	Antiepileptic, sodium and calcium channel blocker ^[86]
(60)	Eszopiclone	 <p>The structure of Eszopiclone features a central benzimidazole ring system. It is substituted with a chlorine atom on the benzimidazole ring, a chlorine atom on a pyridine ring, and a piperazine ring via an amide linkage.</p>	Non- benzodiazepine sedative hypnotic ^[87]
(61)	Oltipraz	 <p>The structure of Oltipraz consists of a pyridine ring substituted with a pyrazole ring. The pyrazole ring has a sulfur atom and a methyl group attached to it.</p>	Antischistosomal agent, Chemoprotective agent ^[88]
(62)	Brimonidine	 <p>The structure of Brimonidine features a benzimidazole ring system with a bromine atom at the 5 position and a piperazine ring attached to the 2 position.</p>	Antiglaucoma agent A2 adrenergic agonist ^[89]

Aims and objectives of the study

Main objective of the study

The main objective of this study is to explore the possibility of designing novel pyrazine based molecules endowed with cytotoxic activity. The study is based on the design and preparation of 2,3-disubstituted pyrazine derivatives that will possibly exert activity against cancer cell lines by acting mainly as cyclin dependent kinase inhibitors.

Specific objectives of the study

- a. To synthesize a series of novel 2,3-disubstituted pyrazine derivatives.
- b. To explore different synthetic strategies that affords the final compounds in shorter time and higher yields.
- c. To characterize the synthesized compounds using available physical methods such as Fourier Transform Infrared spectroscopy (FT-IR), nuclear magnetic resonance (NMR) and mass spectroscopy (MS).
- d. To evaluate the cytotoxic activity of a set of the synthesized derivatives.
- e. To predict the possible biological activities of the newly synthesized compounds using PASS software.
- f. To investigate the drug likeness of the synthesized derivatives according to the rule of five.
- g. To gain insight into the binding mode and affinities of the synthesized derivatives with inactive monomeric CDK-2 using SwissDock software.

Chapter Two

Experiments and methods

2. Experiments and methods

2.1. Synthetic chemistry

2.1.1. Materials:

2,3-dichloropyrazine, ethanol amine, phenylenediamine, 4-aminophenol, 4-aminobenzoic acid, phenol, 2-methylamino-ethanol, glycine, 2-aminopyridine, 2-piperazin-1-yl-ethanol, 2-piperazin-1-yl-ethanol, [1,4']piperidinyl, 2-piperazin-1-yl-pyrimidine, 1-(3-trifluoromethylpyridin-2-yl)-piperazine, 1-(5-trifluoromethylpyridin-2-yl)-piperazine, ethylenediamine, sodium, paracetamol, *N*-bromosuccinimide (NBS), tetrahydrofuran (THF), dicyclohexylcarbodiimide (DCC), *N*-hydroxysuccinimide (NHS), sodium sulfate (Na₂SO₄), diisopropylethylamine (DIPEA), potassium carbonate (K₂CO₃), calcium chloride (CaCl₂), potassium bromide (KBr), dimethylformamide (DMF), dichloromethane (DCM), ethyl acetate (EA), dioxane, ether, triethylamine (TEA), methanol (MeOH), ethanol (EtOH), hexane, isopropanol, chloroform (CHCl₃) and hydrochloric acid (HCl) were purchased from ACROS chemical Ltd or D-Chem and were used without further purification.

Silica gel (silica gel 60 (0.040-0.063 mm)), thin layer chromatography (TLC) (TLC silica gel 60 F254) sheets were all purchased from Merck Ltd.

Deuterated solvents: D₂O, CDCl₃, DMSO-d₆ were purchased from ACROS chemical Ltd.

2.1.2. Instrumentation

2.1.2.1. Nuclear magnetic resonance (¹H-, ¹³C- NMR):

Data were collected using Varian Unity Inova 500 MHz spectrometer equipped with a 5-mm switchable probe and data were processed using the VNMR software. ¹H-NMR chemical shifts are reported in parts per million (ppm, δ) downfield from tetramethylsilane (TMS). Spin multiplicities are described as s (singlet), d (doublet), dd (double doublet), t (triplet), q (quartet), and m (multiplet).

2.1.2.2. Fourier transform infrared spectroscopy (FTIR):

All infrared spectra were obtained from a KBr matrix (4000–400 cm⁻¹) using a Perkin-Elmer spectrum 100, FT-IR spectrometer.

2.1.2.3. Electrospray ionization mass spectrometry (ESIMS):

Mass spectroscopy was performed using a Thermo Quest Finnigan LCQ-Duo in the positive ion mode. Elution was in a mixture of 49:49:2 water/methanol/acetic acid at a flow rate of 15 μ L/minute.

2.1.3. Synthesis of (2-amino-3-chloropyrazine) derivatives under basic condition

To a solution of 2,3-dichloropyrazine (0.5ml, 4.803 mmol) in dioxane or tetrahydrofuran (20 ml), DIEA (0.744 g, 5.763 mmol) or TEA (0.583 g, 5.763 mmol) was added. The mixture was stirred at room temperature for 10 minutes followed by the addition of the corresponding aliphatic or aromatic amine (4.803 mmol). While being stirred, the mixture was heated under reflux for 9-12 hour. The completion of the reaction was monitored by TLC (ethyl acetate: CHCl_3 ; (50:50 v/v)). Upon reaction completion volatiles were evaporated under vacuum. Afterwards, the residue was extracted against ethyl acetate and water (3 x 30 ml), the combined organic extracts were dried over anhydrous sodium sulfate, filtered, and concentrated. The crude product was purified by recrystallization or silica gel column chromatography using (CHCl_3 : hexane) as eluent to give the 2-amino-3-chloropyrazine in 77-91.8 % yield.

2.1.3.1. 2-(3-Chloropyrazin-2-ylamino)-ethanol {A1 (1)}

TLC (EA: CHCl_3 (50:50; v/v)), R_f = 0.26; dark brown oil, 0.764g; yield = 91.8%.

$^1\text{H-NMR}$ 300 MHz (DMSO- d_6 , δ ppm): 7.98(d, 1H pyrazine), 7.53(m, 1H pyrazine), 6.86(s, 1H amine), 4.75(t, 1H hydroxyl), 3.50(m, 2H), 3.41(m, 2H).

2.1.3.2. 2-[(3-Chloropyrazin-2-yl)-methyl-amino]-ethanol {A2 (2)}

TLC (EA: CHCl_3 (50:50; v/v)), R_f = 0.30; light orange oil, 0.798g; yield = 88.9%.

$^1\text{H-NMR}$ 300 MHz (DMSO- d_6 , δ ppm): 8.13(d, 1H pyrazine), 7.81(d, 1H pyrazine), 4.66(t, 1H hydroxyl), 3.58(m, 4H), 3.02(s, 3H CH_3).

2.1.3.3. (3-Chloropyrazin-2-ylamino)-acetic acid {A3 (3)}

TLC (EA), R_f = 0.08; light brown powder, 0.741g; yield = 82.6%.

$^1\text{H-NMR}$ 300 MHz (DMSO- d_6 , δ ppm): 8.17(d, 1H pyrazine), 7.85(d, 1H pyrazine), 7.76(t, 1H amine), 4.16(d, 2H $\text{CH}_2\text{-NH}$).

2.1.3.4. (3-Chloropyrazin-2-ylamino)-acetic acid methyl ester {A4 (4)}

TLC (EA), $R_f = 0.12$; pale yellow powder, 0.843 g; yield = 87.4%.

$^1\text{H-NMR}$ 300 MHz (DMSO- d_6 , δ ppm): 8.23(d, 1H pyrazine), 7.89(d, 1H pyrazine), 7.76(t, 1H amine), 4.20(d, 2H $\text{CH}_2\text{-NH}$), 3.58(s, 3H CH_3).

2.1.3.5. Butyl-(3-chloropyrazin-2-yl)-amine {A5 (5)}

TLC (EA: CHCl_3 (50:50; v/v)), $R_f = 0.55$; light orange oil, 0.685 g; yield = 77.2%.

$^1\text{HNMR}$ 300 MHz (DMSO- d_6 , δ ppm): 7.96 (d, 1H pyrazine), 7.48 (d, 1H pyrazine), 7.00 (s, 1H amine), 3.30 (m, 2 H), 1.49 (m, 2H), 1.29 (m, 2H), 0.85 (tt, 3H CH_3)

2.1.3.6. 2-(3'-Chloro-2,3,5,6-tetrahydro-[1,2']bipyrazinyl-4-yl)-ethanol {A6 (6)}

TLC (EA), $R_f = 0.07$; beige powder, 0.959g; yield = 82.4 %.

$^1\text{H-NMR}$ 300 MHz (DMSO- d_6 , δ ppm): 8.25(s, 1H pyrazine), 7.97(d, 1H pyrazine), 4.46(t, 1H hydroxyl), 3.51(m, 2H), 3.36(d, 4H piperazine), 2.55(m, 4H piperazine), 2.43(t, 2H)

2.1.3.7. 3'-Chloro-4-(5-trifluoromethylpyridin-2-yl)-3,4,5,6-tetrahydro-2H[1,2']bipyrazinyl {A7 (7)}

TLC (EA: CHCl_3 (50:50; v/v)), $R_f = 0.84$; white yellowish crystals, 1.417g; yield = 86.1 %.

$^1\text{H-NMR}$ 300 MHz (DMSO- d_6 , δ ppm): 8.43(s, 1H CH-pyridine), 8.28(d, 1H pyrazine), 8.02(d, 1H pyrazine), 7.82(dd, 1H), 7.00(d, 1H), 3.78(dd, 4H piperazine), 3.48(dd, 4H piperazine).

$^{13}\text{C-NMR}$ (DMSO- d_6 , δ ppm): 162.49(C), 156.58(C), 144.7 (CH), 139.24 (C), 139 (CH), 137.71 (CH), 131.53 (CH), 123.79 (C), 123.31 (C), 107.87 (CH), 48.91 (CH_2), 44.28 (CH_2).

FT-IR (KBr) (cm^{-1}): 2863.2 Ar-H (C-H stretch), 1617.62 & 1569 aromatic (C=C) and (C=N) stretching, 1498.45 (C-H) bending, 844.3 & 787.96 Ar-H ($\text{CH}_2=\text{CH}_2$ bending), 808.15 (C-Cl) stretch, 706.78 (C-F) stretch.

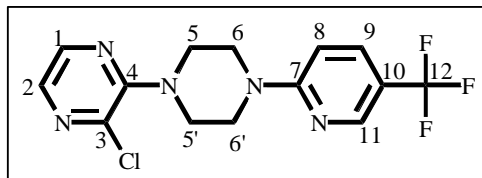


Figure 2.1: Chemical structure of {A7 (7)}

Table 2.1: NMR data for compound {A7 (7)}

Position	¹ H-NMR	¹³ C-NMR
1	8.29(d,1H)	137.71 (CH)
2	8.02(d,1H)	139 (CH)
3	-	139.24 (C)
4	-	156.58 (C)
5,5'	3.79(m,4H)	48.91 (CH ₂)
6,6'	3.48(m,4H)	44.28 (CH ₂)
7	-	162.49 (C)
8	7.00(d,1H)	107.87 (CH)
9	7.83(dd,1H)	131.53 (CH)
10	-	123.79 (C)
11	8.43(d,1H)	144.7 (CH)
12	-	123.31 (C)

Table 2.2: FTIR data for compound {A7 (7)}

Type of bond	Wave number (cm ⁻¹)
Ar-H (C-H stretch)	2863.2
aromatic (C=C) stretching	1617.62
aromatic (C=N) stretching	1569
(C-H) bending	1498.45
Ar-H (CH ₂ =CH ₂ bending)	844.3& 787.96
(C-Cl) stretch	808.15
(C-F) stretch	706.78

2.1.3.8. 3'-Chloro-4-(3-trifluoromethylpyridin-2-yl)-3,4,5,6-tetrahydro-2H-[1, 2'] bipyrazinyl {A8 (8)}

TLC (EA: CHCl₃ (50:50; v/v)), R_f = 0.80; light orange crystals, 1.284g; yield = 78 %.

¹H-NMR300 MHz (DMSO-d₆, δ ppm): 8.54(d, 1H CH-pyridine), 8.28(s, 1H pyrazine), 8.08(d, 1H), 8.01(s, 1H pyrazine), 7.22(m, 1H), 3.49(d, 4H piperazine), 3.33(s, 4H piperazine).

2.1.3.9. 3'-Chloro-4-pyrimidin-2-yl-3,4,5,6-tetrahydro-2H-[1,2']bipyrazinyl {A9 (9)}

TLC (EA), R_f = 0.08; yellow powder, 1.135g; yield = 85.7 %.

¹H-NMR300 MHz (DMSO-d₆, δ ppm): 8.38(d, 2H pyrimidine), 8.33(d, 1H pyrazine), 8.01(s, 1H pyrazine), 6.65(t, 1H), 3.88(s, 4H piperazine), 3.43(s, 4H piperazine).

2.1.3.10. 3'-Chloro-4-pyridin-4-yl-3,4,5,6-tetrahydro-2H-[1,2']bipyrazinyl {A10 (10)}

TLC (EA: CHCl₃ (50:50; v/v)), R_f = 0.71; off-white crystals, 1.074g; yield = 81.4 %.

¹H-NMR300 MHz (DMSO-d₆, δ ppm): 8.34(d, 1H pyrazine), 8.15(d, 2H pyridine), 8.00(d, 1H pyrazine), 6.97(m, 2H), 4.14(m, 4H piperazine), 2.89(m, 4H piperazine).

2.1.3.11. 1'-(3-Chloropyrazin-2-yl)-[1,4']bipiperidinyl {A11 (11)}

TLC (EA), R_f = 0.17; off white crystals, 1.145g; yield = 85.2 %.

¹H-NMR300 MHz (DMSO-d₆, δ ppm): 8.22(d, 1H pyrazine), 7.94(d, 1H pyrazine), 3.90(d, 2H), 3.34(s, 2H), 2.80(t, 2H), 1.80(d, 3H), 1.46(m, 10H)

2.1.3.12. Synthesis of 7-(3-chloropyrazin-2-yl)-7H-purin-6-amine {A12 (12)}

To a solution of 2,3-dichloropyrazine (0.5ml, 4.803 mmol) in dioxane (15 ml), (0.730g, 5.283 mmol) potassium carbonate (K₂CO₃) was added. Afterwards, adenine (0.648g, 4.803 mmol) previously dissolved in DMF (3ml) and water (1ml) was gradually added to the mixture. The reaction was heated under reflux for approximately 16 hour. Reaction completion was confirmed using TLC (ethyl acetate: CHCl₃; (50:50 v/v)). Upon reaction completion volatiles were evaporated under reduced pressure and the residue was extracted against ethyl acetate (3 x 30 ml). The combined organic extracts were dried over anhydrous sodium sulfate and concentrated. For further purification the residue was recrystallized using isopropanol and filtered out leaving the desired product.

TLC (EA: CHCl₃ (50:50; v/v)), R_f = 0.25; yellow powder, 0.978g; yield = 82.48 %.

¹H-NMR300 MHz (DMSO-d₆, δ ppm): 8.76 (m, 2H imidazole and pyrazine), 8.12 (d, 1 H pyrazine), 7.54 (s, 1H), 6.75 (s, 2H amine)

2.1.4. Synthesis of (2-amino-3-chloropyrazine) derivatives under acidic condition

To a solution of 2,3-dichloropyrazine (0.5ml, 4.803 mmol) in dioxane or tetrahydrofuran (20 ml), HCl 12.1M (9.606 mmol) and the corresponding aromatic amine (9.606 mmol) were added respectively. While being stirred, few drops of distilled water were added into the round bottom flask to aid salt solvation. The mixture was heated to reflux for 2-8 hours. Reaction completion was monitored by TLC (ethyl acetate: CHCl₃; (50:50 v/v)). Upon reaction completion, if a precipitate formed the mixture was concentrated and carefully filtered out using suction filtration. If no or little precipitate was formed the volatile components of the mixture were evaporated to dryness under vacuum, and the residue was extracted against ethyl acetate (3 x 30 ml). pH adjustment was made to liberate the compound from its salt form; the organic layer was then pooled, dried using sodium sulfate, and evaporated to afford the desired 2-amino-3-chloropyrazine in 84-93% yield.

2.1.4.1. N-(3-Chloropyrazin-2-yl)-benzene-1,4-diamine {A13 (13)}

TLC (EA: CHCl₃ (50:50; v/v)), R_f=0.14; brown powder, 0.986g; yield = 93.4%.

¹H-NMR300 MHz (DMSO-d₆, δ ppm): 7.97(d, 1H pyrazine), 7.44(s, 1H amine), 7.33(d, 1H pyrazine), 6.81(m, 2H benzene), 6.22(m, 2H benzene), 4.69(s, 1H amine).

2.1.4.2. (3-Chloropyrazin-2-yl)-pyridin-2-yl-amine {A14 (14)}

TLC (EA: CHCl₃ (50:50; v/v)), R_f = 0.4; green oil, 0.830g; yield = 84%.

¹H-NMR300 MHz (DMSO-d₆, δ ppm): 8.27 (d, 2H pyrazine and pyrimidine), 7.89 (dd, 2H pyrazine and pyrimidine), 7.04 (d, 1H), 6.80 (t, 1H), 3.48 (s, 1H amine).

2.1.4.3. 4-(3-Chloropyrazin-2-ylamino)-benzoic acid {A15 (15)}

TLC (EA: CHCl₃ (50:50; v/v)), R_f = 0.07; yellow-orange powder, 1.03g; yield = 86.9%.

¹H-NMR300 MHz (DMSO-d₆, δ ppm): 8.39(d, 1H), 8.04(m, 3H), 7.73(d, 2H), 4 (s, 1H amine).

2.1.4.4. 4-(3-Chloropyrazin-2-ylamino)-phenol {A16 (16)}

TLC (EA: CHCl₃ (50:50; v/v)), R_f = 0.26; yellowish green powder, 0.934g; yield = 88.1%.

¹H-NMR300 MHz (DMSO-d₆, δ ppm): 7.34(d, 2H), 6.81(m, 3H), 6.57(d, 1H), 6.22(s, 1H hydroxyl), 3.99 (s, 1H amine).

2.1.5. Synthesis of mono-alkoxy substituted pyrazine derivatives

To a stirred solution of potassium carbonate (0.796 g, 5.763 mmol) in dioxane (10 ml), the corresponding alcohol acetaminophen (4.803mmol) was added and the mixture was stirred at ambient temperature for 30 minutes. 2,3-dichloropyraizne (0.5ml,4.803mmol) was then added and the mixture was heated to reflux for 7 hours. Reaction completion was monitored by TLC with a suitable elution system of (ethyl acetate: CHCl₃; (50:50 v/v)). Upon reaction completion the solution was evaporated to dryness under vacuum and extracted against ethyl acetate and water. The combined organic extracts were pooled, dried over sodium sulfate and concentrated. The residue was chromatographed on a silica gel column with a mixture of hexane and CHCl₃ to afford A17 (17) as white powder with 95% yield.

2.1.5.1. N-[4-(3-Chloropyrazin-2-yloxy)-phenyl]-acetamide {A17 (17)}

TLC (EA: CHCl₃ (50:50; v/v)), R_f = 0.33; white powder, 1.206g; yield = 95.3%.

¹H-NMR300 MHz (DMSO-d₆, δ ppm): 10.02(s, 1H amide), 8.16(m, 2H pyrazine), 7.61(d, 2H), 7.15(d, 2H), 2.03 (s, 3H CH₃).

2.1.6. Synthesis of 2-amino-3-alkoxypyrazine derivatives

YAN-1 (18) and YAN-2 (19): In a 25 ml round bottom flask equipped with a stirring bar, sodium (0.133 g, 5.818 mmol) was dissolved in the desired alcohol (10 ml) and the mixture was stirred at ambient temperature for 30 minutes. Afterwards, 2,3-dichloropyraizne derivative {(A7), 7} (0.5 g, 1.454 mmol) was added. The reaction mixture was heated to reflux for 12 hours under calcium chloride. Reaction completion was monitored by TLC (ethyl acetate: CHCl₃; (50:50 v/v)). Upon reaction completion the solution was evaporated to dryness under vacuum and extracted against ethyl acetate (3 x 30 ml). The organic phase was dried over sodium sulfate and concentrated. Finally the crude was washed with ether and air dried to afford the desired pure product YAN-1 (18) and YAN-2 (19) in high yields.

2.1.6.1. 3'-Ethoxy-4-(5-trifluoromethylpyridin-2-yl)-3,4,5,6-tetrahydro-2H-[1,2']bipyrazinyl {YAN-1 (18)}

TLC (EA: CHCl₃ (50:50; v/v)), R_f = 0.81; white powder, 0.498g; yield = 97%.

¹H-NMR 300 MHz (DMSO-d₆, δ ppm): 8.42(s, 1H), 7.81(dd, 1H), 7.75(d, 1H pyrazine), 7.60(d, 1H pyrazine), 6.99(d, 1H), 4.36(m, 2H O-CH₂), 3.74(dd, 4H piperazine), 3.56(dd, 4H piperazine), 1.36(td, 3H CH₃).

ESI-MS M/Z for C₁₆H₁₈F₃N₅O 354.18 (M+H)⁺

2.1.6.2. 3'-Isopropoxy-4-(5-trifluoromethylpyridin-2-yl)-3,4,5,6-tetrahydro-2H-[1,2']bipyrazinyl {YAN-2 (19)}

TLC (EA: CHCl₃ (50:50; v/v)), R_f = 0.87; yellow powder, 0.529g; yield = 99%.

¹H-NMR 300 MHz (DMSO-d₆, δ ppm): 8.41(s, 1H), 7.80(dd, 1H), 7.72(d, 1H pyrazine), 7.59(m, 1H pyrazine), 6.99(d, 1H), 5.26(m, 1H O-CH), 3.74(dd, 4H piperazine), 3.54(dd, 4H piperazine), 1.33(dd, 6H (CH₃)₂).

YAN-3 (20): To a stirred solution of sodium (0.133 g, 5.818 mmol) in dry THF (10 ml), the desired alcohol phenol (0.136 g, 1.454 mmol) was added. The mixture was stirred at ambient temperature for 30 minutes. After that 2,3-dichloropyraizne derivative {(A7), 7} (0.5 g, 1.454 mmol) was added and the mixture was heated to reflux for 18 hours under calcium chloride. Reaction completion was monitored by TLC (ethyl acetate: CHCl₃; (50:50 v/v)). Upon reaction completion the solution was evaporated to dryness under vacuum and extracted against ethyl acetate and water, the combined organic extracts were pooled, dried over sodium sulfate, and concentrated. The residue was adsorbed onto Silica and purified by column chromatography (ethyl acetate /hexane) to give the desired product YAN-3 (20) in 89% yield.

2.1.6.3. 3'-Phenoxy-4-(5-trifluoromethylpyridin-2-yl)-3,4,5,6-tetrahydro-2H-[1,2']bipyrazinyl {YAN-3 (20)}

TLC (EA: CHCl₃ (50:50; v/v)), R_f = 0.65; colorless oil, 0.511g; yield = 87.6%.

¹H-NMR 300 MHz (DMSO-d₆, δ ppm): 8.32(s, 1H), 8.18(dd, 1H), 7.91(d, 1H), 7.71(d, 1H pyrazine), 7.03(m, 2H phenol), 6.89(m, 1H phenol), 6.63(m, 3H phenol and pyrazine), 3.65(m, 4H), 3.38 (m, 4H).

2.1.7. Synthesis of (2,3-diamino pyrazine) derivatives under acidic conditions

To a solution of A7 (7) (0.5g, 1.454 mmol) in dioxane or tetrahydrofuran (20 ml), excess of HCl 37% (approximately 1ml) and the corresponding aromatic amine (1.6 mmol) were added respectively. While being stirred, few drops of distilled water were added to aid salt solvation. The mixture was heated to reflux for 10-14 hour. Reaction completion was monitored by TLC (ethyl acetate: CHCl₃; (50:50 v/v)). Upon reaction completion, if a precipitate formed the mixture was concentrated and carefully filtered out using suction filtration. If no or little precipitate formed, volatile components of the mixture were evaporated to dryness under vacuum, the residue was extracted against ethyl acetate (3 x 30 ml). pH adjustment was made to liberate the compound from its salt form. Organic extracts were then pooled, dried using sodium sulfate, and re evaporated to afford the desired product in 69-81 % yield.

2.1.7.1. N-[4-(5-Trifluoromethylpyridin-2-yl)-3,4,5,6-tetrahydro-2H-[1,2']bipyrazinyl-3'-yl]-benzene-1,4-diamine {YAN-4 (21)}

TLC (EA: CHCl₃ (50:50; v/v)), R_f=0.53; brown powder, 0.489g; yield = 81.01%.

¹H-NMR300 MHz (DMSO-d₆, δ ppm): 8.73(m, 2H pyridine N-CH and NH), 7.99(d, 1H pyrazine), 7.90(m, 1H pyridine), 7.84(d, 1H pyrazine), 7.67(m, 2H benzene), 6.66(d, 1H pyridine), 6.28(m, 2H benzene), 4.52(s, 2H amine), 4.15(m, 6H piperazine), 3.97(m, 2H piperazine).

2.1.7.2. 4-[4-(5-Trifluoromethylpyridin-2-yl)-3,4,5,6-tetrahydro-2H-[1,2']bipyrazinyl-3'-ylamino]-benzoic acid {YAN-5 (22)}

TLC (EA: CHCl₃ (50:50; v/v)), R_f=0.27; orange powder, 0.467g; yield = 72.3%.

¹H-NMR300 MHz (DMSO-d₆, δ ppm): 8.41(s, 1H pyridine N-CH), 7.87(d, 3H benzene and pyridine), 7.10(m, 4H pyrazine and benzene), 6.75(d, 1H pyridine), 4.14(m, 4Hpiperazine), 3.85(m, 4H piperazine).

2.1.7.3. 4-[4-(5-Trifluoromethylpyridin-2-yl)-3,4,5,6-tetrahydro-2H-[1,2']bipyrazinyl-3'-ylamino]-phenol {YAN-6 (23)}

TLC (EA: CHCl₃ (50:50; v/v)), R_f=0.34; dark brown powder, 0.422g; yield = 69.1%.

¹H-NMR300 MHz (DMSO-d₆, δ ppm): 10.22(s,1H hydroxyl), 8.32(d, 1H pyridine N-CH), 7.95(m, 1H pyridine), 7.13(dd, 2H pyrazine), 6.79(m, 6H), 6.08(s, 1H amine), 4.22 (s, 2H), 3.86(dt, 3H), 3.51(d, 2H).

2.1.7.4. Pyridin-2-yl-[4-(5-trifluoromethylpyridin-2-yl)-3,4,5,6-tetrahydro-2H-[1,2']bipyrazinyl-3'-yl]-amine {YAN-7 (24)}

TLC (EA: CHCl₃ (50:50; v/v)), R_f = 0.62; white powder, 0.435g; yield = 74.5%.

¹H-NMR300 MHz (DMSO-d₆, δ ppm): 8.41(s, 1H pyridine N-CH), 8.19(d, 2H pyridine N-CH amine), 7.90(m, 3H pyrazine), 7.03(m, 1Hpyridine), 6.81(m, 3Hpyridine), 5.40(s, 1H), 4.15(s, 2H piperazine), 3.83(m, 4H piperazine), 3.49(d, 2H piperazine).

2.1.8. Synthesis of symmetrical (2,3-diamino pyrazine) derivatives

2.1.8.1. N, N'-Di-pyridin-2-yl-pyrazine-2,3-diamine {YAN-8 (25)}

To a solution of 2,3-dichloropyrazine (0.5 ml, 4.8 mmol) and 2-aminopyridine (0.99 g, 10 mmol) in dioxane (10 ml), excess HCl 37% (2 ml) was added. While being stirred, few drops of distilled water were added to aid salt solvation, and the reaction mixture was heated to reflux for 18 hour. Upon reaction completion a precipitate formed and the mixture was concentrated and carefully filtered out using suction filtration and washed to give the desired product.

TLC (EA: CHCl₃ (50:50; v/v)), R_f = salt; off-white powder, 1.161g; yield = 91.5%.

¹H-NMR300 MHz (DMSO-d₆, δ ppm): 7.84 (m, 2H pyridine), 7.51 (m, 4H pyrazine and pyridine), 6.66 (d, 2H pyridine), 6.45 (d, 2H pyridine).

2.1.8.2. 2,3-bis(4-(5-trifluoromethyl)pyridine-2-yl)piperazine-1-ylpyrazine {YAN-9 (26)}

To a stirred solution of 1-(5-trifluoromethyl-pyridin-2-yl)-piperazine (3.21 g, 10 mmol) and K₂CO₃ (1.46 g, 10 mmol) in DMSO (5 ml), 2,3-dichloropyrazine (0.5 ml, 4.8 mmol) in DMSO (5 ml) was gradually added. The reaction mixture was refluxed at 100 °C for 10-12h. The completion of the reaction was indicated by TLC (CHCl₃). Upon reaction completion the mixture was evaporated to dryness and the crude product was extracted by ethyl acetate (3 x 30 ml). The organic extracts were collected, dried over sodium sulfate, and concentrated. Finally recrystallization using ethanol was done to give the desired product.

TLC (CHCl₃), R_f = 0.69; brown oil, 2.296g; yield = 88.7%.

¹H-NMR300 MHz (DMSO-d₆, δ ppm): 8.40(d, 2H), 8.07(s, 2H pyrazine), 7.80(d, 2H), 6.99(d, 2H), 3.63(m, 8H piperazine), 3.44(m, 8H piperazine).

2.1.9. Synthesis of YAN-5 (22) analogues via coupling reactions

To a solution of YAN-5 (22) (0.5g, 1.12 mmol) in dioxane (10 ml), *N*-hydroxysuccinimide (NHS) (0.28 g, 2.47 mmol), dicyclohexyl carbodiimide (DCC) (0.5g, 2.47 mmol) and TEA (0.59 g, 6.75 mmol) were added. The mixture was stirred at room temperature for 5 hours followed by the addition of the desired amine (ethanol amine or glycine methyl ester, 2 mmol). Reaction progress was monitored using TLC (ethyl acetate). If needed, the reaction was heated for 2-3 hours to speed up the coupling process. Upon reaction completion the mixture was evaporated to dryness and dissolved in cold ethyl acetate to precipitate the DCU. Suction filtration and washing with cold ethyl acetate were used to remove the precipitate. Finally, the filtrate was evaporated to yield the product YAN-11 (28) in good yield (87%).

In case of YAN-10 (27) further purification was needed, the crude was adsorbed to silica gel column chromatography and eluted using (ethyl acetate /DCM). The compound was retrieved with a yield of 64%.

2.1.9.1. {4-[4-(5-Trifluoromethylpyridin-2-yl)-3,4,5,6-tetrahydro-2H [1,2']bipyrazinyl-3'-ylamino]-benzoylamino}-acetic acid methyl ester {YAN-10 (27)}

TLC (EA), $R_f = 0.3$; pale yellow powder, 1.142g; yield = 87%.

$^1\text{H-NMR}$ 300 MHz (DMSO- d_6 , δ ppm): 8.70(m, 1H N-CH pyridine), 8.01(d, 1H pyrazine), 7.88(m, 2H pyrazine), 7.77(m, 2H benzene), 7.70(m, 2H benzene), 6.66(d, 1H), 4.15(m, 8H amide CH_2 , piperazine), 3.98(m, 2H piperazine), 3.65(s, 3H O- CH_3).

2.1.9.2. N-(2-Hydroxy-ethyl)-4-[4-(5-trifluoromethylpyridin-2-yl)-3,4,5,6-tetrahydro-2H-[1,2']bipyrazinyl-3'-ylamino]-benzamide {YAN-11 (28)}

TLC (EA), $R_f = 0.27$; off white powder, 0.624g; yield = 64%.

$^1\text{H-NMR}$ 300 MHz (DMSO- d_6 , δ ppm): 8.72(d, 1H N-CH pyridine), 8.67(t, 1H NH amide), 8.0(d, 1H pyrazine), 7.88(m, 2H pyrazine), 7.74(m, 2H benzene), 7.70(m, 2H benzene), 6.66(d, 1H), 4.15(m, 6H piperazine), 3.98(m, 2Hpiperazine), 3.55(m, 2H NH- CH_2), 3.38(m, 2H OH- CH_2).

2.1.10. Bromination of pyrazine derivative A1 (1)

To a stirred solution of {(A-1), 1} (1.5g, 8.6mmol) in ACN (8 ml), *N*-bromosuccinimide (NBS) (1.69 g, 9.46 mmol) was gradually added. The reaction mixture was stirred at room temperature

overnight. The completion of the reaction was monitored by TLC with a suitable elution system (ethyl acetate: CHCl_3 ; (50:50 v/v)). Upon reaction completion the precipitate was collected using suction filtration, washed with cold water and dried to provide the desired pure product.

2.1.10.1. 2-(5-Bromo-3-chloropyrazin-2-ylamino)-ethanol {YAN-12 (29)}

TLC (EA: CHCl_3 (50:50; v/v)), $R_f = 0.52$; dark yellow powder, 2.05g; yield = 94.3%.

$^1\text{H-NMR}$ 300 MHz (DMSO- d_6 , δ ppm): 8.16(d, 1H pyrazine position 6), 7.08(s, 1H amine), 4.69(s, 1H hydroxyl), 3.51(m, 2H), 3.39(d, 2H).

2.1.11. Synthesis of 2-amino-5-alkoxy pyrazine derivatives

To a stirred solution of sodium (0.133 g, 5.818 mmol) in the desired alcohol (10 ml), YAN-12 (29) (0.3g, 1.18mmol) was added and the mixture was heated to reflux for 19 h under calcium chloride. Reaction completion was monitored by TLC (ethyl acetate: CH_2Cl_2 ; (50:50 v/v)). Upon reaction completion volatiles were evaporated to dryness under vacuum and the crude was extracted against ethyl acetate and water (3 x 30 ml). The combined organic extracts were pooled, dried over sodium sulfate, and concentrated. Recrystallization using ether was performed to afford YAN-13 (30) and YAN-14 (31) in yields 98.2 % and 96.4%.

2.1.11.1. 2-((3-chloro-5-ethoxypyrazin-2-yl)amino)ethanol {YAN-13 (30)}

TLC (EA: CH_2Cl_2 (50:50; v: v)), $R_f = 0.76$; white powder, 0.253g; yield = 98.2%.

$^1\text{H-NMR}$ 300 MHz (DMSO- d_6 , δ ppm): 7.69(s, 1H pyrazine), 4.75(m, 1H hydroxyl), 4.30(m, 2H O- CH_2), 3.64 (m, 4H CH_2 - CH_2), 1.35(t, 3H CH_3)

2.1.11.2. 2-((3-chloro-5-isopropoxy pyrazin-2-yl)amino)ethanol {YAN-14 (31)}

TLC (EA: CH_2Cl_2 (50:50; v: v)), $R_f = 0.830$; white powder, 0.266g; yield = 96.4%.

$^1\text{H-NMR}$ 300 MHz (DMSO- d_6 , δ ppm): 7.69(s, 1H pyrazine), 4.82(m, 1H O-CH), 4.75(m, 1H hydroxyl), 3.63 (m, 4H CH_2 - CH_2), 1.27(m, 6H (CH_3) $_2$)

**2.1.11.3. N-(3-((6-chloro-5-((2-hydroxyethyl)amino)pyrazin-2-yl)oxy)phenyl)acetamide
{YAN-15 (32)}**

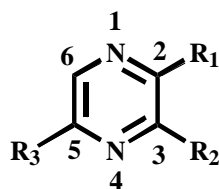
To a stirred solution of potassium carbonate (0.19 g, 1.41 mmol) in dioxane (10 ml), acetaminophen (0.179 g, 1.18mmol) was added and the mixture was stirred at room temperature for 15 minutes. Afterwards, YAN-12 (29) (0.3g, 1.18mmol) was added and the mixture was heated to reflux overnight. Reaction completion was monitored by TLC (ethyl acetate: CHCl₃; (50:50 v/v)). Upon reaction completion volatiles were evaporated to dryness and extracted against ethyl acetate (3 x 30 ml). The combined organic extracts were pooled, dried over sodium sulfate, and concentrated. The residue was purified by column chromatography (ethyl acetate /hexane) to give YAN-15 (32) in good yield.

TLC (EA: CHCl₃ (50:50; v/v)), R_f = 0.22; white powder, 0.339g; yield = 94%.

¹H-NMR 300 MHz (DMSO, δ ppm): 10.05(s, 1H amide), 7.75 (s, 1H pyrazine), 7.62(d, 1H), 7.14 (d, 1H), 3.54 (d, 2H benzene ring), 3.37 (d, 2H benzene ring), 1.99(s, 3H CH₃) .Melting point: 143-145 C.

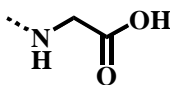
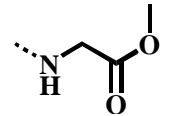
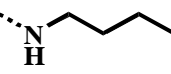
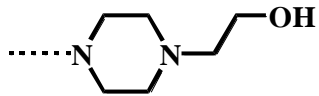
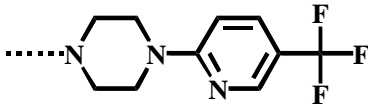
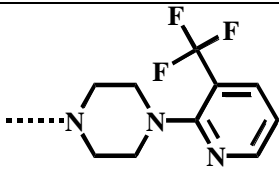
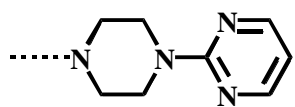
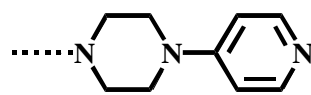
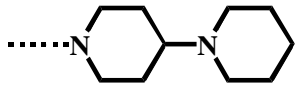
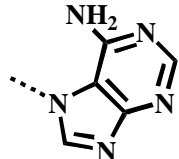
A summary of the mono and disubstituted synthesized compounds is shown in table 2.3 below.

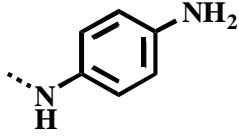
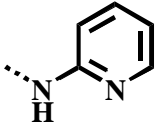
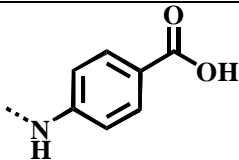
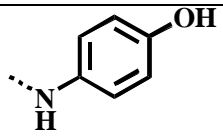
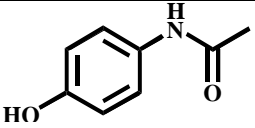
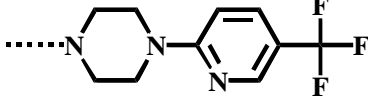
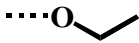
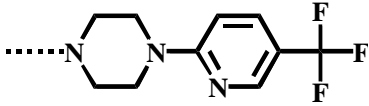
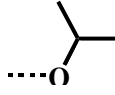
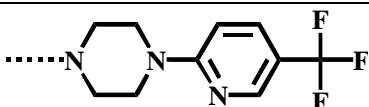
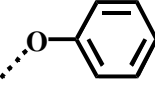
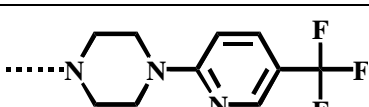
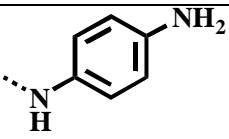
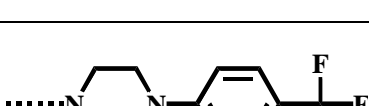
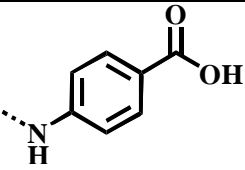
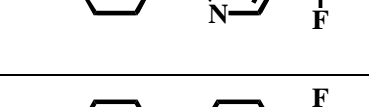
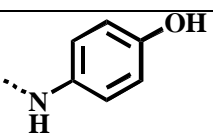
Table 2.3: List of synthesized compounds showing their chemical and structural formalms



General formula

Com #	Com. code	R1	R2	R3	Chemical formula
1	A1*		Cl	H	C ₆ H ₈ ClN ₃ O
2	A2*		Cl	H	C ₇ H ₁₀ ClN ₃ O

3	A3		Cl	H	C ₆ H ₆ ClN ₃ O ₂
4	A4		Cl	H	C ₇ H ₈ ClN ₃ O ₂
5	A5		Cl	H	C ₈ H ₁₂ ClN ₃
6	A6		Cl	H	C ₁₀ H ₁₅ ClN ₄ O
7	A7		Cl	H	C ₁₄ H ₁₃ ClF ₃ N ₅
8	A8		Cl	H	C ₁₄ H ₁₃ ClF ₃ N ₅
9	A9		Cl	H	C ₁₂ H ₁₃ ClN ₆
10	A10		Cl	H	C ₁₃ H ₁₄ ClN ₅
11	A11		Cl	H	C ₁₄ H ₂₁ ClN ₄
12	A12		Cl	H	C ₉ H ₆ ClN ₇

13	A13		Cl	H	C ₁₀ H ₉ ClN ₄
14	A14		Cl	H	C ₉ H ₇ ClN ₄
15	A15		Cl	H	C ₁₁ H ₈ ClN ₃ O ₂
16	A16		Cl	H	C ₁₀ H ₈ ClN ₃ O
17	A17		Cl	H	C ₁₂ H ₁₀ ClN ₃ O ₂
18	YAN-1			H	C ₁₆ H ₁₈ F ₃ N ₅ O
19	YAN-2			H	C ₁₇ H ₂₀ F ₃ N ₅ O
20	YAN-3			H	C ₂₀ H ₁₈ F ₃ N ₅ O
21	YAN-4			H	C ₂₀ H ₂₀ F ₃ N ₇
22	YAN-5			H	C ₂₁ H ₁₉ F ₃ N ₆ O ₂
23	YAN-6			H	C ₂₀ H ₁₉ F ₃ N ₆ O

24	YAN-7			H	$C_{19}H_{18}F_3N_7$
25	YAN-8			H	$C_{14}H_{12}N_6$
26	YAN-9			H	$C_{24}H_{24}F_6N_8$
27	YAN-10			H	$C_{24}H_{24}F_3N_7O_3$
28	YAN-11			H	$C_{23}H_{24}F_3N_7O_2$
29	YAN-12		Cl	Br	$C_6H_7BrClN_3O$
30	YAN-13		Cl		$C_8H_{12}ClN_3O_2$
31	YAN-14		Cl		$C_9H_{14}ClN_3O_2$
32	YAN-15		Cl		$C_{14}H_{15}ClN_4O_3$

A1* CAS number: 84066-20-6

A2* CAS number: 1353960-18-5

2.2. Initial *in vitro* biological activity

Some of the synthesized pure and well characterized compounds were initially assessed for their *in vitro* biological activity at professor's Bjørn Tore Gjertsen lab, department of clinical science. University of Bergen- NORWAY.

Cell line

Acute monocytic leukemia (Molm-13) cell line was utilized in the *in vitro* assessment. They were obtained from a 20 years old acute myeloid leukemia (AML) patient. Part of the cell line had been stably transfected by sh-RNA while the other part was transfected by sh-p53 RNA.

Medium

RPMI1640 medium, originally developed by Moore and his coworkers at Roswell Park Memorial Institute in 1966, was used to cultivate the cell line that was used for testing our compounds. RPMI has successfully been used for the cultivation of normal human and neoplastic leukocytes. It has been widely used in fusion protocols and in the growth of hybrid cells. It was formulated to support lymphoblastoid cells in suspension culture.

In vitro assay

WST-1 assay was used to determine cells viability, the assay is based on the cleavage of tetrazolium salt into a colored soluble formazan dye by a complex cellular mechanism that involves mitochondrial dehydrogenase enzymes. As the bio-reduction process is largely dependent on the glycolytic production of NADPH in viable cells, the amount of formazan dye formed directly correlates to the number of metabolically active cells in the given culture. Cells grown in the culture plate are incubated with the WST-1 reagent for 0.5 - 4 hours. Afterwards, the formazan dye formed is quantitated with a scanning multi-well spectrophotometer (ELISA reader). The measured absorbance directly correlates to the number of viable cells.

2.3. Computational chemistry of the synthesized compounds

2.3.1. Computer-aided prediction of biological activity spectra of the synthesized compounds

Biological activity is defined as the inherent capacity of a substance to alter any chemical or physiological functions of a biological entity. A biologically active compound may exert its action via various mechanisms; the specificity of action is always relative and is defined by a number of peculiarities including but not limited to object, dose, and route. On the other hand, the biological potential of compound includes all activities, which can be discovered under some specific experimental conditions, and it is called the biological activity spectrum. The spectrum of compound can be predicted on the basis of structure-activity relationships found by the analysis of the known data from the training set.^[90] PASS (Prediction of Activity Spectra for Substances) is one such program that predicts the possibility of a drug to be active against a target based on the physico-chemical methods using various algorithms and comparisons^[91].

This Computer program was the product of ideas originated more than 25 years ago within the framework of the National Registration System of New Chemical Compounds organized in the USSR in 1972^[92]. First the idea was introduced by V.Avidon who suggested that many kinds of biological activity could be predicted on the basis of structural formula of chemical compound^[93]. Meanwhile, Similar approach was under development by V.Golender and A.Rozenblit^[94].

PASS concurrently predicts several hundreds of biological activities (pharmacological main and side effects, mechanisms of action, mutagenicity, carcinogenicity, teratogenicity and embryotoxicity). The biological activity spectrum of a compound shows all compound's actions despite the difference in essential conditions of its experimental determination process. If the difference in (species, sex, age, dose, route, etc) is ignored, the biological activity can be only qualitatively identified. As a result, "the biological activity spectrum" is defined as the "intrinsic" property of a compound depending only on its structure and physico-chemical characteristics. Prediction of this spectrum by PASS is based on SAR analysis of the training set containing more than 35,000 compounds which have more than 500 kinds of biological activity^[95]. Thus, PASS once trained is able to predict simultaneously all biological activities which are included in the training set (library). To provide the best quality of prediction new information about

biologically active compounds is collected permanently from papers and electronic sources, evaluated and then regularly added to the training set^[95].

PASS uses CSV, SD or MOL-files as input, data Analysis using this program is based on a number of chemical descriptors that are called multilevel neighborhoods of atoms (MNA), the descriptors are automatically generated on the basis of MOL-file of the assisted molecule. The list of MNA descriptors currently consists of more than 35700 different items. Frequently, new descriptors are added to this list in order to refresh it. Those descriptors are effectively applied in SAR, QSAR and similarity analysis. Finally the output results of prediction can be obtained as TXT or SD-files. Since the prediction of biological activity spectra for 1,000 compounds in usual PC takes about 1 minute, PASS can be effectively applied to predict biological potential of separate compounds and to analyze large chemical databases.

PASS algorithm was selected by theoretical and empirical comparison of many different mathematical methods to provide high accuracy of prediction and robustness of calculated estimated data. The mean accuracy of biological activity prediction with PASS is 70±80% both in prediction for independent test and leave-one-out cross validation. However, the reliability of predictions relates to the researcher's purpose. The ultimate decision on how many and which structures should be selected for testing depends on the estimated probabilities for a compound to be active (Pa) and inactive (Pi), experimental facilities and the researcher's aspiration concerning the extent of innovation in the result sets of about 5000 compounds diverse in both structure and activity^[96, 97].

Biological Activity Spectra Prediction

Biological activity of the synthesized compounds was assisted using PASS. The structure of the compounds was first drawn using ISIS draw version 2.4. Then all the calculations were performed using PASS 2012 demo version. Description of current version of computer system PASS and feasibility for its free testing are available via Internet on:

<http://www.genexplain.com/pass>

2.3.2. Lipinski's rule of five: computational approach to predict drug-likeness of the synthesized compounds

Several computational approaches were used to estimate solubility and permeability of chemical structures in discovery and development stages. Lipinski's rule of five or simply the Rule of five (RO5) evaluate drug likeness or determine if the chemical entity has properties that would make it a likely orally active compound, in addition it describes the required molecular features that are considered important for a drug's pharmacokinetics "ADME" (absorption, distribution, metabolism, excretion) in vivo. Christopher A. Lipinski lunched this rule in 1997, based on the observation that most orally administered drugs are relatively small and moderately lipophilic in nature.

The rule of 5' states that good absorption or permeation is more likely when there are less than 5 H-bond donors, 10 H-bond acceptors, the molecular weight (MWT) is smaller than 500 Dalton's and the calculated octanol-water partition coefficient (Log P) is not greater than 5. Afterward, and In an attempt to improve the predictions of drug-likeness, the rules have spawned many extensions, indicating that the chemical entity should meet the following criteria : Partition coefficient (log P) in -0.4 to +5.6 range, Molar refractivity ranges from 40 to 130, Molecular weight between 180 to 500, total Number of atoms from 20 to 70, and Polar surface area not greater than 140 Å².

Drug-likeness of the synthesized compounds was assisted using Chemicalize, A public web resource which gives structure-based predictions. The structure and IUPAC name of the compounds was generated using ChemDraw ultra. Then all the calculations were performed using Chemicalize. Description of the public resource of Chemicalize and feasibility for its free testing are available via Internet on: <http://cds.rsc.org/chemicalize.asp>.

2.3.3. Docking of the synthesized compounds using SwissDock, a protein-small molecule docking web service based on EADock DSS.

Currently, it is well known that most of the vitality processes in life involve complex interactions between two molecules at least. Moreover, the prediction of binding modes occurring between a small molecule and a target protein of biological interest is crucial for drug development and can be performed by the aid of so-called docking software.

In our study, docking calculations were conducted with SwissDock, a protein small molecule docking web service based on EADock DSS. SwissDock algorithm consists of many steps; first the structure of the target protein, as well as that of the ligand must be specified. In our study the crystal structure of human cyclin-dependent kinase was obtained from the PDB with the accession code 1HCL. Ligand 3D structure was obtained by the conversion of ChemDraw (Cdxml) file for each compound into (MOL2) file using Open Babel GUI software version 2.4.1.

Once the target and ligand have been designed the prediction parameters were selected and the docking assay was submitted. All calculations were performed on the server side and the output results were sent to user by email. Many binding modes were generated in the vicinity of all target cavities (blind docking), their CHARMM energies were estimated, the binding modes with the most favorable energies were evaluated and clustered, and the most favorable clusters can be visualized online and downloaded on a personal computer.

Finally the interpretation of docking results was greatly facilitated by the visualization of docking predictions in the UCSF Chimera1.11.2 molecular viewer, which can be launched directly from the web browser.

Chapter three

Results and discussion

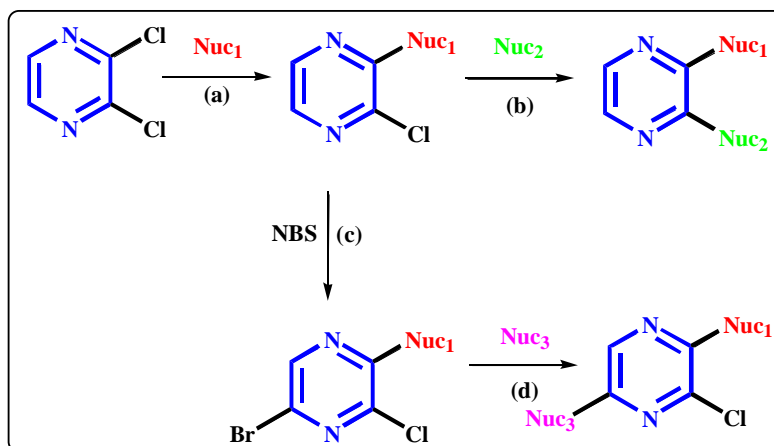
3. Results and discussion

3.1. Chemical synthesis of compounds

Pyrazine, one of the naturally occurring diazines is an aromatic heterocyclic ring with two nitrogen atoms located in the 1 and 4 positions of the heterocycle. Pyrazine bear multiple functionalities that may be transformed into diverse derivatives using a sequence of chemical reactions. Pyrazine is considered less reactive compared to other related diazines, this is mainly due to the symmetrical *Para* position of the electron-attracting nitrogen atoms which makes pyrazine a weaker base ($pK_b = 13.49$) than its isomeric analogous pyrimidine ($pK_b = 12.77$), or pyridazine ($pK_b = 10.76$) and hence decreases its reactivity.

Since pyrazine is considered a 6π -electron-deficient aromatic system -Nitrogen in pyrazine withdraws electrons from the ring rather than donates to it - it could undergo sequential aromatic substitution reaction (S_NAr). In S_NAr a nucleophile attacks an electron deficient aromatic ring with a good leaving group. A resonance stabilized carboanion is formed, and the leaving group departs as the aromatic ring π system is reestablished. Taking a deep look at pyrazine scaffold it can be seen that the electron deficiencies are at 2, 3, 5 and 6 positions of the ring. Therefore, nucleophilic reagents could attack these positions. Still yet, halogenated forms of pyrazine at the previously mentioned positions are needed to make the substitution easier. The presence of “halogen” another electron withdrawing group that normally deactivates the ring in electrophilic aromatic substitutions makes pyrazine more electrons deficient and a good candidate for S_NAr . Different commercially available chloro and poly-chloropyrazines where used to create a wide panel of pyrazine based derivatives. Even so, few studies were concerned in developing 2,3-disubstituted pyrazine derivatives so it was the subject of our research.

In the current study commercially available 2,3-dichloropyrazine was used as the core scaffold, and the derivatives were synthesized by sequential aromatic substitution reaction (S_NAr) under different conditions depending on the nucleophile itself and the order of substitution. The overall Strategy for synthesis of the desired disubstitued pyrazine derivatives is depicted in **Scheme 3.1**.



Scheme 3.1: Sequential substitution of 2,3-dichloropyrazine by various nucleophiles. Typical method for preparation of monosubstituted and disubstituted pyrazines. Nuc: nucleophile, NBS: N-bromosuccinimide used for C-H activation.

As indicated in **scheme 3.1** different groups of compounds have been synthesized in the course of the current study. The final products classified as 2,3-disubstituted pyrazines were synthesized in a way to mimic CDK inhibitors mainly pyrollopyrazine. All the functional groups were selected to accommodate the CDK binding site.

3.1.1.1. Synthesis of mono-amino substituted pyrazines (1-16)

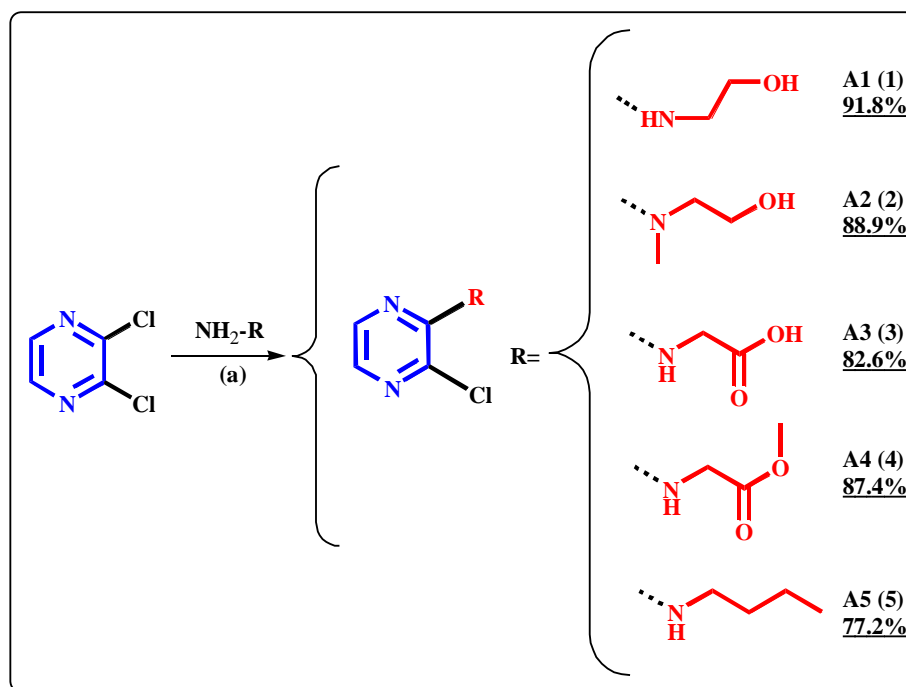
First we aimed at exploring the possibility of introducing different nucleophilic moieties (aliphatic and aromatic amines) as first substituent on the pyrazine core. The reactions were done using reported procedures according to the type of nucleophile used.

3.1.1.1.1. Synthesis of 2-amino-3-chloropyrazine derivatives under basic conditions (1-12)

The planned compounds were prepared starting from commercially available 2,3-dichloropyrazine which was reacted with the corresponding aliphatic amine under basic conditions using TEA or DIPEA as base and dioxane or tetrahydrofuran as solvent. The reaction proceeds via aromatic nucleophilic substitution $S_{N}Ar$. The amine attacks the electron deficient pyrazine aromatic ring. A resonance stabilized carboanion is formed. Resonance delocalizes the negative charge over the entire ring causing the “chlorine” leaving group to leave the ring. The nucleophilic displacement of chlorine by aliphatic amines proceeded under elevated temperatures. After reaction completion, volatiles were evaporated under vacuum. The residue was extracted against ethyl acetate and water and the organic layer was then pooled, dried using

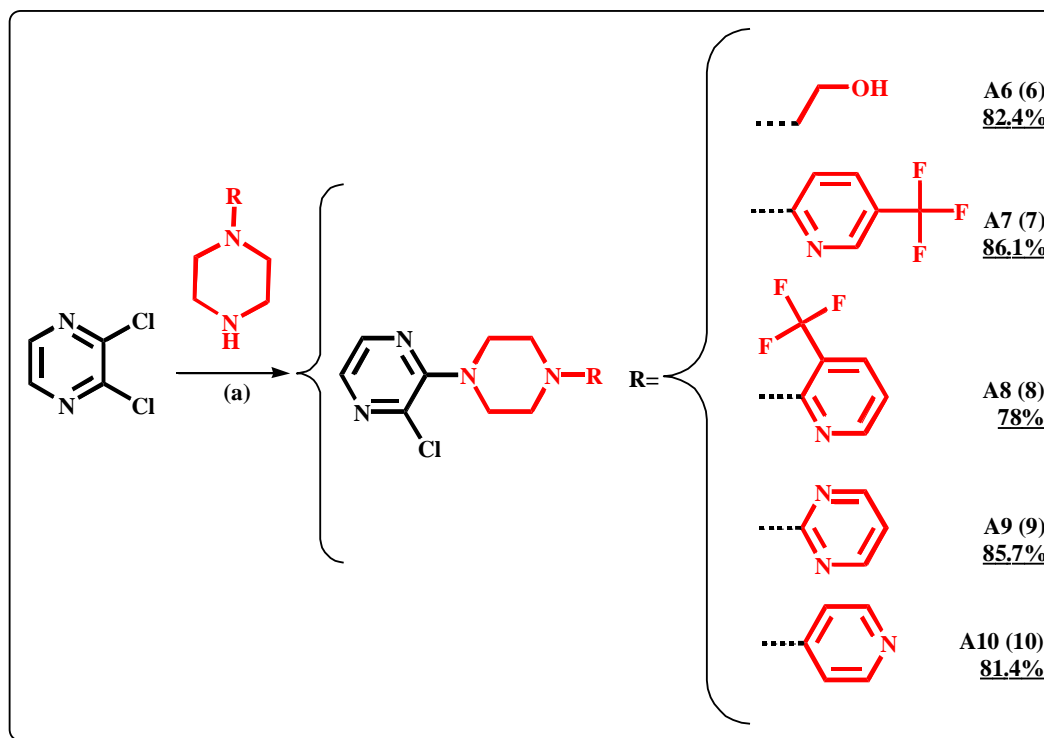
sodium sulfate and condensed. If needed the crude product was purified using recrystallization or silica gel column chromatography using (CHCl₃: hexane) as eluent to give the 2-amino-3-chloropyrazine derivatives in good yields ranging from 77-91%.

Different aliphatic acyclic amines were used to displace the chlorine group on position 2 of the pyrazine core including ethanol amine, 2-methylethanolamine, glycine, glycine methyl ester, and n-butylamine as shown in scheme 3.2.



Scheme 3.2: Representative procedure for the synthesis of (2-amino-3-chloropyrazine) derivatives using acyclic amines under basic conditions. (a) Dioxane or THF, TEA or DIPEA, stirring at reflux, R= aliphatic linear amine.

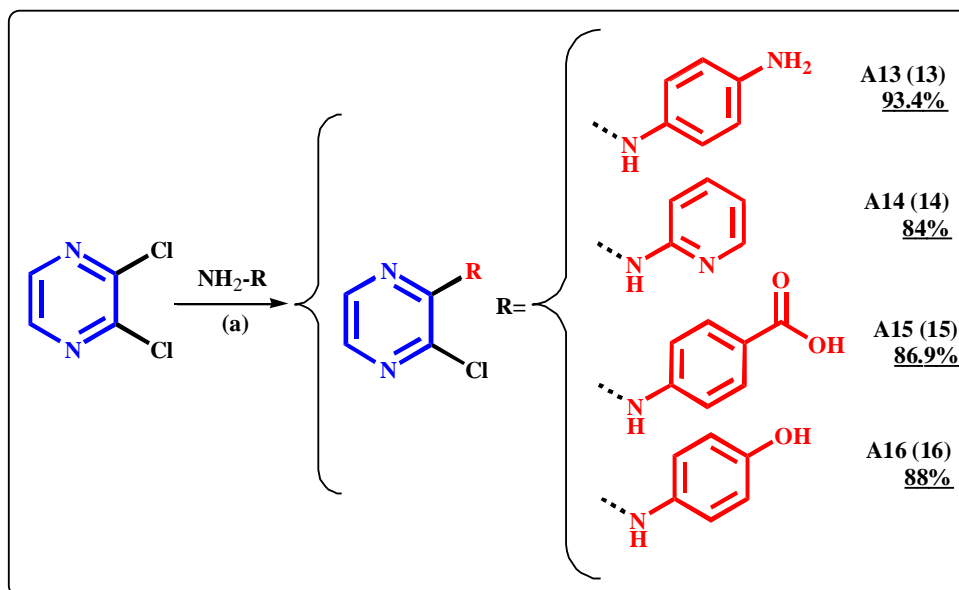
Furthermore, wide range of pyridine heterocyclic amines were introduced to the pyrazine core including piperazine and pyridine derivatives such as 2-piperazin-1-yl-ethanol, 1-(5-trifluoromethylpyridin-2-yl)-piperazine, 1-(3-trifluoromethylpyridin-2-yl)-piperazine, 1-pyridin-4-yl-piperazine, 2-piperazin-1-yl-pyrimidine, [1,4'] bipiperidinyl-piperazine as shown in scheme 3.3. Pyridine containing derivatives are considered among the important aliphatic heterocyclic moieties, they are found in various compound classes exhibiting wide range of pharmacological activities that's mainly the reason why they were chosen.



Scheme 3.3: Representative procedure for the synthesis of (2-amino-3-chloropyrazine) derivatives using cyclic amines under basic conditions. (a) Dioxane or THF, TEA or DIPEA, stirring at reflux, R= aliphatic cyclic amines.

3.1.1.2. Synthesis of 2-amino-3-chloropyrazine derivatives under acidic conditions

The compounds were prepared starting from commercially available 2,3-dichloropyrazine which was reacted with the corresponding aromatic amine under acidic conditions using HCl (37%) and dioxane or tetrahydrofuran as solvent as shown in scheme 3.4. It is unclear which mechanistic pathway this reaction proceeds through. However, the presence of HCl makes it difficult to consider a nucleophilic aromatic substitution mechanism. Indicatively, amines are basic so they tend to neutralize the added acid forming a salt product; few drops of distilled water were added to aid salt solvation. This whole process may increase the solubility of the amine thereby increase the rate of the reaction. The mixture was heated to reflux for 2-8 hours which is a short time in comparison to basic conditions. Upon reaction completion - in most cases- a precipitate was formed and carefully filtered out using suction filtration. However, if no or little precipitate formed the volatiles were evaporated under vacuum, the residue was extracted against ethyl acetate and water, pH adjustment was made to liberate the compound from its salt form, the organic layer was then pooled, dried using sodium sulfate and re evaporated to afford the desired 2-amino-3-chloropyrazine derivative in 84-93 % yield.

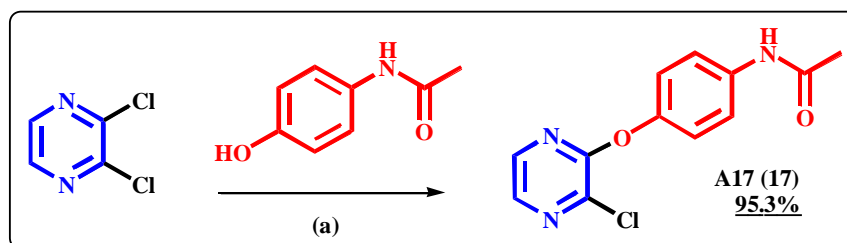


Scheme 3.4: Representative procedure for the synthesis of (2-amino,3-chloropyrazine) derivatives using aromatic amines under acidic conditions. (a) Dioxane or THF, HCl, stirring at reflux, R= aromatic amines.

From our experimental trials we noticed that aromatic amines tend to slowly react with 2,3-dichloropyrazine under basic conditions, so new alternative approach was needed to speed up the reaction. Surprisingly, the use of acidic conditions along with aromatic amines increased the rate and the yields of the reactions in comparison with basic conditions using the same amount of reactants.

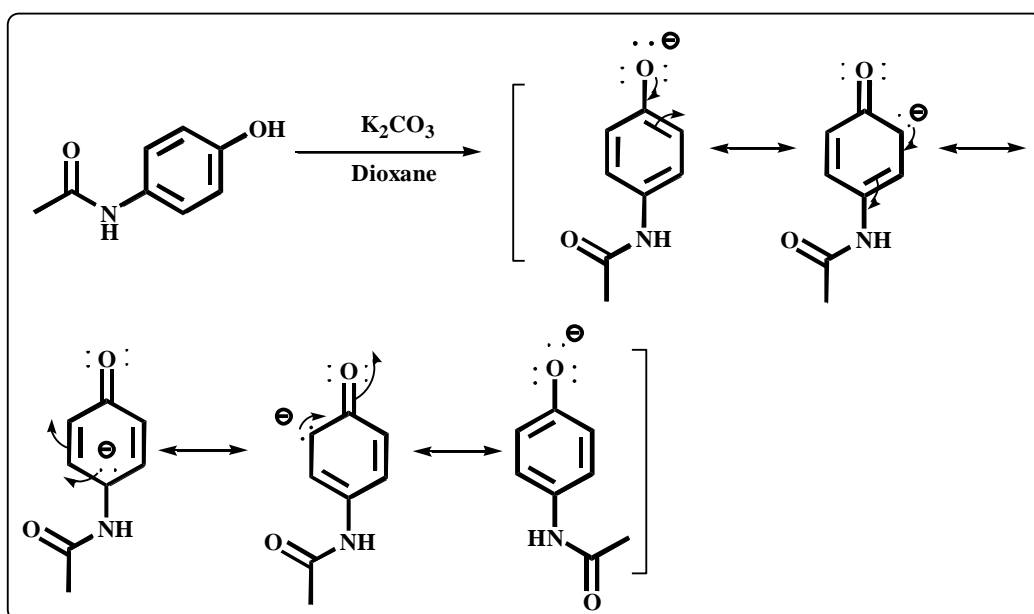
3.1.2. Synthesis of mono-alkoxy substituted pyrazine derivatives (17)

2,3-Dichloropyrazine was reacted with acetaminophen in dioxane under basic condition using K_2CO_3 as shown in scheme 3.5. The mixture was heated to reflux for 7 h, the completion of the reaction was monitored by TLC with a suitable elution system of (ethyl acetate: $CHCl_3$; (50:50 v/v)). Upon reaction completion the solution was evaporated under vacuum and extracted against ethyl acetate and water, the combined organic extracts were pooled, dried over sodium sulfate and concentrated to afford **A17 (17)** as white powder with 95% yield.



Scheme 3.5: Synthesis of (2-alkoxy-3-chloropyrazine) derivative **A17 (17)**. (a) Dioxane, K_2CO_3 , reflux.

Acetaminophen itself is not a good nucleophile; therefore, a base must be added to deprotonate acetaminophen creating a stronger nucleophile (Scheme 3.6). Phenolic hydroxyl group shows a pKa range of 16.47-15.28 (in DMSO) while N-acetyl-amino group shows a pKa of approximately 25 (in DMSO), this information indicates that phenol is more acidic than N-acetyl-amino group hence it can be deprotonated using mild bases like K_2CO_3 . The conjugate base of phenol is resonance stabilized in a way that allows this type of acid-base reaction to occur, and the negatively charged phenoxide anion become a strong nucleophile and attacks 2,3-dichloropyrazine on carbon 2.



Scheme 3.6: Deprotonation and resonance stabilization of the phenolic hydroxyl group in acetaminophen using potassium carbonate.

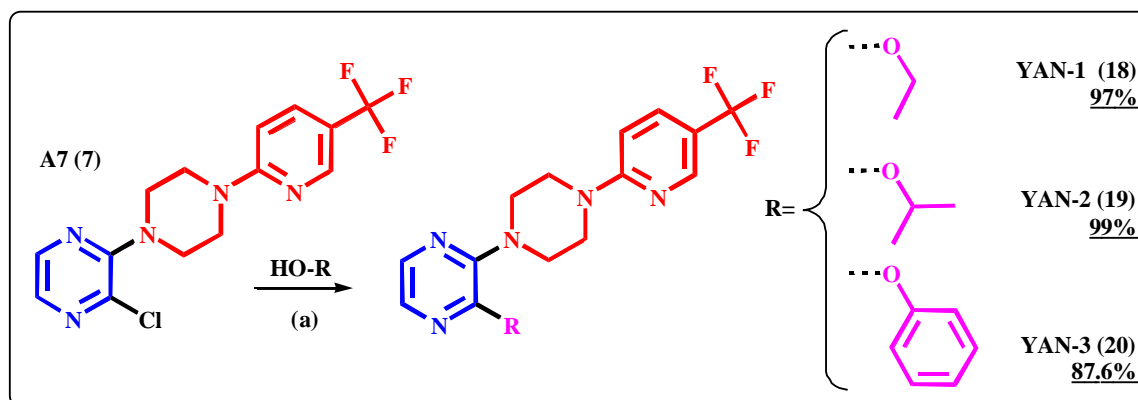
3.1.3. Synthesis of 2-amino-3-alkoxy pyrazine derivatives (18-20)

To prepare the planned derivatives, the intermediate A7 (7) was reacted with the desired protonated aliphatic or aromatic alcohol as shown in scheme 3.7. Since aliphatic alcohols have higher pKa values than phenols they require stronger bases to deprotonate them. Hence, Sodium metal a stronger base than K_2CO_3 was used for these reactions. Sodium metal converts the alcohol to alkoxide. Hydrogen gas liberated during the reaction that's why it should be done with great caution, under calcium chloride, and using dry glassware.

During the synthesis of YAN-1 (18) or YAN-2 (19) the alcohol itself (ethanol or isopropanol respectively) was used as both solvent and nucleophile, this means that the solvent was the conjugate acid of the alkoxide. Sufficient volume of the alcohol was first stirred with sodium at ambient temperature. A7 (7) was added and the mixture was heated to reflux for 12 hours (for both 18, 19). Upon reaction completion volatiles were evaporated. The residue was extracted using ethyl acetate. Organic fractions were dried using sodium sulfate, concentrated, and washed with ether and air dried to afford YAN-1 (18) and YAN-2 (19) in high yields of 97% and 99%, respectively.

Regarding YAN-3 (20) phenol was added to a previously stirred solution of sodium in dry tetrahydrofuran. The mixture was stirred at ambient temperature for additional 30 minutes. A7 (7) was then added and the mixture was heated to reflux for 18 hours (in total). Upon reaction completion volatiles were evaporated. Further purification using column chromatography (ethyl acetate: dichloromethane) was needed to produce (20) in 87.6% yield.

We noticed that introducing alcohol directly to 2,3-dichloropyrazine was much easier as seen in the preparation of A17 (17), took less time, and needed milder basic condition in comparison with introducing alcohol to 2-amino-3-chloropyrazine derivatives. It is believed that the successive introduction of an electron donating substituent at position 2 decreased the rate of nucleophilic substitution and decreased the tendency of chlorine at position 3 to act as leaving group.

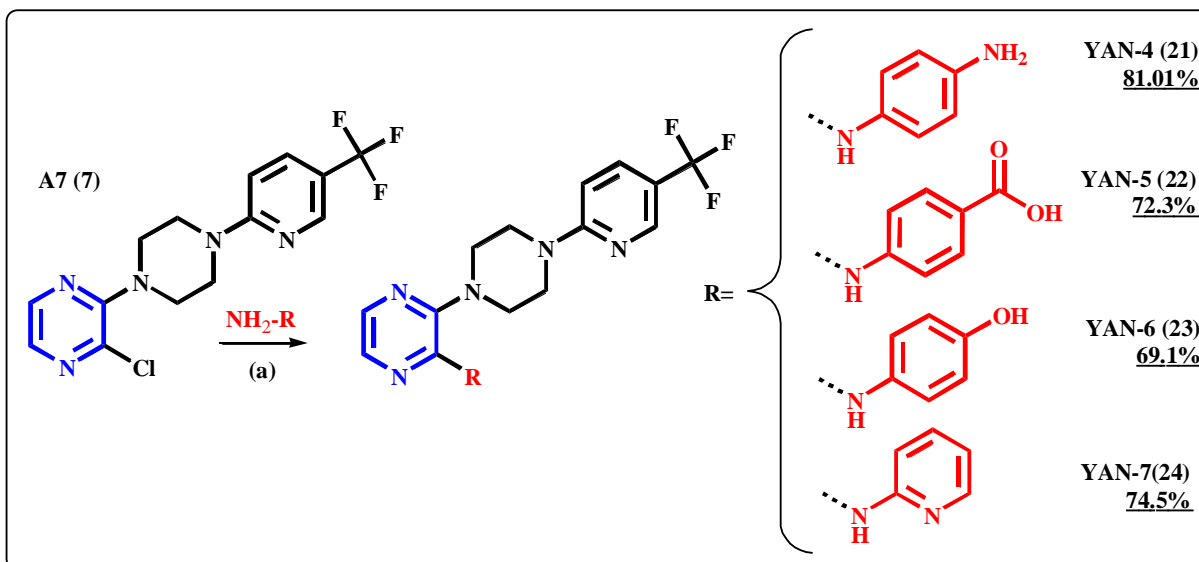


Scheme 3.7: Synthesis of 2-amino-3-alkoxy pyrazine derivatives using A7 (7) and different aliphatic or aromatic alcohols, (a) sodium, reflux 12h under calcium chloride for YAN-1 (18), and YAN-2 (19). (a) Sodium, dry THF, reflux 18h under calcium chloride for YAN-3 (20).

3.1.4. Synthesis of di-amino substituted pyrazines

3.1.4.1. Synthesis of asymmetrical 2,3-diaminopyrazine derivatives (21-24)

To prepare the planned 2,3-diamino pyrazine, A7 (7) was reacted with the corresponding aromatic amine under acidic conditions using HCl (37%) and dioxane or tetrahydrofuran as solvent. It is unclear which mechanistic pathway this reaction proceeds through. However, the presence of HCl makes it difficult to consider a nucleophilic aromatic substitution mechanism. Indicatively, amines tend to neutralize the added acid forming a salt product; few drops of distilled water were added to aid salt solvation. The mixture was heated to reflux for 10-14 hour. Upon reaction completion in case of (21) and (22) a precipitate formed and carefully filtered out using suction filtration. In case of (23) and (24) volatiles were evaporated under vacuum, the residue was extracted against ethyl acetate and water. pH adjustment was made to liberate the compound from its salt form, the organic extracts were pooled, dried using sodium sulfate and re evaporated. In case of (23) further purification using column chromatography was performed.

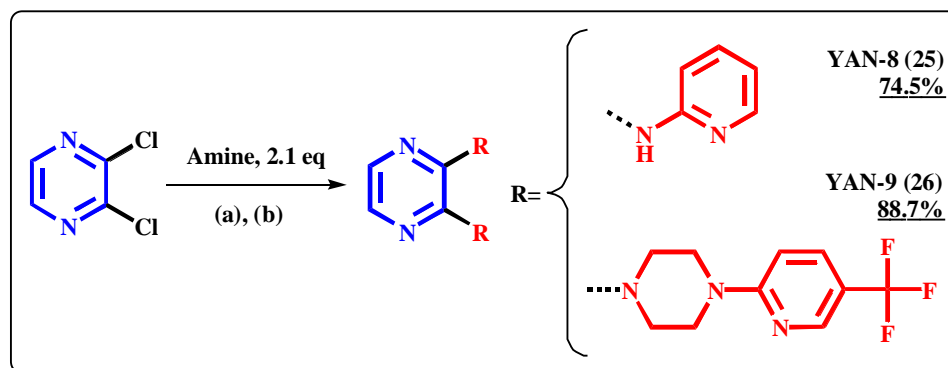


Scheme 3.8: Synthesis of 2,3-diaminopyrazine derivatives using A7 (7) and different aromatic amines, (a) HCl, Dioxane, reflux.

The introduction of the first amine - an electron donating group - at position 2 of pyrazine will exert a resonance donating effect and decrease the rate of nucleophilic substitution therapy inducing a significant deactivation toward the second amination. This deactivation may also rise from the steric bulk introduced by the substituent at position 2 and the decreased tendency of the chlorine atom at position 3 of pyrazine core to act as leaving group. Hence, elevated temperatures, higher concentration of nucleophiles and prolonged reaction time were needed.

3.1.4.2. Synthesis of symmetrical 2,3-diaminopyrazine derivatives (25,26)

YAN-8 (25) was prepared starting from commercially available 2,3-dichloropyrazine which was reacted with 2.1 equivalents of 2-aminopyridine under acidic conditions using 37% HCl and dioxane as shown in scheme 3.9. While being stirred, few drops of distilled water were added to aid salt solvation and the mixture was heated to reflux for 18 hour. After reaction completion a precipitate formed and the mixture was concentrated and carefully filtered out and washed using suction filtration to give the desired product as off white powder with a yield of 74.5%.



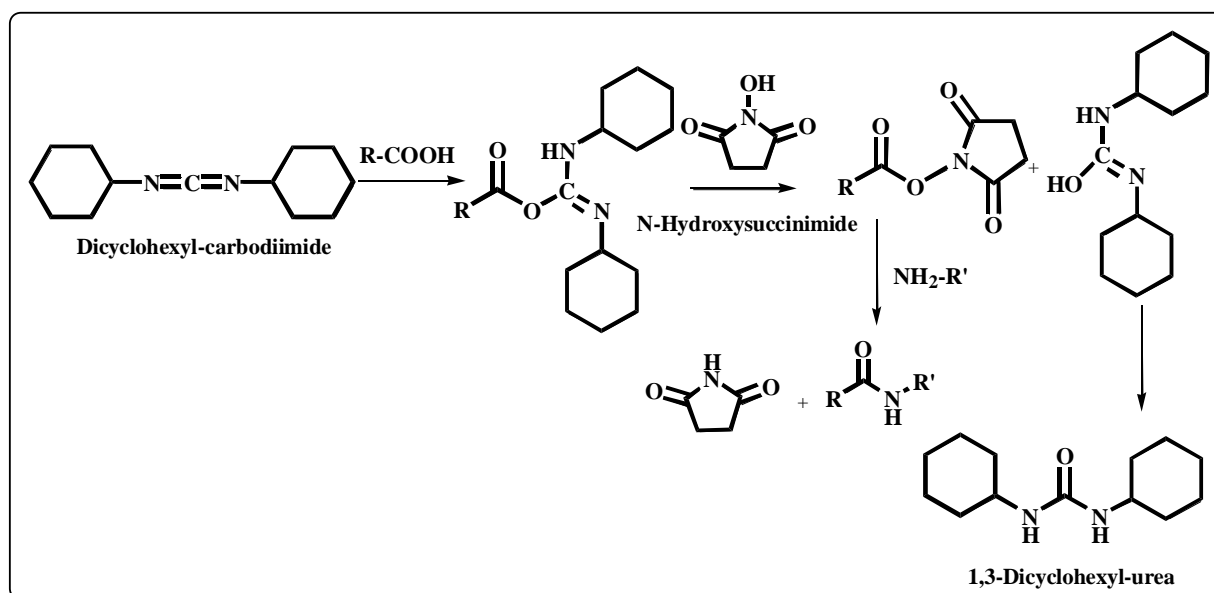
Scheme 3.9: Synthesis of 2,3-diaminopyrazine symmetrical derivatives (YAN-8 (25), YAN-9 (26)) using 2,3-dichloropyrazine and different amines, (a) HCl, Dioxane and DMF, reflux (b) K_2CO_3 , DMSO, reflux.

YAN-9 (26) was prepared starting from commercially available 2,3-dichloropyrazine which was reacted with 2.1 equivalents of 1-(5-trifluoromethylpyridin-2-yl)-piperazine under basic conditions using K_2CO_3 as base and DMSO as solvent as shown in scheme 3.9. After reaction completion the mixture was evaporated, cold water (ice) was added and then the mixture was extracted with chloroform multiple times. Organic extracts were pooled, dried using sodium sulfate, and concentrated to give the desired product as brown oil with a yield of 88.7%.

We have noticed that the synthesis of symmetrical 2,3-diaminopyrazine derivatives require special reaction conditions, including longer reaction time, higher concentration of reactants, stronger acid/base. Moreover, aprotic solvents such as DMSO and DMF were used in S_NAr because they could increase the solubility of the reactants and thereby increase the kinetic of reaction.

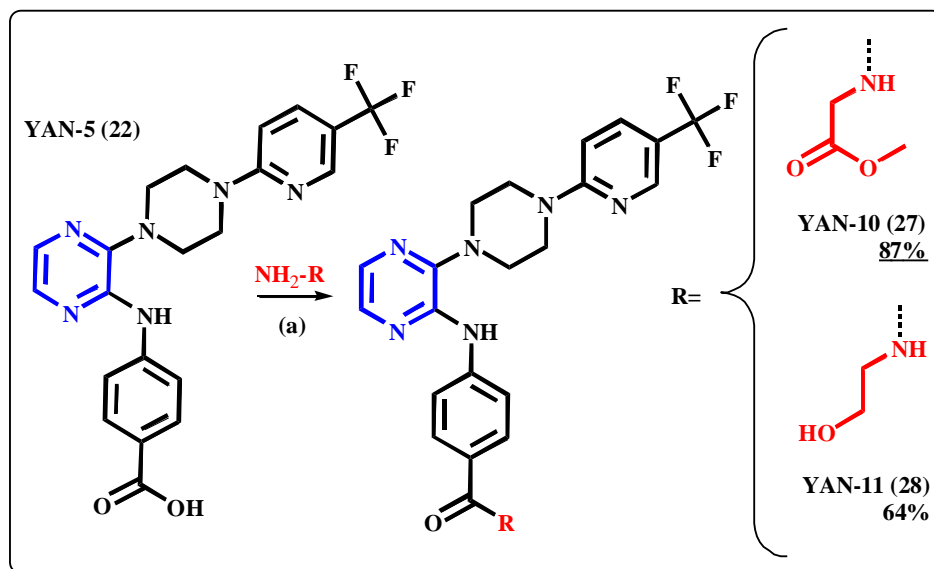
3.1.5. Extending the carboxylic acid terminus of YAN-5 (22) via amide bond formation

The reaction of carboxylic acid with amine in presence of DCC and NHS coupling system is frequently used in practice for amide bond formation. First DCC (dicyclohexyl-carbodiimide) reacts with the carboxylic acid terminus of the compound creating an *o*-acylisourea intermediate which is considered a good leaving group. Afterwards, *N*-hydroxysuccinimide attacks the intermediate forming 1,3-dicyclohexyl-isourea which is directly converted to the side product 1,3-dicyclohexyl-urea (DCU), the new intermediate is then subjected to the desired amine which results in amide bond formation as shown in scheme 3.10.



Scheme 3.10: Detailed mechanism showing the coupling of the carboxylic acid terminus with different amines, using DCC, NHS coupling system.

As shown in scheme 3.11. YAN-5 (22) was added to a solution of DCC and NHS in dioxane and TEA, the mixture was stirred at room temperature for 5 h. The intended amines were dissolved in small amount of dioxane and added to the activated YAN-5 (22) solution. While being stirred, the reaction was left at room temperature overnight. Upon reaction completion the crude mixture was evaporated and re-dissolved in cold ethyl acetate. Insoluble DCU was removed by filtration and washed with cold ethyl acetate. The filtrate was condensed to give YAN-10 (27) in 87% yield. Regarding YAN-11 (28) further purification using column chromatography was needed to remove the remaining by-products; the compound was recovered with a yield of 64%.



Scheme 3.11: Synthesis of YAN-10 (27) and YAN-11(28) by extending the carboxylic acid terminus of YAN-5 (22) via amide bond formation using different amines, (a) DCC, NHS, Dioxane, TEA, room temperature overnight

3.1.6. Bromination of pyrazine derivative A1 (1)

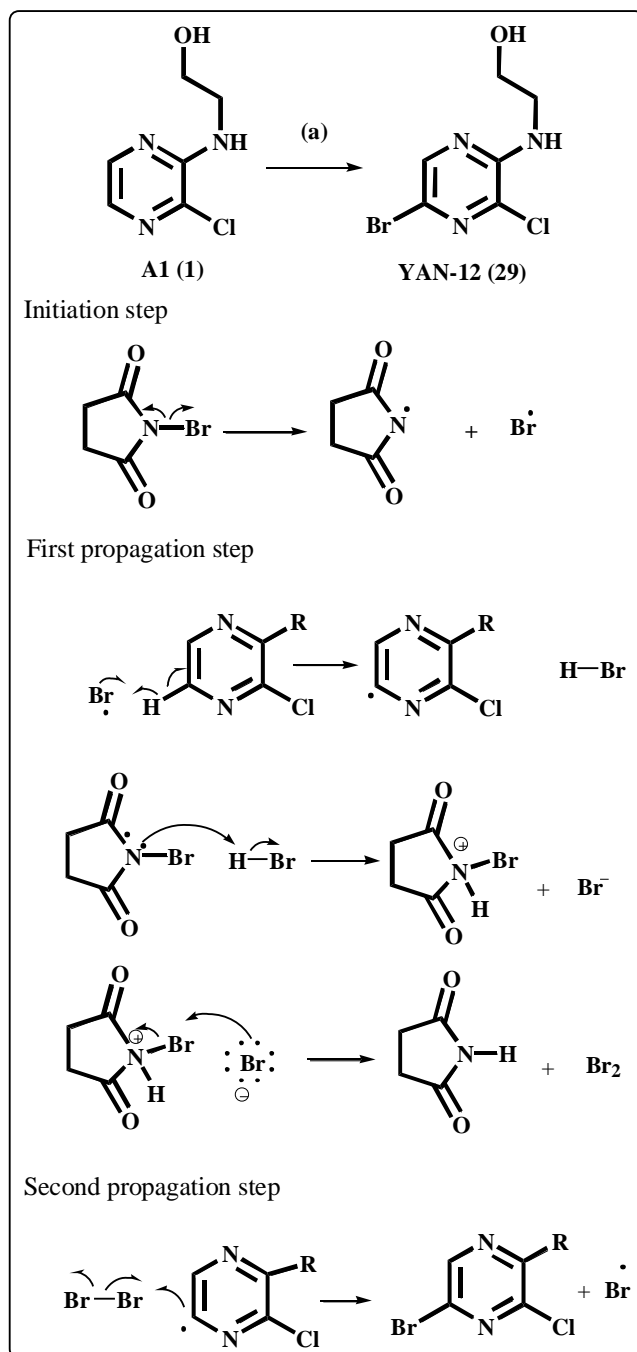
A1 (1) was subjected to radical reaction conditions to explore the possibility of pyrazine ring activation. NBS was used for bromination; it produces a controlled amount of Br radicals which allows controlling the number of bromines added. First NBS was gradually added to a solution of A1 (1) in acetonitrile at room temperature. The initiation step started with a heterolytic cleavage of the N-Br bond in NBS. Afterwards, NBS nitrogen abstracted a proton from HBr, and a bromide ion attacked the protonated NBS bromine forming Br₂. Finally, pyrazine radical abstracted a bromine radical from Br₂ to form the desired product. The detailed activation mechanism is described in scheme 3.12.

The reaction of bromine atom with pyrazine is considered endothermic (energy of activation is high and the transition state is closer in energy to products than reactants) so no heating was needed and the reaction rate was very fast. A change in colour of the reaction and formation of precipitate was noticed with time. TLC showed almost a complete reaction after 2 hours, however, the reaction was left at room temperature overnight to ensure product formation. Upon reaction completion, the reaction mixture was cooled and YAN-12 (29) was collected by suction filtration as a solid orange-brown powder with 96.3% yield.

Bromination with NBS is highly selective because bromine forms a stable radical; the reactivity-stability principle states that with increased reactivity selectivity decreases.

It was reported that bromination position is highly affected by the used solvent. Two separated studies disclosed that starting from 2-aminopyrazine, if the bromination reaction was carried out using NBS in acetonitrile or dichloromethane the bromination will take place at carbon 5 of pyrazine (*Para* to the amine) and the resulted derivative will be 2-amino-5-bromopyrazine^[98, 99]. In contrast, *B. Jiang et al.* claimed that if the same reaction was done using DMSO the bromination will take place at both carbon 3 and 5 of the ring and the resulted derivative will be 2-amino-3,5-dibromopyrazine^[100].

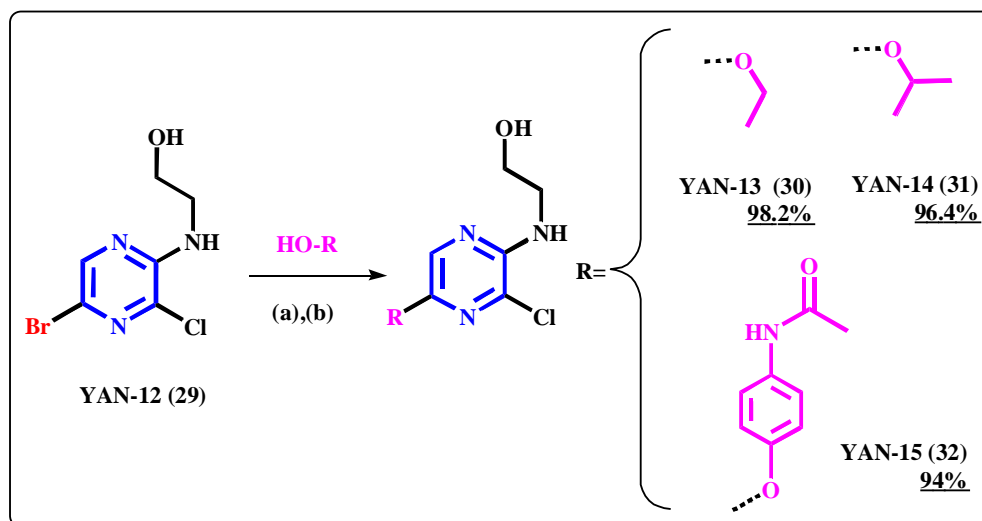
In our procedure acetonitrile was used as solvent therefore the bromination is likely takes place at position 5, *para* to the amine. Comparing ¹H-NMR spectrum of A1 (1) and YAN-12 (29) revealed that the peak for the proton at position 5 of the pyrazine ring disappeared from (29) ¹H-NMR spectrum, which confirms that bromination occurred at position 5.



Scheme 3.12: Detailed mechanism showing C-H activation of A1 (1) using NBS. (a) NBS, acetonitrile, stirring at room temperature overnight. R= ethanolamine.

3.1.7. Synthesis of 2-amino-3-chloro-5-alkoxy pyrazine derivatives (30-32)

The previously synthesized intermediate YAN-12 (29) was reacted with acetaminophen in dioxane under basic condition using K_2CO_3 as shown in scheme 3.13. Potassium carbonate deprotonates the phenolic hydroxyl group of acetaminophen as previously shown in Scheme 3.6. The conjugate base of phenol is resonance stabilized creating negatively charged phenoxide anion which as a strong nucleophile attacks YAN-12 (29) on carbon 5. The reaction was refluxed for 24 hours. Upon reaction completion YAN-15 (32) was isolated by column chromatography in 94% yield.



Scheme 3.13: Synthesis of 2-amino-3-chloro-5-alkoxy pyrazine derivatives (30) and (31), (a) Sodium, reflux, synthesis of (32): (b) K_2CO_3 , Dioxane, reflux.

During the synthesis of YAN-13 (30) and YAN-14 (31), YAN-12 (29) was reacted with deprotonated aliphatic alcohols, Sodium which is considered a stronger base than K_2CO_3 was used since aliphatic alcohols have high pKa values and therefore requires stronger bases to deprotonate them. Aliphatic alcohol itself (ethanol and isopropanol, respectively) was used as both solvent and nucleophile. Sufficient volume of the alcohol was first stirred at ambient temperature with sodium to allow the alcohol to deprotonate. Hydrogen gas bubbles were noticed at this point indicating the deprotonation process. After the addition of (29), the mixture was heated to reflux for 19 hours (for both 30, 31). Upon reaction completion volatiles were evaporated, the crude was extracted with ethylacetate. The organic extracts were pooled, dried using sodium sulfate and concentrated. The product was washed with cold ether and air dried to afford YAN-13 (30) and YAN-14 (31), in high yields of 98.2 % and 96.4%, respectively.

YAN-12 (29) has two possible positions that could be attacked by the protonated alcohol. However, substitution at position 5 is preferred. Bromine is considered a better leaving group than chlorine because bromine is larger in size and is more polarizable, which lowers the overall energy of the reaction transition state.

The presence of a substituent at the pyrazine ring will highly affect the rate and orientation of nucleophilic substitution; in fact it is a combination of resonance and inductive effects. The electron withdrawing substituents (Cl and Br) play an inductive effect on the other carbons which creates an electron deficient aromatic ring. Whereas the already existed amine -electron donating group- substituent at position 2 will increase the electron density on the ring through a resonance donating effect and decrease the rate of nucleophilic substitution. The resonance only allows electron density to be positioned at the *ortho*- and *para*- positions. Hence, these sites are more nucleophilic, and the system tends to react with electrophiles at these *ortho*- and *para* sites. In addition, substitution at position 2 creates a steric bulk that favors the second substitution to take place at *para* position.

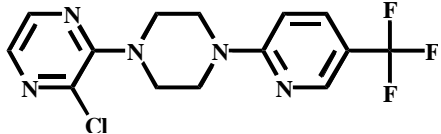
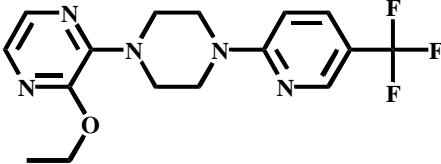
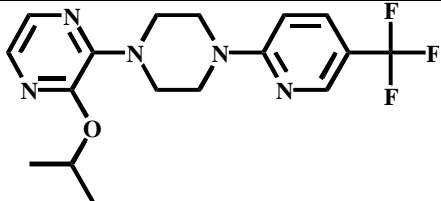
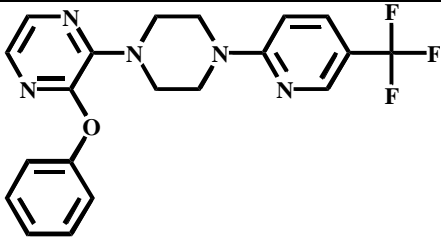
3.2. Initial *in vitro* biological activity

Some of the synthesized compounds were assessed for their *in vitro* biological activity against Acute Myeloid Leukemia (AML) cell lines. Aggressive AML is receptor tyrosine kinase mutant driven. As a result screening our compounds using AML cell line may reveal whether they work as tyrosine kinase inhibitors or not. The rationale behind choosing this cell line was that 2,3-disubstituted pyrazines may act as kinase inhibitors. P53 “the guardian of the genome” is a protein produced by the tumor suppressor p53 gene, this protein has the ability to detect any abnormality in cells growth or division and hence terminate the abnormal cells. Recent studies showed that p53 gene is mutated in more than 50% of human cancers^[101, 102].

To evaluate whether our compounds act in a p53 dependent or independent manner, acute monocytic leukemia (Molm-13) cell lines were transfected with a short hairpin RNA (sh-RNA). sh-RNA is RNA sequence engineered to suppress the expression of desired gene via RNA interference. Two forms of (Molm-13) cell lines were used; the first (Molm-13) transfected with sh-RNA empty vector and the second (Molm-13 sh-p53) transfected with sh-p53 RNA. (Molm-13 sh-p53) are p53 knocked down. To develop an initial structure activity

relationship, A-7 (7) and three different analogues carrying ether functionality at position 3 of pyrazine were tested against the two forms of (Molm-13) cell lines and the viability of the cells was determined using WST-1 assay. The tested compounds have shown weak to moderate activity against Molm-13 cell line (empty vector) [IC_{50} = 39 to 63 μ M] and Molm-13 cell line (sh-p53) [IC_{50} = 18 to 63 μ M]. A-7 (7) was relatively more potent than its analogues with IC_{50} of 18 and 39 μ M against Molm-13 (sh-p53) and Molm-13 (empty vector), respectively. It could be concluded from IC_{50} values (table 3.1) that introducing an alkoxy substituent at position 3 result in a drop in the activity. Moreover, increasing the size of the alkoxy derivative at position 3 is directly proportional to decreasing the activity of the compound as shown in the case of YAN-1 (18), YAN-2 (19), and YAN-3 (20) which possesses ethanol, isopropanol and phenol derivatives, respectively.

Table 3.1: Structure activity relationship and IC_{50} values of compounds (7, 18, 19, and 20).

Com number	Com code	Compound structure	IC_{50} (μ M) Molm-13 Empty vector	IC_{50} (μ M) Molm-13 sh-p53
7	A7		39	18
18	YAN-1		NA	26
19	YAN-2		NA	39
20	YAN-3		63	63

YAN-1 (18) and YAN-2 (19) have shown a remarkable difference between the concentration response curve and the IC₅₀ values derived from the two forms of Molm-13 cell lines (empty vector and sh-p35) suggesting that the compounds mechanism of action is p53 dependent (Figures 3.1, and 3.2).

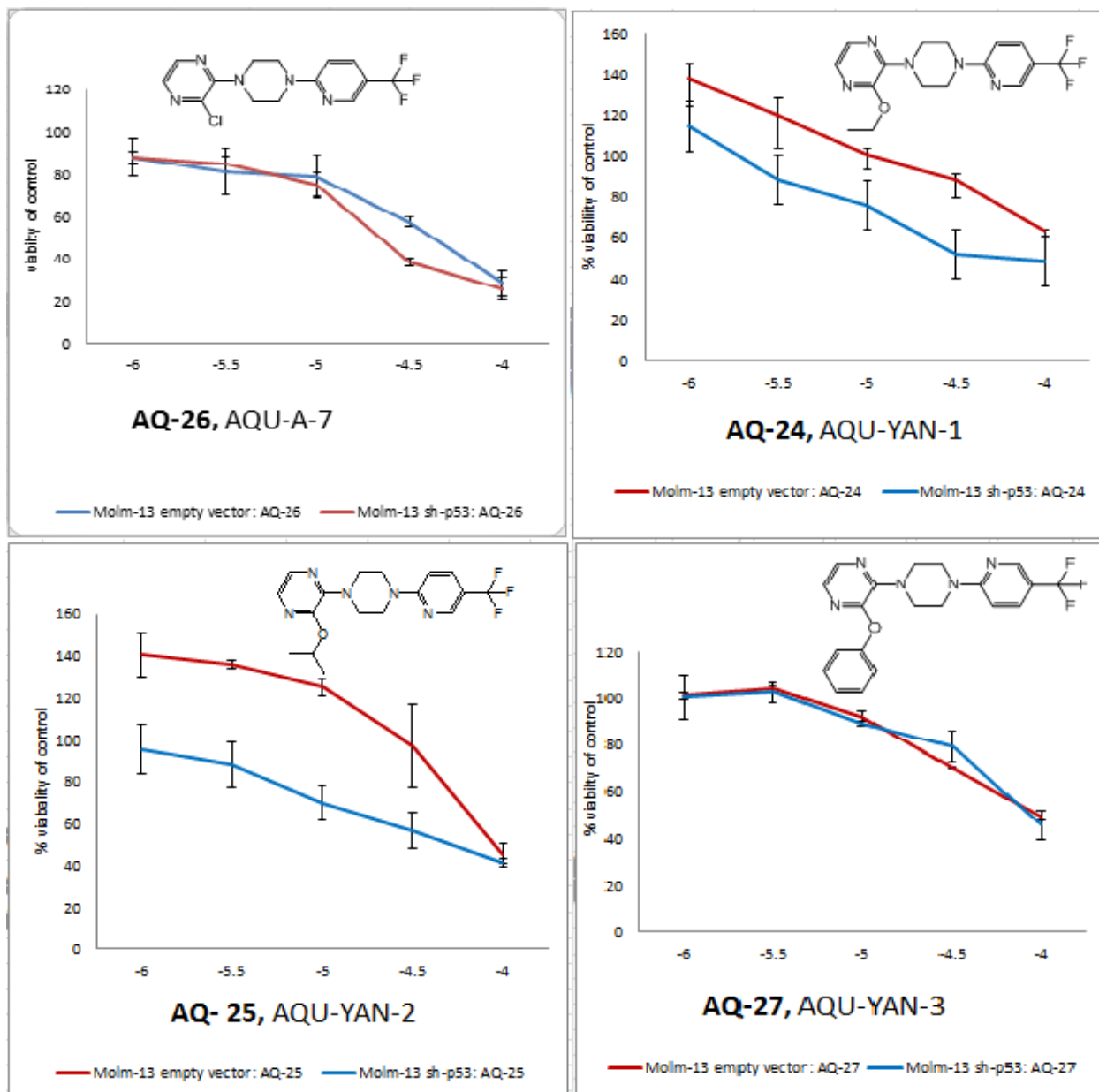


Figure 3.1: Concentration-response effect of A-7 (7), YAN-1 (18), YAN-2 (19), and YAN-3 (20) on Molm-13 cancer cell lines. Cell viability was measured using WST-1 assay and the data expressed as the mean+SD of two independent experiments.

Although p53 mutations have been detected in only about 5% of acute myeloid leukemia patients, they are considered an adverse factor for disease prognosis and response to chemotherapeutic agents.

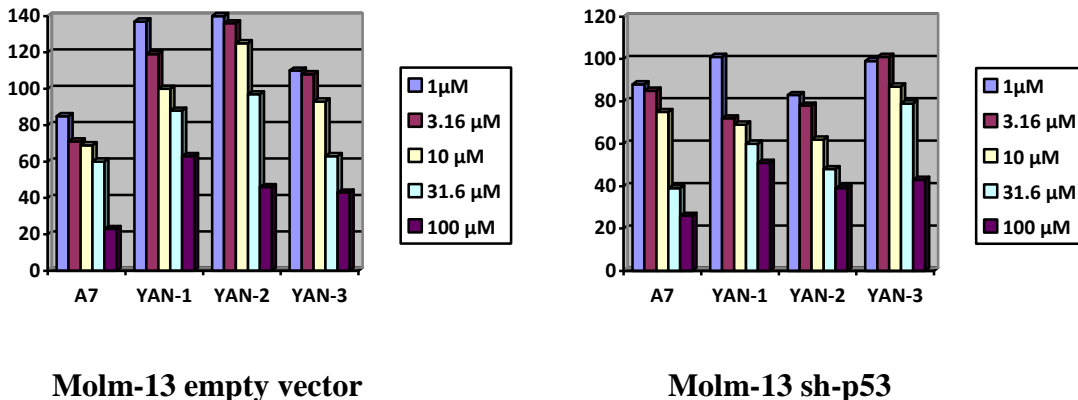


Figure 3.2: Viability chart of molm-13 empty vector and molm-13 sh-p53 cells at different concentration (1, 3.16, 10, 31.6, and 100 μM) of A-7 (7), YAN-1 (18), YAN-2 (19), and YAN-3 (20).

From this initial biological screening we concluded that 1-(5-trifluoromethylpyridin-2-yl)-piperazine moiety is a good pharmacophore for the antineoplastic activity, so it was fixed at position 2 of the pyrazine ring and A-7 (7) was chosen as a lead compound, however we also concluded that different non-alkoxy substituents must be introduced at position 3 of the ring in order to increase the activity.

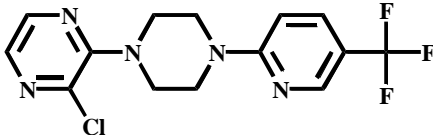
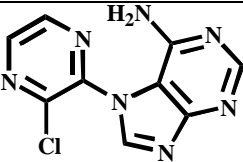
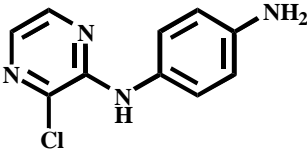
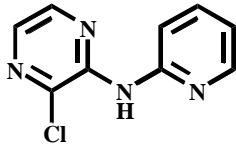
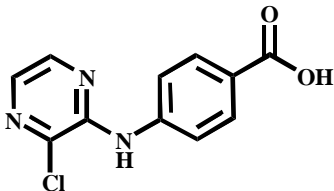
The biological results were confirmed using “PASS” prediction of activity spectra software (see section 3.3 for details), the software predicted the same sequence of activity for A-7 (7), YAN-1 (18), YAN-2 (19), and YAN-3 (20). Furthermore, and in aim to increase the chance of preparing new active compounds, different amine substituents were introduced to A-7 (7) (position 3 of pyrazine ring) computationally and their activity was predicted using PASS. Afterwards the active derivatives were synthesized.

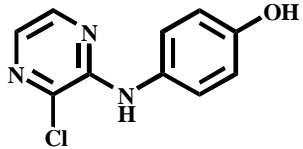
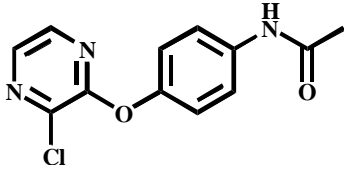
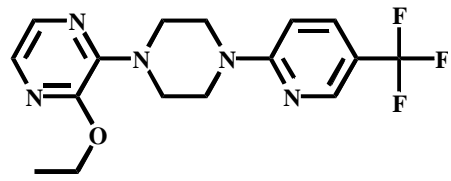
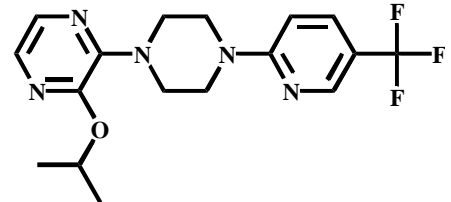
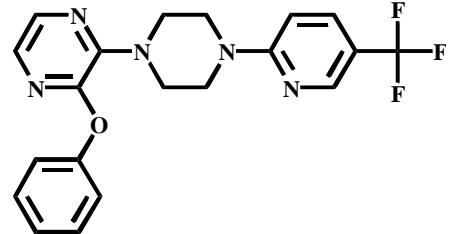
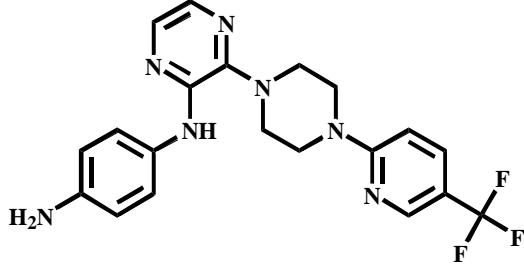
3.3. Computational chemistry of synthesized compounds

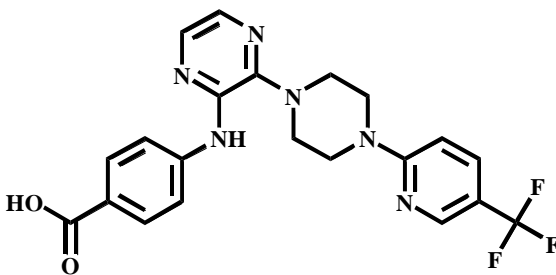
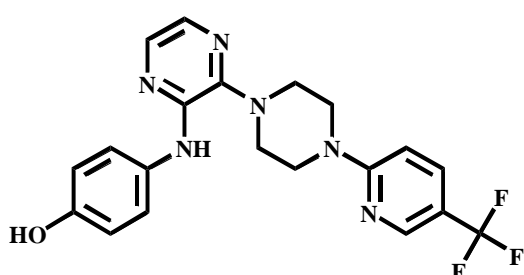
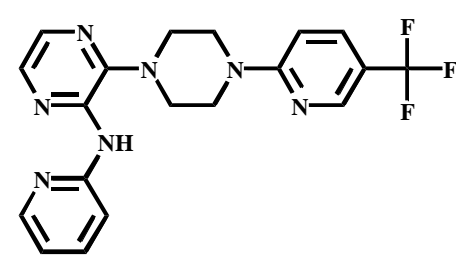
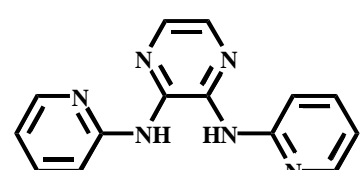
3.3.1. Computer-aided prediction of biological activity spectra of the synthesized

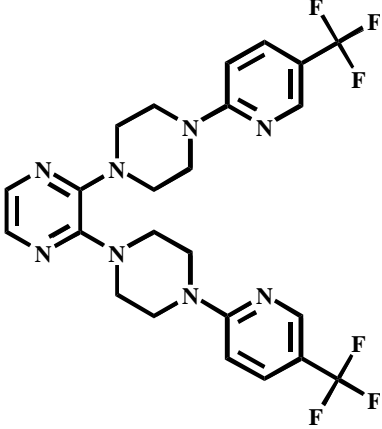
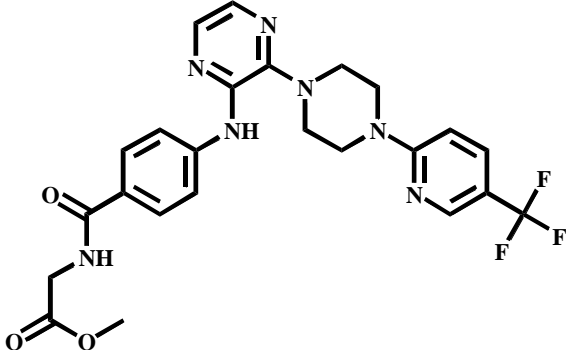
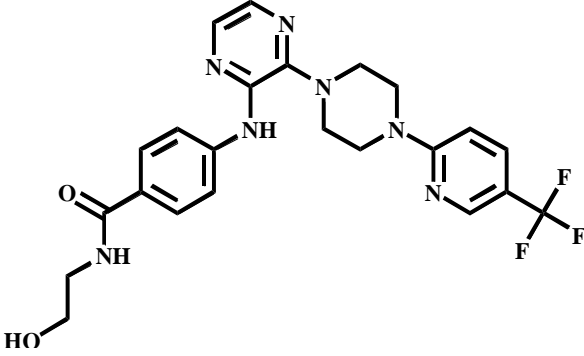
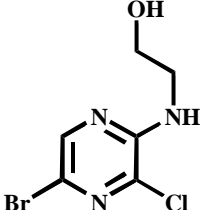
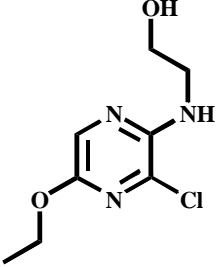
compounds: The PASS (prediction of activity spectra for substances) software was used to predict the pharmacological effect and the biochemical mechanism of the newly synthesized compounds according to their structural formula. Table 3.2 shows the results

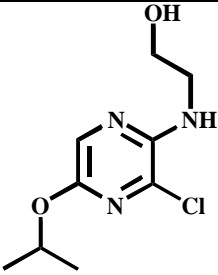
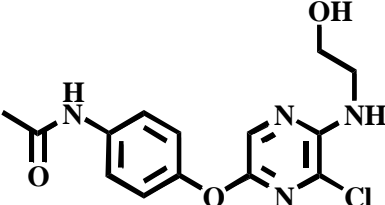
Table 3.2: Computer-aided prediction of biological activity spectra (PASS) results of the synthesized compounds.

Com. number	Com. Code	Structure	Expected activity	Pa value
7	A7		Antineoplastic (non-Hodgkin's lymphoma)	0.604
			Autoimmune disorder treatments	0.683
12	A12		Antineoplastic	0.735
			Signal transduction pathway inhibitor	0.444
13	A13		Signal transduction pathway inhibitor	0.927
			Antineoplastic (solid tumors)	0.824
			Preneoplastic conditions treatment	0.478
14	A14		Signal transduction pathway inhibitor	0.962
			Antineoplastic (solid tumors)	0.862
15	A15		Signal transduction pathway inhibitor	0.682
			Antineoplastic (solid tumors)	0.693
			Preneoplastic conditions treatment	0.668

16	A16		Signal transduction pathway inhibitor	0.853
			Antineoplastic (solid tumors)	0.753
			Preneoplastic conditions treatment	0.645
17	A17		Antineoplastic (solid tumors)	0.543
			Signal transduction pathway inhibitor	0.459
18	YAN-1		Antineoplastic (non-Hodgkin's lymphoma)	0.611
			Anti-obesity	0.810
19	YAN-2		Antineoplastic (non-Hodgkin's lymphoma)	0.585
			Anti-obesity	0.794
20	YAN-3		Antineoplastic (non-Hodgkin's lymphoma)	0.589
			Anti-obesity	0.925
21	YAN-4		Antineoplastic (non-Hodgkin's lymphoma)	0.612
			Signal transduction pathway inhibitor	0.734

22	YAN-5		Antineoplastic (non-Hodgkin's lymphoma)	0.582
			Signal transduction pathway inhibitor	0.464
23	YAN-6		Antineoplastic (non-Hodgkin's lymphoma)	0.600
			Signal transduction pathway inhibitor	0.604
24	YAN-7		Antineoplastic (non-Hodgkin's lymphoma)	0.606
			Signal transduction pathway inhibitor	0.803
25	YAN-8		Signal transduction pathway inhibitor	0.961
			Angiogenesis inhibitor	0.825
			Antineoplastic	0.779
			Preneoplastic conditions treatment	0.506

26	YAN-9		Antineoplastic (non-Hodgkin's lymphoma)	0.667
27	YAN-10		Antineoplastic (non-Hodgkin's lymphoma)	0.552
			Signal transduction pathway inhibitor	0.337
28	YAN-11		Antineoplastic (non-Hodgkin's lymphoma)	0.607
			Signal transduction pathway inhibitor	0.455
29	YAN-12		Signal transduction pathway inhibitor	0.665
30	YAN-13		Antineoplastic(solid tumors)	0.344

31	YAN-14		Antineoplastic(solid tumors)	0.381
32	YAN-15		Antineoplastic(solid tumors)	0.256

Notes:

Antineoplastics are agents that prevent or inhibit the maturation and proliferation of neoplasms in the body.

Signal transduction pathway inhibitors are chemical structures that may prevent the ability of cancer cell to multiply quickly and invade other tissues

Preneoplastic conditions treatment: treatment that is given to patients with genetically clinically, or morphologically defined conditions that are associated with high risk to develop cancer and increased incidence of malignant neoplasia with time.

Non-Hodgkin's lymphomas: a group of lymphoproliferative disorders that originates in the lymphocytes (a type of white blood cells).

Angiogenesis inhibitors: are agents that inhibit the formation and growth of new blood vessels.

Regarding our compounds, results were interpreted as the possible mechanisms of actions for each compound (structural unit) along with Pa value which indicates the estimated probabilities for a compound to be active, or pi value which indicates the estimated probabilities for a compound to be inactive. Usual interpretation of prediction results is based on the Pa values. If Pa value > 0.7 the chance to find the activity in experiment is high, and the compound may occur to be close analogue of known pharmaceutical agents. If $0.5 < Pa < 0.7$ the chance to find the activity in experiment is less, but the compound is not so similar to known pharmaceutical agents. If Pa < 0.5 the chance to find the activity in experiment is even more less, but if it will be confirmed the compound might occur to be a New Chemical Entity.

Result demonstrated that mono substituted derivatives possessing amine substituent at position 2 of the pyrazine ring (A7 (7), A12 (12), A13 (13), A14 (14), A15 (15), and A16 (16)) exhibited different antineoplastic activities. For instance A7 showed good antineoplastic activity especially in (non-Hodgkin's lymphoma), while (A12 - A16) showed excellent antineoplastic activity mainly against solid tumors with Pa value > 0.7 . Moreover, the later derivatives (A12 - A16) were able to act as signal transduction pathway inhibitors with very high Pa values that reached 0.962 for A14. On the other hand, (A13, A15, and A16) were good candidates for preneoplastic conditions treatment.

A17 (17), a mono substituted derivative with alkoxy substituent at position 2 of the pyrazine ring showed similarity to (A12 - A16) series in manner of predicted activity, but with lower Pa values. A structural activity relationship could be derived from this prediction indicating that position 2 must be substituted with an amine for better Pa results.

2-amino-3-alkoxy disubstituted derivatives (YAN-1 (18), YAN-2 (19), and YAN-3 (20)) showed moderate antineoplastic activity especially in case of (non-Hodgkin's lymphoma). From SAR point of view these derivatives are structurally related to A7 (7), they share a common structural moiety (1-(5-trifluoromethyl-pyridin-2-yl)-piperazine) which is likely responsible for the antineoplastic activity. On the contrary, introducing aliphatic or aromatic alcohol to position 3 of the already substituted pyrazine ring resulted in a new cancer non related activity. (YAN-1, YAN-2, and YAN-3) showed excellent anti-obesity activity with relatively high Pa values that reached 0.925 in case of YAN-3 (20). This again confirms the large spectrum of activity for pyrazine derivatives.

Asymmetrical 2,3-diamino substituted derivatives (YAN-4 (21) - YAN-7 (24)) exhibited good antineoplastic activity against (non-Hodgkin's lymphoma) with Pa values ≥ 0.6 . They also showed ability to act as signal transduction pathway inhibitors with different Pa values. This difference was structurally related to the presence of certain functional groups at the terminal of the derivative, for example having terminal hydrophilic moieties such as hydroxyl or carboxylic acid decreased the Pa value of the derivative as signal transduction pathway inhibitor while having terminal amine (aliphatic or aromatic) increased the Pa values.

Symmetrical di-amino substituted pyrazine derivatives (YAN-8 (25) and YAN-9 (26)) showed good antineoplastic activity, particularly (YAN-8 (25) exhibited excellent Pa values. It mainly acts as signal transduction pathway inhibitor with Pa value of 0.961, angiogenesis inhibitor with Pa value of 0.825, antineoplastic with Pa value of 0.779, and also preneoplastic conditions treatment with Pa value of 0.506. These combined mechanisms might result in synergistic effect that could increase the possibility of this compound to be active in experiment at lower concentrations.

YAN-10 (27) and YAN-11 (28) are analogous of YAN-5 (22); they were designed by extending the carboxylic acid terminal via amide bond. The analogues exhibited the same activities as YAN-5 including antineoplastic (non-Hodgkin's lymphoma) and signal transduction pathway inhibitory activity. However, the Pa values were different, in case of YAN-10 the Pa values are lower than YAN-5 this may refer to the introduction of the methylated carboxylic ester to the structure. On the other hand, YAN-11 showed a slightly higher Pa value (as antineoplastic agent) than YAN-5.

In order to investigate the importance of derivatization position at the pyrazine ring, the activity of 2-amino-5-alkoxy disubstituted derivatives (YAN-13 (30) and YAN-14 (31)) was predicted. According to PASS results, the derivatives showed antineoplastic activity against solid tumors with very low Pa values of ≤ 0.4 . This indicates poor activity in comparison with the 2,3-disubstituted pyrazine derivatives and hence confirms the importance of the derivatization position.

PASS software also predicts the mechanism of action, most of the mono amino derivatives (A13 - A16) exhibited the same mechanism of action which is protein kinase inhibitor with different Pa values, A14 had the highest Pa value (0.873), followed by A13 with Pa value of (0.706), A15 and A16 showed lower Pa values of (0.338) and (0.527), respectively.

Accordingly, di-amino substituted pyrazine derivatives (YAN-4 (21) - YAN-8 (25)) possessed the same mechanism of action, YAN-8 (25) a symmetrical disubstituted analogue of A14 (posses 2-aminopyridine in position 2 and 3 of the pyrazine ring) displayed the highest Pa value among

the disubstituted derivatives which is (0.954), followed by YAN-7 (24) , YAN-4 (21), and YAN-6 (23) with Pa values of 0.827, 0.707, and 0.705 respectively. The remaining derivatives showed relatively small Pa values ≤ 0.5 .

According to different publications PASS managed to provide robustness of calculated estimated data and high accuracy of prediction. The mean accuracy of biological activity prediction with PASS is $70 \pm 80\%$ both in prediction for independent test and leave-one-out cross validation (LOO)^[103, 104]. Therefore, the results could be used to select the most prospective compounds from the set of predicted derivatives for both synthesis and experimental biological screening. On top of that, the informative pass predictions could be used to determine the cell lines and biological assay that are relevant to the predicted biological activity and mechanism of action for each compound.

Some of the predicted derivatives were already synthesized when the PASS prediction was carried on; however, other derivatives were synthesized according to their promising activity results.

3.3.2. **Lipinski's rule of five: computational approach to predict drug-likeness of the synthesized compounds.** Drug-likeness of the synthesized compounds was assisted using Chemicalize, A public web resource which gives structure-based predictions. Table 3.3 depicts the results.

Table 3.3: drug-likeness prediction results of the synthesized compounds using Lipinski's rule of five.

Com. #	Com. name	H-bond donors	H-bond acceptors	molar mass g/mol	log <i>P</i>	Molar refractivity Cm ³ /mol	Atoms count	Pass rule of five
1	2-(3-Chloropyrazin-2-ylamino)-ethanol	2	4	173.6	-0.26	44.41	19	yes
2	2-[(3-Chloropyrazin-2-yl)-methyl-amino]-ethanol	1	4	187.63	0.37	48.64	22	yes
3	(3-Chloropyrazin-2-ylamino)-acetic acid	2	5	187.58	-0.21	44.20	18	yes
4	(3-Chloropyrazin-2-ylamino)-acetic acid methyl ester	1	4	201.61	0.05	48.97	21	yes
5	Butyl-(3-chloropyrazin-2-yl)-amine	1	3	185.66	1.75	51.99	24	yes
6	2-(3'-Chloro-2,3,5,6-tetrahydro-[1,2']bipyrazinyl-4-yl)-ethanol	1	5	242.71	0.22	64.69	31	yes
7	3'-Chloro-4-(5-trifluoromethylpyridin-2-yl)-3,4,5,6-tetrahydro-2H [1,2'] bipyrazinyl	0	5	343.74	3.06	83.03	36	yes
8	3'-Chloro-4-(3-trifluoromethylpyridin-2-yl)-3,4,5,6-tetrahydro-2H-[1,2']bipyrazinyl	0	5	344.74	3.06	83.03	36	yes
9	3'-Chloro-4-pyrimidin-2-yl-3,4,5,6-tetrahydro-2H-[1,2']bipyrazinyl	0	6	276.73	1.56	75.51	32	yes

10	3'-Chloro-4-pyridin-4-yl-3,4,5,6-tetrahydro-2H-[1,2']bipyrazinyl	0	5	275.74	1.59	76.74	33	yes
11	1'-(3-Chloropyrazin-2-yl)-[1,4']bipiperidinyl	0	4	280.8	1.94	79.95	40	yes
12	7-(3-Chloropyrazin-2-yl)-7H-purin-6-amine	1	6	247.65	0.29	75.08	23	yes
13	N-(3-Chloropyrazin-2-yl)-benzene-1,4-diamine	2	4	220.66	1.57	61.11	24	yes
14	(3-Chloropyrazin-2-yl)-pyridin-2-yl-amine	1	4	206.63	1.77	54.57	21	yes
15	4-(3-Chloropyrazin-2-ylamino)-benzoic acid	2	5	249.65	2.01	63.67	25	yes
16	4-(3-Chloropyrazin-2-ylamino)-phenol	2	4	221.64	5.10	58.39	23	yes
17	N-[4-(3-Chloropyrazin-2-yloxy)-phenyl]-acetamide	1	3	263.68	6.08	69.03	28	yes
18	3'-Ethoxy-4-(5-trifluoromethylpyridin-2-yl)-3,4,5,6-tetrahydro-2H-[1,2']bipyrazinyl	0	6	353.34	3.03	88.69	43	yes
19	3'-Isopropoxy-4-(5-trifluoromethylpyridin-2-yl)-3,4,5,6-tetrahydro-2H-[1,2']bipyrazinyl	0	6	367.37	3.44	93.11	46	yes
20	3'-Phenoxy-4-(5-trifluoromethylpyridin-2-yl)-3,4,5,6-tetrahydro-2H-[1,2']bipyrazinyl	0	5	401.39	4.33	103.72	47	yes
21	N-[4-(5-Trifluoromethylpyridin-2-yl)-3,4,5,6-tetrahydro-2H-[1,2']bipyrazinyl-3'-yl]-benzene-1,4-diamine	2	7	415.42	3.44	110.67	50	yes

22	4-[4-(5-Trifluoromethylpyridin-2-yl)-3,4,5,6-tetrahydro-2H-[1,2']bipyrazinyl-3'-ylamino]-benzoic acid	2	8	444.41	3.00	113.22	51	yes
23	4-[4-(5-Trifluoromethylpyridin-2-yl)-3,4,5,6-tetrahydro-2H-[1,2']bipyrazinyl-3'-ylamino]-phenol	2	7	416.40	3.96	107.95	49	yes
24	Pyridin-2-yl-[4-(5-trifluoromethylpyridin-2-yl)-3,4,5,6-tetrahydro-2H-[1,2']bipyrazinyl-3'-yl]-amine	1	7	401.39	3.64	104.12	47	yes
25	N,N'-Di-pyridin-2-yl-pyrazine-2,3-diamine	2	6	264.29	7.47	75.66	32	yes
26	2,3-Bis({4-[5-(trifluoromethyl)pyridin-2-yl]piperazin-1-yl})pyrazine	0	8	538.50	4.93	132.59	62	no
27	{4-[4-(5-Trifluoromethylpyridin-2-yl)-3,4,5,6-tetrahydro-2H [1,2']bipyrazinyl-3'-ylamino]-benzoylamino}-acetic acid methyl ester	2	8	515.49	2.97	130.79	61	no
28	N-(2-Hydroxy-ethyl)-4-[4-(5-trifluoromethylpyridin-2-yl)-3,4,5,6-tetrahydro-2H-[1,2']bipyrazinyl-3'-ylamino]-benzamide	3	8	487.48	2.65	126.23	59	yes
29	2-(5-Bromo-3-chloropyrazin-2-ylamino)-ethanol	2	4	252.5	0.71	52.87	19	yes
30	2-((3-Chloro-5-ethoxypyrazin-2-yl)amino)ethanol	2	5	217.65	0.53	55.94	26	yes

31	2-(3-Chloro-5-isopropoxy-pyrazin-2-ylamino)-ethanol	2	5	231.68	0.95	60.35	29	yes
32	N-(3-((6-Chloro-5-((2-hydroxyethyl)amino)pyrazin-2-yl)oxy)phenyl)acetamide	3	5	322.75	1.07	85.83	37	yes

The results demonstrate the number of H-bond donors and acceptors, molecular weight, partition coefficient, molar refractivity and atoms count for each compound. Rule of 5' states that the compound should possess less than 5 H-bond donors, 10 H-bond acceptors, molecular weight (MWT) smaller than 500 Dalton (preferred MWT between 180 to 500), calculated octanol-water partition coefficient (Log P) in -0.4 to +5.6 range, molar refractivity in 40 to 130 range, and finally total number of atoms from 20 to 70.

From the collected data all of the tested compounds successfully met the rule of 5 requirements except two of them YAN-9 (26) and YAN-10 (27). This was mainly due to the large molecular mass of these compounds which rise from the large implicated substituents.

3.3.3. Docking of the synthesized compounds using SwissDock, a protein-small molecule docking web service based on EADock DSS.

3.3.3.1. Docking study using inactive monomeric CDK-2 model

In order to gain insight into the binding mode of pyrazine derivatives with CDK-2, a series of 16 compounds were docked with a crystallographic structure of human cyclin dependent kinase-2 using SwissDock software. First, the crystallographic structure of the target was obtained from the Protein Data Bank (PDB), accession code 1-HCL and viewed using chimera software (Figure 3.3).

The monomeric CDK2 consists of 298 amino acids and folds into a typical bi-lobal structure, consisting of a smaller *N*-terminal lobe (residues 1–85) that contains an antiparallel five-strand β -sheet along with a major *C*-helix, and a larger *C*-terminal lobe composed of α -helix predominantly. The two terminal domains are connected through a single peptide strand (residues 81–83) which acts as a hinge linker to ensure the lobes rotation without disruption of the kinase secondary structure. It is well known that most small agents inhibit CDK2 through competition with ATP for the ATP catalytic binding site which is located deep at the junction connecting the *N* and *C* domains, the binding site consists of 136 consecutive amino acids (10–145) on the CDK2 including the hinge linker region (residues 81–83). Various inhibitors bind to the ATP binding pocket and normally occupy the adenine ring (subsite) of the ATP.

As the target was determined and prior the docking of our compounds, we need to ensure the efficiency of docking and validate the selected target. Therefore, ‘Aloisine B’ a synthetic ligand with a known affinity to CDK-2 was re-docked with the selected target (PDB1-HCL) using SwissDock software (Figure 3.4).

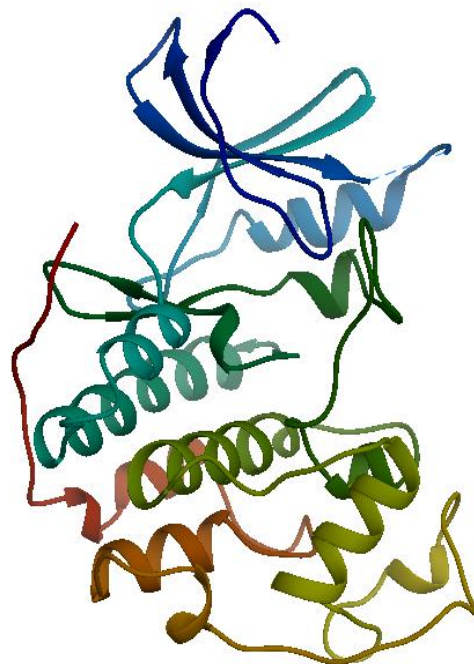


Figure 3.3: CDK2 (1-HCL.PDB) structure in ribbon representation. The *N*-terminal lobe is dominated by a five-stranded antiparallel β -sheet, and the *C*-terminal lobe is predominantly α -helical. Picture was taken from chimera software.

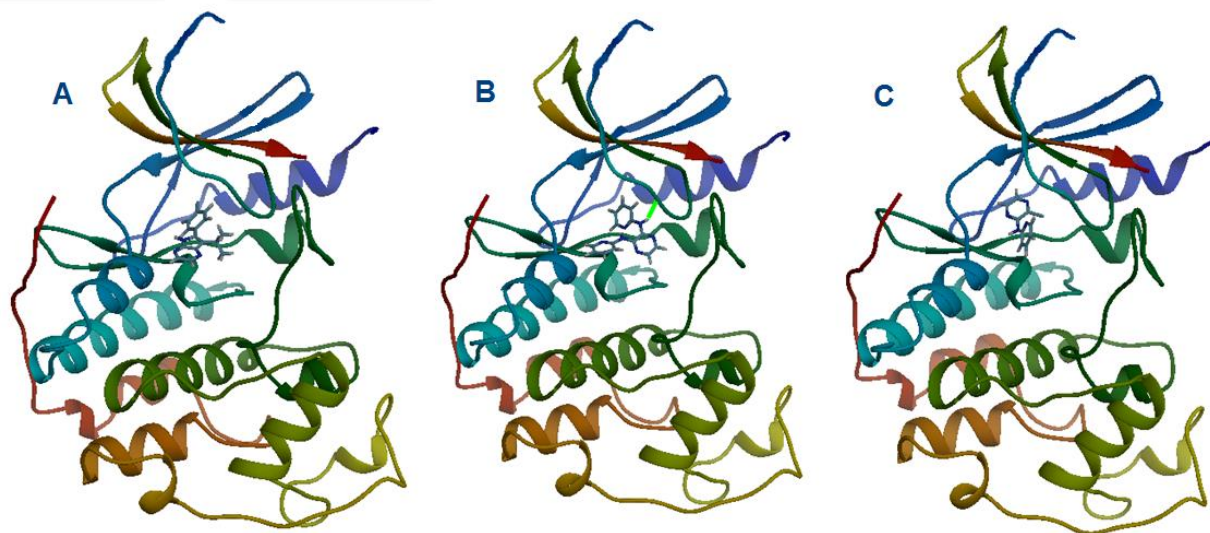


Figure 3.4. Docking of CDK2 (1-HCL.PDB) with Aloisine B (A), YAN-8 (25) (B) and A14 (14) (C). The compounds soak into the CDK-2 ATP binding site. Crystallographic structure was taken from chimera software.

Docking results demonstrated that Aloisine B occupies the CDK-2 ATP binding site and makes hydrogen bonds to the kinase backbone within the hinge sequence that links the two lobes of the kinase. These results are in full agreement with the docking results conducted by Yvette Mettey and his colleagues in 2002^[72], which indicates the efficiency of docking and the validity of the selected target.

After target determination and validation, our compounds were docked to CDK-2 using SwissDock software. Results showed all the possible binding modes of each compound with target cavities (blind docking) and their CHARMM energies. The binding modes with the most favorable energies were evaluated and clustered, and the most favorable clusters were selected and visualized in the UCSF Chimera molecular viewer. Finally, compounds were ranked according to their predicted binding energies and full fitness values (Table 3.4).

The docked compounds exhibited distinct binding affinities to the target, compound 25 showed the highest full fitness value (-1422.14 kcal/mol) whilst compound 26 showed the lowest full fitness value(-1299.70 kcal/mol). In terms of binding mode, pyrazine derivatives occupied the CDK-2 ATP binding site and made hydrogen bonds to the kinase backbone within the hinge sequence that links the two lobes of the kinase.

Table 3.4: docking outcomes of derivatives 14 ,18 ,20 ,21 ,22 ,23 ,24 ,25 ,26 ,27 ,28 ,30 ,31, 32 and Aloisine B with monomeric CDK-2. Results include estimated binding energies and full fitness values as seen in SwissDock and chimera software.

Compound Number	Compound Code	Chimera Model Number	Full Fitness (kcal/mol)	Estimated ΔG (kcal/mol)	Simple fitness energy
14	A14	#1.116	-1405.48	-6.23	24.2
18	YAN-1	#1.57	-1355.46	-6.87	35.89
18	YAN-1	#1.73	-1355.39	-6.74	36.9
19	YAN-2	#1.9	-1353.53	-7.01	38.29
20	YAN-3	#1.40	-1331.50	-7.29	60.49
20	YAN-3	#1.231	-1326.08	-7.22	60.04
21	YAN-4	#1.65	-1348.45	-7.02	62.8
21	YAN-4	#1.240	-1343.88	-7.05	65.1
21	YAN-4	#1.157	-1345.51	-7.67	60.30
22	YAN-5	#1.36	-1342.90	-7.06	64.11
22	YAN-5	#1.110	-1340.87	-6.91	64.0
22	YAN-5	#1.183	-1338.29	-7.36	59.87
23	YAN-6	#1.33	-1347.95	-7.21	59.6
23	YAN-6	#1.67	-1346.70	-7.24	59.9
24	YAN-7	#1.29	-1364.35	-7.16	51.92
24	YAN-7	#1.69	-1362.08	-7.14	53.67
24	YAN-7	#1.93	-1361.39	-7.39	49.45
25	YAN-8	#1.11	-1422.14	-6.66	36.9
25	YAN-8	#1.104	-1417.4	-6.75	36.4
25	YAN-8	#1.108	-1409.0	-7.0	45.0
26	YAN-9	#1.130	-1299.70	-7.04	70.31
26	YAN-9	#1.138	-1299.35	-6.94	78.4
27	YAN-10	#1.1	-1330.16	-8.13	53.4
28	YAN-11	#1.41	-1330.74	-8.24	59.1

30	YAN-13	#1.32	-1382.33	-6.46	10.4
31	YAN-14	#1.51	-1377.98	-6.67	14.95
32	YAN-15	#1.76	-1378.22	-6.77	33.3
32	YAN-15	#1.222	-1375.15	-7.15	28.2
Aloisine B		#1.44	-1406.92	-6.64	7.79

Full Fitness: a common docking outcome in SwissDock and Chimera that reflects the fitness of the tested compound within a given target.

Simple fitness energy: the energy of binding that is related to the degree of fitness

Estimated ΔG : SwissDock outcome representing the estimated difference in free energy of binding.

Both the full fitness and energy values indicated that YAN-8 (25) (-1422.14 kcal/mol) has higher affinity to the target in comparison to Aloisine B (-1406.92 kcal/mol) and the remaining compounds. In terms of structure it is a symmetrical derivative possessing 2-amino pyridine substituent at position 2 and 3 of the pyrazine ring, the structure activity relationship that could be drawn from that indicated the importance of 2-amino pyridine moiety in binding; moreover, this SAR claim was confirmed by A14 (14) which has a mono 2-amino pyridine substituent at position 2 of the pyrazine ring and showed high fitness results (-1405.48 kcal/mol). YAN-8 (25) showed higher probability of binding because of having 2 hydrogen bond donors and 5 hydrogen bond acceptors in its structure whilst A14 (14) has only 1 hydrogen bond donor and 5 hydrogen bond acceptors which reduced the chance of binding. Fortunately, these findings are also of high agreement to PASS results and scores.

YAN-9 (26) (2,3-bis({4-[5-(trifluoromethyl)pyridin-2-yl]piperazin-1-yl})pyrazine) showed the lowest full fitness value (-1299.70 kcal/mol) among the tested compounds. This is mainly due to the large molecular weight and bulkiness of this compound which reduced the chance of fitting into the ATP binding site cavity. Moreover, this compound was rejected in terms of Lipinski's rule of five.

Chapter Four

Conclusion

Conclusion

Cyclin dependent kinase CDK2 is now recognized as a promising target for structure based design of antitumor agents. So far, structural feedback in the rational design of CDK2 inhibitors has been derived from complexes of inhibitors with inactive monomeric form of the enzyme.

This research focuses on the synthesis of disubstituted pyrazine derivatives possessing cytotoxic and CDK2 inhibitory activity. A set of 2,3-disubstituted pyrazine derivatives were synthesized during this study through sequential substitution of the chlorides in 2,3-dichloropyrazine using different aliphatic and aromatic amines or alkoxide. The synthesized compounds were purified using chromatography techniques, characterized by ¹H-NMR, FT-IR and ESIMS spectroscopy.

Some of the synthesized compounds were initially assessed for their cytotoxic activity, intermediate A-7 (7) and three different disubstituted analogues carrying alcohol substituent at position 3 of pyrazine were *in vitro* screened for their inhibitory activity against two forms of acute myeloid leukemia cells (Molm-13). The viability of the cells was determined using WST-1 assay. A-7 (7) was relatively more potent than its analogues with IC₅₀ of 18 and 39 μM against Molm-13 (sh-p53) and Molm-13 (empty vector), respectively. It was noticed that introducing an alkoxide substituent at position 3 result in a drop in the activity. However, 1-(5-trifluoromethyl-pyridin-2-yl)-piperazine pharmacophore showed good antineoplastic activity; hence A-7 (7) was chosen as a lead intermediate.

The biological activity of the synthesized compounds was predicted using PASS software. Initial results demonstrated that A13 (13), A14 (14), YAN-7 (24), YAN-8 (25) exhibited potent activities as cytotoxic agents and signal transduction pathway inhibitors with relatively high Pa values. The previously mentioned compounds also shared the same mechanism of action “protein kinase inhibitor” with Pa values larger than 0.8. SAR analysis derived from PASS proved that the activity of the synthesized derivative is highly affected by the site and type of the substituent on the pyrazine ring. The 2,3-disubstituted derivatives showed better Pa values when compared to the corresponding 2,5- disubstituted ones. In addition amine substituents at positions 2 and 3 of pyrazine ring were preferred over alkoxide substituents in terms of antineoplastic activity.

The concept of drug likeness of the mono and di substituted synthesized derivatives was investigated by applying the rule of five (RO5). All of the tested compounds successfully met the rule of 5 requirements except YAN-9 (26) and YAN-10 (27) which possessed molecular weights larger than 500 Dalton.

In order to gain insight into the binding mode of pyrazine derivatives with CDK-2, a series of 16 compounds along with 'Aloisine B' -a synthetic ligand with a known affinity to CDK-2- were docked with a crystallographic structure of inactive monomeric cyclin dependent kinase-2 using SwissDock software. The binding modes with the most favorable energies were evaluated and visualized in the UCSF Chimera molecular viewer. Compounds were ranked according to their predicted binding energies and full fitness values.

In terms of binding mode, pyrazine derivatives occupied the CDK-2 ATP binding site and made hydrogen bonds to the kinase backbone within the hinge sequence that links the two lobes of the kinase which means that they belong to the family of ATP-competitive inhibitors.

The docked compounds exhibited distinct binding affinities to the target, YAN-8 (25) showed the highest full fitness value (-1422.14 kcal/mol) among the synthesized compounds. Moreover, both the full fitness and energy values indicated that YAN-8 (25) has higher affinity to the target in comparison to Aloisine B (-1406.92 kcal/mol), a well-known CDK-2 inhibitor.

Chapter Five

References

References

1. Abu-Rmeileh, N.M., et al., *Cancer mortality in the West Bank, Occupied Palestinian Territory*. BMC public health, 2016. **16**(1): p. 1.
2. Myadaraboina, S., et al., *Structure activity relationship studies of imidazo [1, 2-a] pyrazine derivatives against cancer cell lines*. European journal of medicinal chemistry, 2010. **45**(11): p. 5208-5216.
3. Miller, M.M. and A.J. DelMonte, *Six-Membered Ring Systems: Diazines and Benzo Derivatives*. Progress in heterocyclic chemistry, 2011. **23**: p. 371.
4. Meher, C., A. Rao, and M. Omar, *Piperazine-pyrazine and their multiple biological activities*. Asian J. Pharm. Sci. Res, 2013. **3**(4).
5. Joule, J.A. and K. Mills, *Heterocyclic chemistry at a glance*2012: John Wiley & Sons.
6. Asif, M., *The pharmacological importance of some diazine containing drug molecules*. Sop Transactions on Organic Chemistry, 2014. **1**(1): p. 1-16.
7. DAVIDSON, D., M. WEISS, and M. JELLING, *The action of ammonia on benzoin*. The Journal of Organic Chemistry, 1937. **2**(4): p. 328-334.
8. Kress, T. and D. Varie, *Six-Membered Ring Systems: Diazines & Benzo Derivatives*. Progress in Heterocyclic Chemistry: A Critical Review of the 1989 Literature Preceded by One Chapter on a Current Heterocyclic Topic, 2013: p. 185.
9. Damani, L. and P. Crooks, *Oxidative metabolism of heterocyclic ring systems*. Metabolic basis of detoxication. Academic, New York, 1982: p. 69-89.
10. Alvarez-Builla, J., J.J. Vaquero, and J. Barluenga, *Modern Heterocyclic Chemistry: Vol. 12*2011: John Wiley & Sons.
11. Dewick, P.M., *Essentials of organic chemistry: for students of pharmacy, medicinal chemistry and biological chemistry*2006: John Wiley & Sons.
12. Scarborough, T.D., D.B. Foote, and C.J. Uiterwaal, *Ultrafast resonance-enhanced multiphoton ionization in the azabenzenes: Pyridine, pyridazine, pyrimidine, and pyrazine*. J Chem Phys, 2012. **136**(5): p. 054309.
13. Henderson, A.S., et al., *Nucleophilic Aromatic Substitution (S_NAr) as an Approach to Challenging Carbohydrate–Aryl Ethers*. Org Lett, 2015. **17**(19): p. 4846-4849.
14. Mąkosza, M., *Nucleophilic substitution of hydrogen in electron-deficient arenes, a general process of great practical value*. Chemical Society Reviews, 2010. **39**(8): p. 2855-2868.
15. Walsh, K., H.F. Sneddon, and C.J. Moody, *Amination of Heteroaryl Chlorides: Palladium Catalysis or S_NAr in Green Solvents?* ChemSusChem, 2013. **6**(8): p. 1455-1460.
16. Doležal, M. and K. Kráľová, *Synthesis and evaluation of pyrazine derivatives with herbicidal activity*2011: INTECH Open Access Publisher.
17. Müller, R. and S. Rappert, *Pyrazines: occurrence, formation and biodegradation*. Applied microbiology and biotechnology, 2010. **85**(5): p. 1315-1320.
18. Wagner, R., et al., *Structure-odour-activity relationships of alkylpyrazines*. Zeitschrift für Lebensmitteluntersuchung und-forschung A, 1999. **208**(5-6): p. 308-316.
19. Mahboobi, S., et al., *Synthesis of Naturally Occurring Pyrazine and Imidazole Alkaloids from Botryllus Leachi*RID=" a" ID=" a" Dedicated to Prof. G. Märkl on the occasion of his 75 th birthday. Monatshefte für Chemie/Chemical Monthly, 2004. **135**(3): p. 333-342.

20. Doležal, M., *Biologically active pyrazines of natural and synthetic origin*. Feedback, 1997. **91**.
21. Hwang, H.-I., et al., *Formation of Pyrazines from the Maillard Reaction of Glucose and Lysine- α -amine-15N*. J Agric Food Chem, 1994. **42**(4): p. 1000-1004.
22. Krems, I.J. and P.E. Spoerri, *The pyrazines*. Chemical Reviews, 1947. **40**(2): p. 279-358.
23. Krems, I.J. and P.E. Spoerri, *The pyrazines*. Chem Rev, 1947. **40**(2): p. 279-358.
24. Gastaldi, G., *Pyrazines synthesis*. Gazz Chim Ital, 1921. **51**: p. 233-55.
25. Ghosh, P. and A. Mandal, *Greener approach toward one pot route to pyrazine synthesis*. Green Chemistry Letters and Reviews, 2012. **5**(2): p. 127-134.
26. Shaabani, A. and A. Maleki, *Green and Efficient Synthesis of Quinoxaline Derivatives via Ceric Ammonium Nitrate Promoted and in Situ Aerobic Oxidation of ALPHA.-Hydroxy Ketones and ALPHA.-Keto Oximes in Aqueous Media*. Chemical and Pharmaceutical Bulletin, 2008. **56**(1): p. 79-81.
27. Latha, B.M., V. Sadasivam, and B. Sivasankar, *A highly selective synthesis of pyrazine from ethylenediamine on copper oxide/copper chromite catalysts*. Catalysis Communications, 2007. **8**(7): p. 1070-1073.
28. Anand, R. and B. Rao, *Synthesis of 2-methyl pyrazine over zinc-modified ferrierite (FER) catalysts*. Catalysis Communications, 2002. **3**(1): p. 29-35.
29. Utsukihara, T., et al., *Microwave-assisted synthesis of α -hydroxy ketone and α -diketone and pyrazine derivatives from α -halo and α , α' -dibromo ketone*. Tetrahedron Lett, 2006. **47**(52): p. 9359-9364.
30. Cherng, Y.-J., *Efficient nucleophilic substitution reactions of pyrimidyl and pyrazyl halides with nucleophiles under focused microwave irradiation*. Tetrahedron, 2002. **58**(5): p. 887-890.
31. Wu, G., et al., *One-pot synthesis of useful heterocycles in medicinal chemistry using a cascade strategy*. Green Chemistry, 2012. **14**(3): p. 580-585.
32. Polshettiwar, V. and R.S. Varma, *Greener and expeditious synthesis of bioactive heterocycles using microwave irradiation*. Pure and Applied Chemistry, 2008. **80**(4): p. 777-790.
33. Goya, P., et al., *Heterocyclic structures useful in medicinal chemistry: the case of pyrazino [2, 3-c][1, 2, 6] thiadiazine 2, 2-dioxide*. Farmaco (Società chimica italiana: 1989), 1997. **52**(5): p. 283.
34. Voss, M.E., et al., *Synthesis and SAR studies of imidazo-[1, 2-*c*]-pyrazine Aurora kinase inhibitors with improved off-target kinase selectivity*. Bioorganic & medicinal chemistry letters, 2012. **22**(10): p. 3544-3549.
35. Shi, R., N. Itagaki, and I. Sugawara, *Overview of anti-tuberculosis (TB) drugs and their resistance mechanisms*. Mini reviews in medicinal chemistry, 2007. **7**(11): p. 1177-1185.
36. Judge, V., B. Narasimhan, and M. Ahuja, *A Review of Biological potential of Pyrazinamide derivatives*. Hygeia J Drugs Med, 2012. **4**: p. 1-6.
37. Foks, H., et al., *Studies on pyrazine derivatives III: Antibacterial and antifungal activity of nitrogen heterocyclic compounds obtained by pyrazinamidrazone usage*. Heteroatom Chemistry, 2012. **23**(1): p. 49-58.
38. Doležal, M. and K. Kráľová, *Synthesis and evaluation of pyrazine derivatives with herbicidal activity*. Herbicides, Theory and Applications, 2011: p. 581-610.

39. Deng, L., et al., *Ligustrazine Derivatives. Part 4: Design, Synthesis, and Biological Evaluation of Novel Ligustrazine-based Stilbene Derivatives as Potential Cardiovascular Agents*. *Chemical biology & drug design*, 2012. **79**(5): p. 731-739.
40. Silva, Y.K.C.d., et al., *Synthesis and pharmacological evaluation of pyrazine-*N*-acylhydrazone derivatives designed as novel analgesic and anti-inflammatory drug candidates*. *Bioorganic & medicinal chemistry*, 2010. **18**(14): p. 5007-5015.
41. France, C., et al., *Mirfentanil: pharmacological profile of a novel fentanyl derivative with opioid and nonopioid effects*. *Journal of Pharmacology and Experimental Therapeutics*, 1991. **258**(2): p. 502-510.
42. B Miniyar, P., et al., *Unequivocal role of pyrazine ring in medicinally important compounds: A review*. *Mini Rev Med Chem*, 2013. **13**(11): p. 1607-1625.
43. Dolezal, M. and J. Zitko, *Pyrazine derivatives: a patent review (June 2012–present)*. *Expert Opin Ther Pat*, 2015. **25**(1): p. 33-47.
44. Chauhan, D., et al., *Proteasome inhibitor therapy in multiple myeloma*. *Molecular cancer therapeutics*, 2005. **4**(4): p. 686-692.
45. Dick, L.R. and P.E. Fleming, *Building on bortezomib: second-generation proteasome inhibitors as anti-cancer therapy*. *Drug discovery today*, 2010. **15**(5): p. 243-249.
46. Dias, N., et al., *Synthesis of 2, 6-diphenylpyrazine derivatives and their DNA binding and cytotoxic properties*. *European journal of medicinal chemistry*, 2005. **40**(12): p. 1206-1213.
47. Jiang, B. and X.-H. Gu, *Syntheses and cytotoxicity evaluation of bis (indolyl) thiazole, bis (indolyl) pyrazinone and bis (indolyl) pyrazine: analogues of cytotoxic marine bis (indole) alkaloid*. *Bioorganic & medicinal chemistry*, 2000. **8**(2): p. 363-371.
48. Niculescu-Duvaz, I., et al., *Novel inhibitors of B-RAF based on a disubstituted pyrazine scaffold. Generation of a nanomolar lead*. *Journal of medicinal chemistry*, 2006. **49**(1): p. 407-416.
49. Kassis, P., et al., *Synthesis and biological evaluation of new 3-(6-hydroxyindol-2-yl)-5-(Phenyl) pyridine or pyrazine V-Shaped molecules as kinase inhibitors and cytotoxic agents*. *European journal of medicinal chemistry*, 2011. **46**(11): p. 5416-5434.
50. Whelligan, D.K., et al., *Aminopyrazine inhibitors binding to an unusual inactive conformation of the mitotic kinase Nek2: SAR and structural characterization*. *J Med Chem*, 2010. **53**(21): p. 7682-7698.
51. Zhao, H., J.L. Watkins, and H. Piwnica-Worms, *Disruption of the checkpoint kinase 1/cell division cycle 25A pathway abrogates ionizing radiation-induced S and G2 checkpoints*. *Proceedings of the National Academy of Sciences*, 2002. **99**(23): p. 14795-14800.
52. Li, G., et al., *Synthesis and biological evaluation of 1-(2, 4, 5-trisubstituted phenyl)-3-(5-cyanopyrazin-2-yl) ureas as potent Chk1 kinase inhibitors*. *Bioorg Med Chem Lett*, 2006. **16**(8): p. 2293-2298.
53. Wang, G.T., et al., *1-(5-Chloro-2-alkoxyphenyl)-3-(5-cyano-pyrazi-2-yl) ureas as potent and selective inhibitors of Chk1 kinase: synthesis, preliminary SAR, and biological activities*. *J Med Chem*, 2005. **48**(9): p. 3118-3121.
54. Han, Y., et al., *Novel pyrazinone mono-amides as potent and reversible caspase-3 inhibitors*. *Bioorg Med Chem Lett*, 2005. **15**(4): p. 1173-1180.

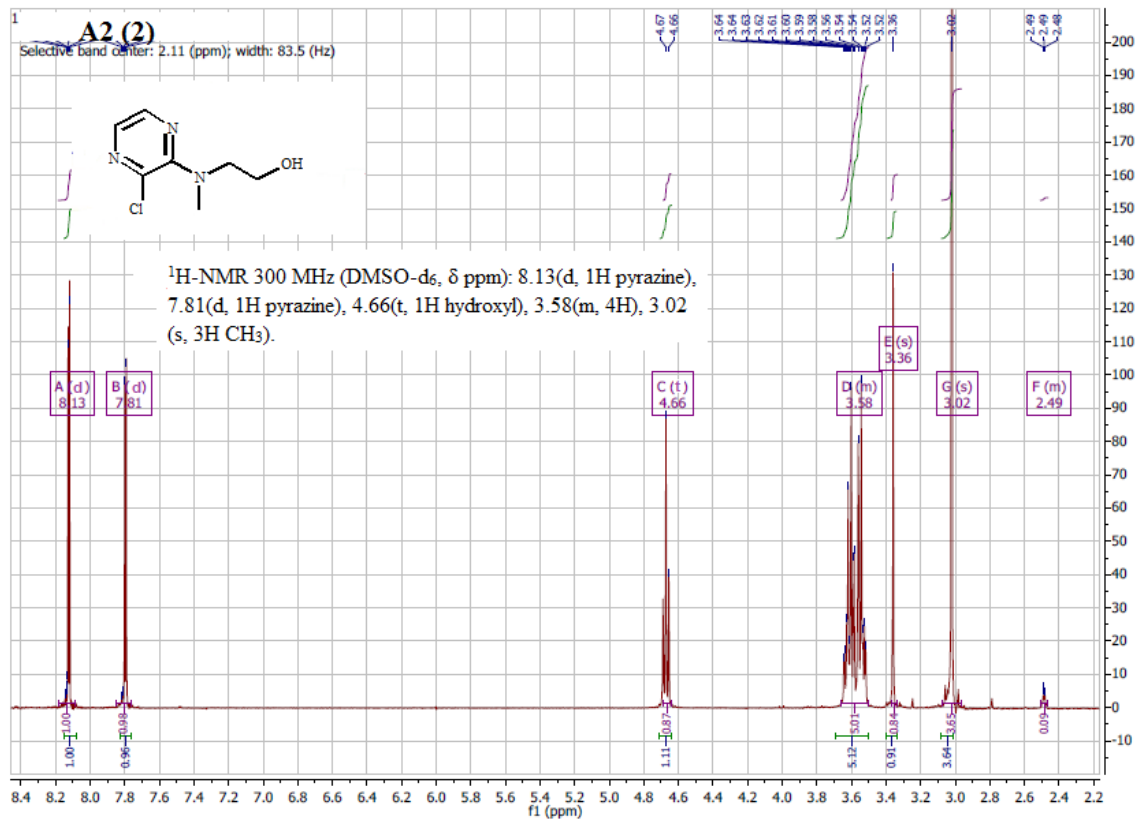
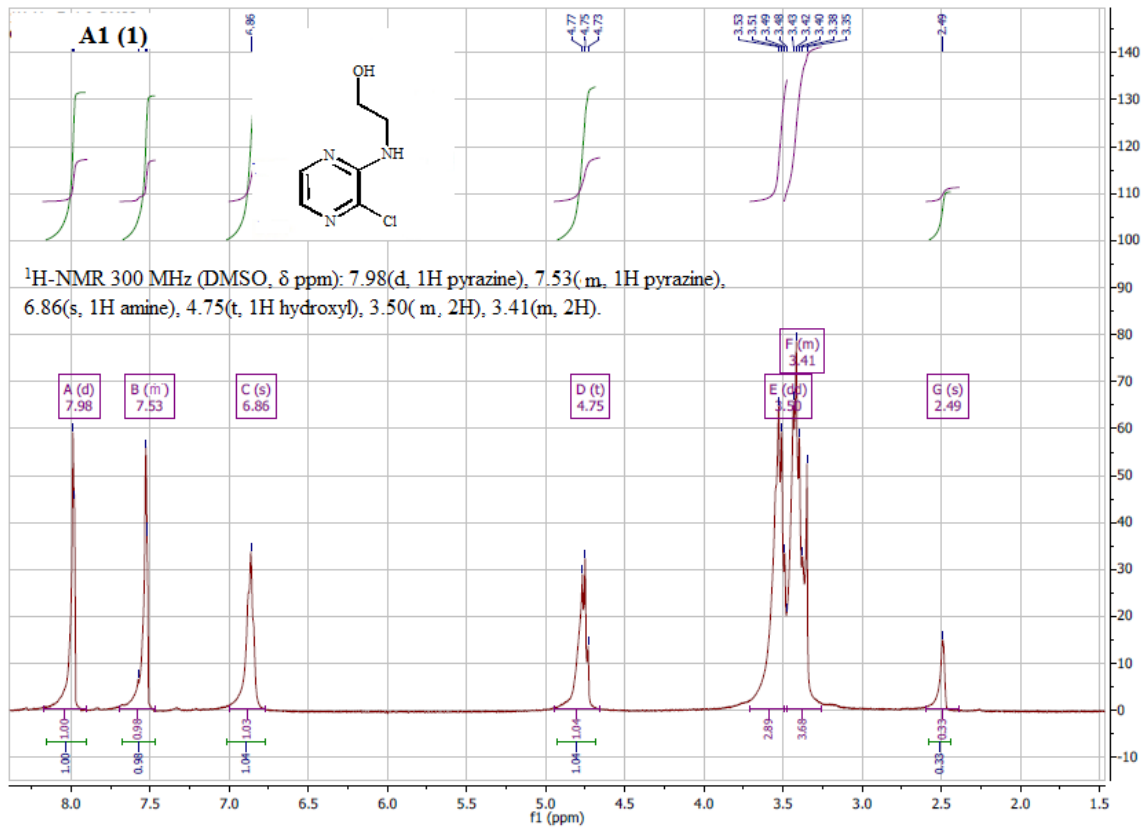
55. Kerekes, A.D., et al., *Aurora kinase inhibitors based on the imidazo [1, 2-a] pyrazine core: fluorine and deuterium incorporation improve oral absorption and exposure*. J Med Chem, 2010. **54**(1): p. 201-210.
56. Belanger, D.B., et al., *Discovery of imidazo [1, 2-a] pyrazine-based Aurora kinase inhibitors*. Bioorg Med Chem Lett, 2010. **20**(17): p. 5170-5174.
57. GIL, I.K. and S. Demirayak, *Synthesis of some 2, 3, 6, 8-tetraarylimidazo [1, 2-a] pyrazine derivatives by using either reflux or microwave irradiation method, and investigation their anticancer activities*. Turk J Chem, 2011. **35**: p. 13-24.
58. Currie, K.S., et al., *Imidazo [1, 2-a] pyrazin-8-ylamines, method of making, and method of use thereof*, 2005, Google Patents.
59. DeSimone, R.W., et al., *6-aryl-imidazo [1, 2-a] pyrazin-8-ylamines, method of making, and method of use thereof*, 2007, Google Patents.
60. Gong, Y.-D., et al., *A novel 3-arylethynyl-substituted pyrido [2, 3-< i> b</i>] pyrazine derivatives and pharmacophore model as Wnt2/ β -catenin pathway inhibitors in non-small-cell lung cancer cell lines*. Bioorganic & medicinal chemistry, 2011. **19**(18): p. 5639-5647.
61. Dorsch, D., et al., *Pyrido [2, 3 - b] pyrazine derivatives and their therapeutical uses*, 2012, Google Patents.
62. Chekmarev, D.S., et al., *Highly selective substitutions in 2, 3-dichloropyrazine. A novel general approach to aloisines*. Tetrahedron, 2006. **62**(42): p. 9919-9930.
63. Dubinina, G., et al., *Novel 5, 7-disubstituted 6-amino-5H-pyrrolo [3, 2-b] pyrazine-2, 3-dicarbonitriles, the promising protein kinase inhibitors with antiproliferative activity*. European journal of medicinal chemistry, 2006. **41**(6): p. 727-737.
64. Everitt, S., et al., *Compounds useful as inhibitors of atr kinase*, 2012, Google Patents.
65. Mazanetz, M.P. and P.M. Fischer, *Untangling tau hyperphosphorylation in drug design for neurodegenerative diseases*. Nature reviews Drug discovery, 2007. **6**(6): p. 464-479.
66. Morgan, D.O., *The cell cycle: principles of control* 2007: New Science Press.
67. Akin, S., et al., *A novel targeted therapy in breast cancer: Cyclin dependent kinase inhibitors*. Journal of BU ON.: official journal of the Balkan Union of Oncology, 2014. **19**(1): p. 42.
68. Bártoová, I., et al., *Activation and inhibition of cyclin-dependent kinase-2 by phosphorylation; a molecular dynamics study reveals the functional importance of the glycine-rich loop*. Protein science, 2004. **13**(6): p. 1449-1457.
69. Saeed, U., N. Jalal, and M. Ashraf, *Roles of cyclin dependent kinase and cdk-activating kinase in cell cycle regulation: contemplation of intracellular interactions and functional characterization*. Global Journal of Medical Research, 2013. **12**(11).
70. Anastassiadis, T., et al., *Comprehensive assay of kinase catalytic activity reveals features of kinase inhibitor selectivity*. Nature biotechnology, 2011. **29**(11): p. 1039-1045.
71. Mariaule, G. and P. Belmont, *Cyclin-dependent kinase inhibitors as marketed anticancer drugs: where are we now? A short survey*. Molecules, 2014. **19**(9): p. 14366-14382.
72. Mettey, Y., et al., *Aloisines, a new family of CDK/GSK-3 inhibitors. SAR study, crystal structure in complex with CDK2, enzyme selectivity, and cellular effects*. J Med Chem, 2003. **46**(2): p. 222-236.

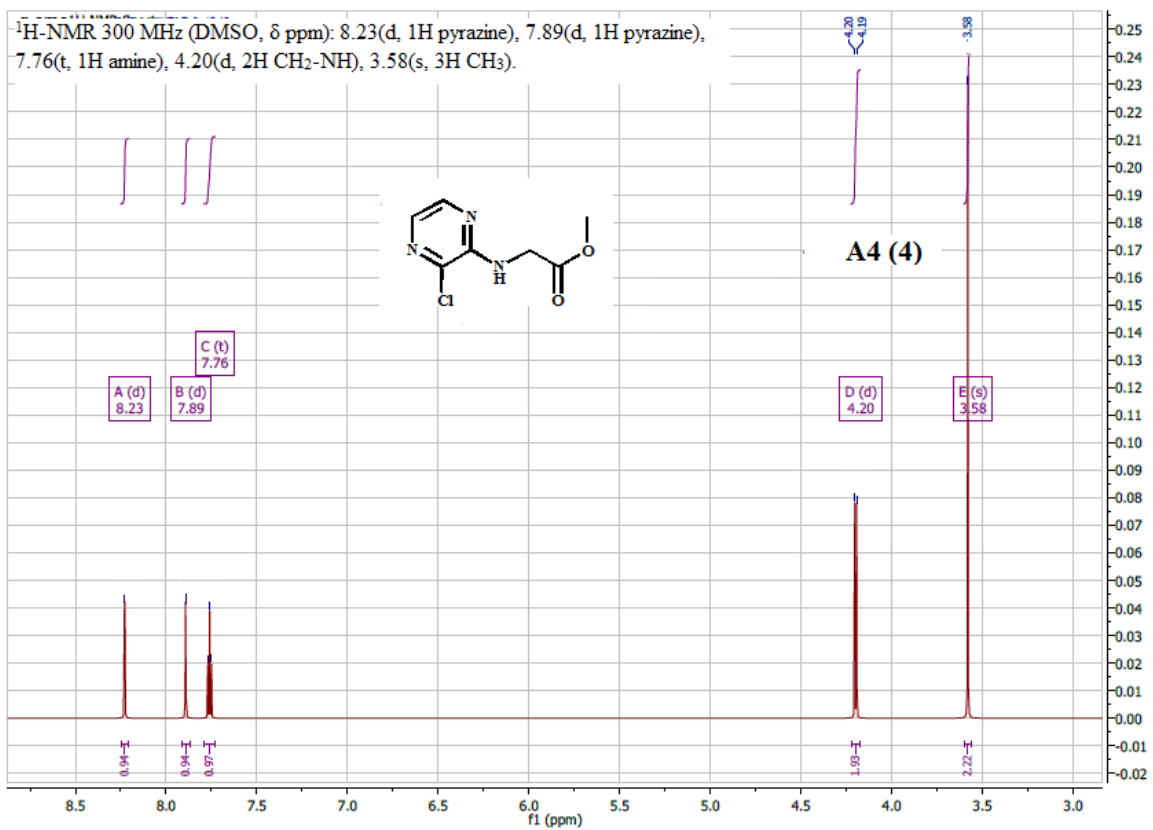
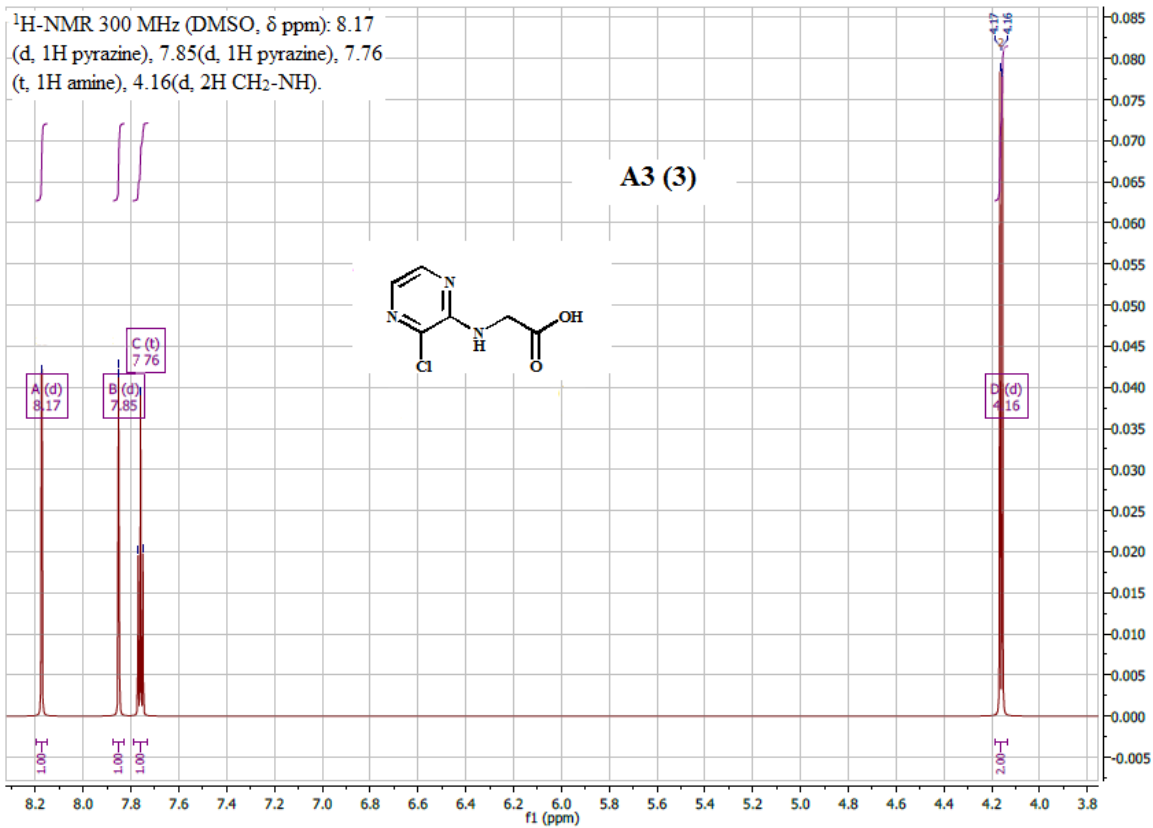
73. Fischer, P.M., *Functions and pharmacological inhibitors of cyclin-dependent kinases (CDKs)*. Cell Transm, 2003. **19**: p. 3-9.
74. Zimhony, O., et al., *Pyrazinamide inhibits the eukaryotic-like fatty acid synthetase I (FASI) of Mycobacterium tuberculosis*. Nature medicine, 2000. **6**(9): p. 1043-1047.
75. Singh, S.B. and J.E. Tomassini, *Synthesis of natural flutimide and analogous fully substituted pyrazine-2, 6-diones, endonuclease inhibitors of influenza virus*. J Org Chem, 2001. **66**(16): p. 5504-5516.
76. Furuta, Y., et al., *T-705 (favipiravir) and related compounds: Novel broad-spectrum inhibitors of RNA viral infections*. Antiviral Res, 2009. **82**(3): p. 95-102.
77. Edelman, M.J., et al., *Phase II trial of pyrazine diazohydroxide in androgen-independent prostate cancer*. Invest New Drugs, 1998. **16**(2): p. 179-182.
78. Ambrogi, V., et al., *Anti-lipolytic activity of a series of pyrazine-N-oxides*. Eur J Med Chem, 1980. **15**(2): p. 157-163.
79. Roblin Jr, R.O., et al., *Chemotherapy. II. Some Sulfanilamido Heterocycles1*. J Am Chem Soc, 1940. **62**(8): p. 2002-2005.
80. Ambrogi, V., et al., *Synthesis of pyrazine derivatives as potential hypoglycemic agents*. J Pharm Sci, 1972. **61**(9): p. 1483-1486.
81. Qi, C., et al., *Glipizide, an antidiabetic drug, suppresses tumor growth and metastasis by inhibiting angiogenesis*. Oncotarget, 2014. **5**(20): p. 9966.
82. Adams, J. and M. Kauffman, *Development of the proteasome inhibitor Velcade™(Bortezomib)*. Cancer investigation, 2004. **22**(2): p. 304-311.
83. Coe, J.W., et al., *Varenicline: an $\alpha 4\beta 2$ nicotinic receptor partial agonist for smoking cessation*. J Med Chem, 2005. **48**(10): p. 3474-3477.
84. Cragoe Jr, E.J., O.W. Woltersdorf Jr, and M.G. Bock, *Pyrazine-2-carbonyloxyguanidines*, 1979, Google Patents.
85. Zeuzem, S., et al., *Telaprevir for retreatment of HCV infection*. New England Journal of Medicine, 2011. **364**(25): p. 2417-2428.
86. Foreman, M.M., et al., *In vivo pharmacological effects of JZP-4, a novel anticonvulsant, in models for anticonvulsant, antimania and antidepressant activity*. Pharmacology Biochemistry and Behavior, 2008. **89**(4): p. 523-534.
87. Cotrel, C., C. Jeanmart, and M.N. Messer, *Pyrrolo (3, 4-b) pyrazine derivatives*, 1975, Google Patents.
88. Clapper, M.L., *Chemopreventive activity of oltipraz*. Pharmacology & therapeutics, 1998. **78**(1): p. 17-27.
89. Gluchowski, C., *(2-imidazolin-2-ylamino) tetrahydroquinoxalines and methods for using same*, 1994, Google Patents.
90. Poroikov, V. and D. Filimonov, *Computer-aided prediction of biological activity spectra. Application for finding and optimization of new leads*. Rational Approaches to Drug Design, 2001: p. 403-407.
91. De Britto, A.J., T. Raj, and D.A. Chelliah, *Prediction of biological activity spectra for few anticancer drugs derived from plant sources*. Ethnobotanical Leaflets, 2008. **2008**(1): p. 109.

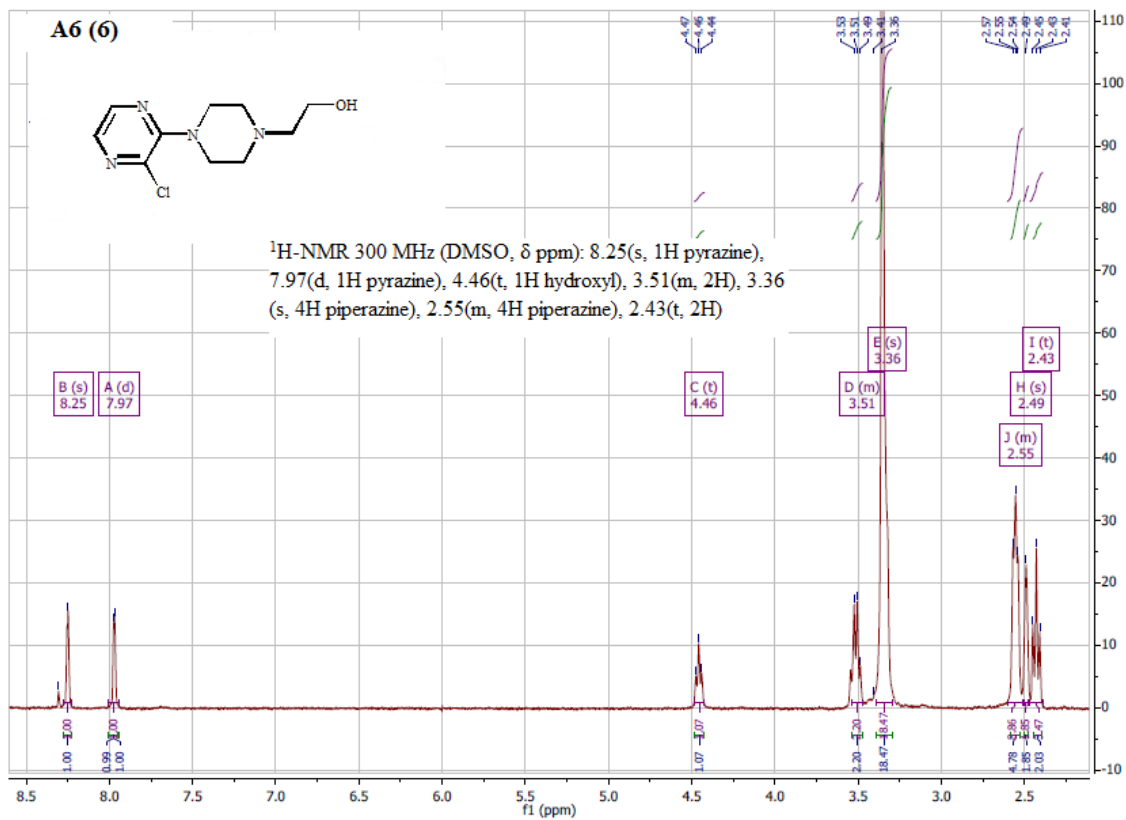
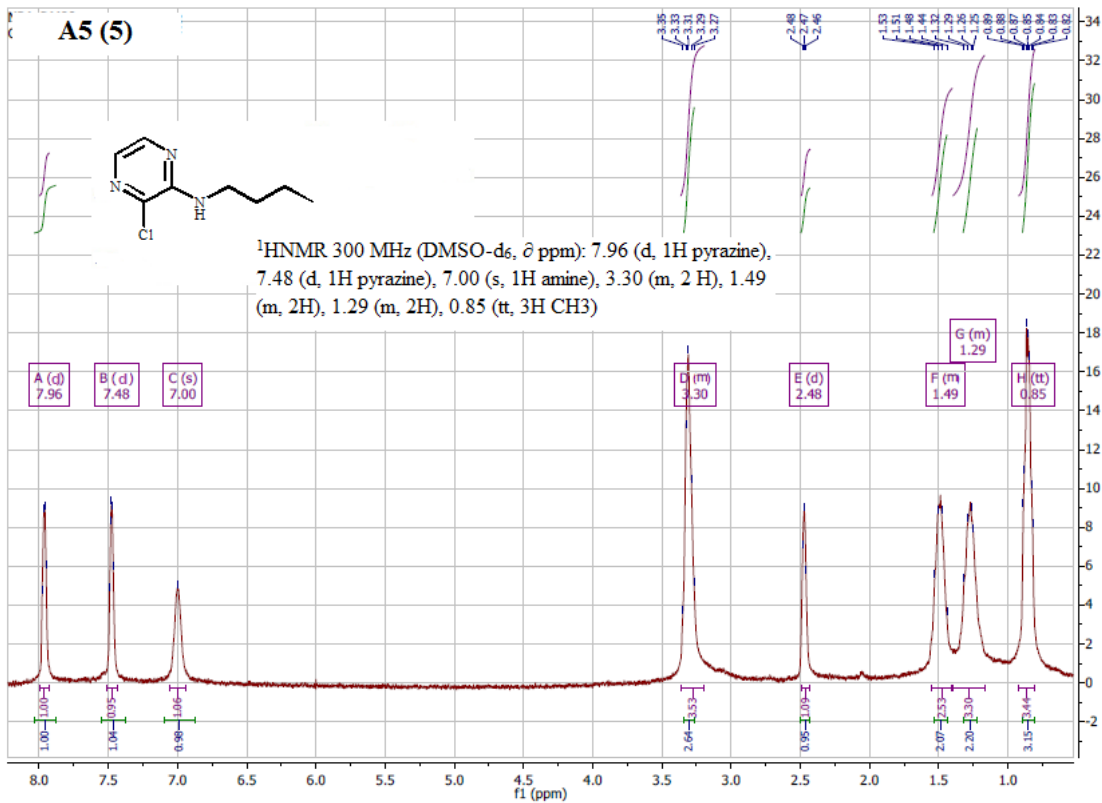
92. Burov, Y.V., V. Poroikov, and L. Korolchenko, *National system for registration and biological testing of chemical compounds: facilities for new drugs search*. Bull. Natl. Center for Biologically Active Compounds (Rus.), 1990. **1**: p. 4-25.
93. Avidon, V., *The criteria of chemical structures similarity and the principles for design of description language for chemical information processing of biologically active compounds*. Chim.-Pharm. J.(Rus), 1974. **8**: p. 22-25.
94. Golender, V.E. and A.B. Rozenblit, *Logical and combinatorial algorithms for drug design*. Vol. 6. 1983: Research Studies Press Letchworth, Hertfordshire, England.
95. Lagunin, A., et al., *PASS: prediction of activity spectra for biologically active substances*. Bioinformatics, 2000. **16**(8): p. 747-748.
96. Poroikov, V., D. Filimonov, and A. Boudunova. *Computer assisted prediction of biological activity spectra: estimating the effectivity of use in high throughput screening*. in *XIVth International Symposium on Medicinal Chemistry (8-12 September, Maastricht)*. 1996.
97. Poroikov, V., D. Filimonov, and A. Budanova, *Comparison of the results of prediction of the spectrum of biological activity of chemical compounds by experts and the PASS computer system*. AUTOMATIC DOCUMENTATION AND MATHEMATICAL LINGUISTICS TRANSLATIONS OF SELECTED ARTICLES FROM NAUCHNO-TEKHNICHESKAIA INFORMATSIIA, 1993. **27**: p. 40-40.
98. De Wael, F., et al., *In vitro and in vivo studies of 6, 8-(diaryl) imidazo [1, 2-a] pyrazin-3 (7H)-ones as new antioxidants*. Bioorg Med Chem, 2009. **17**(13): p. 4336-4344.
99. Jiang, B., et al., *Synthesis and cytotoxicity evaluation of novel indolylpyrimidines and indolylpyrazines as potential antitumor agents*. Bioorg Med Chem, 2001. **9**(5): p. 1149-1154.
100. Stadler, A.M., et al., *Rull Multinuclear Metallosupramolecular Rack-Type Architectures of Polytopic Hydrazone-Based Ligands: Synthesis, Structural Features, Absorption Spectra, Redox Behavior, and Near-Infrared Luminescence*. Chemistry-A European Journal, 2010. **16**(19): p. 5645-5660.
101. Ozaki, T. and A. Nakagawara, *Role of p53 in cell death and human cancers*. Cancers, 2011. **3**(1): p. 994-1013.
102. Greenblatt, M., et al., *Mutations in the p53 tumor suppressor gene: clues to cancer etiology and molecular pathogenesis*. Cancer Res, 1994. **54**(18): p. 4855-4878.
103. Poroikov, V., et al., *Robustness of biological activity spectra predicting by computer program PASS for noncongeneric sets of chemical compounds*. Journal of chemical information and computer sciences, 2000. **40**(6): p. 1349-1355.
104. Sadym, A., et al., *Prediction of biological activity spectra via the Internet*. SAR and QSAR in Environmental Research, 2003. **14**(5-6): p. 339-347.

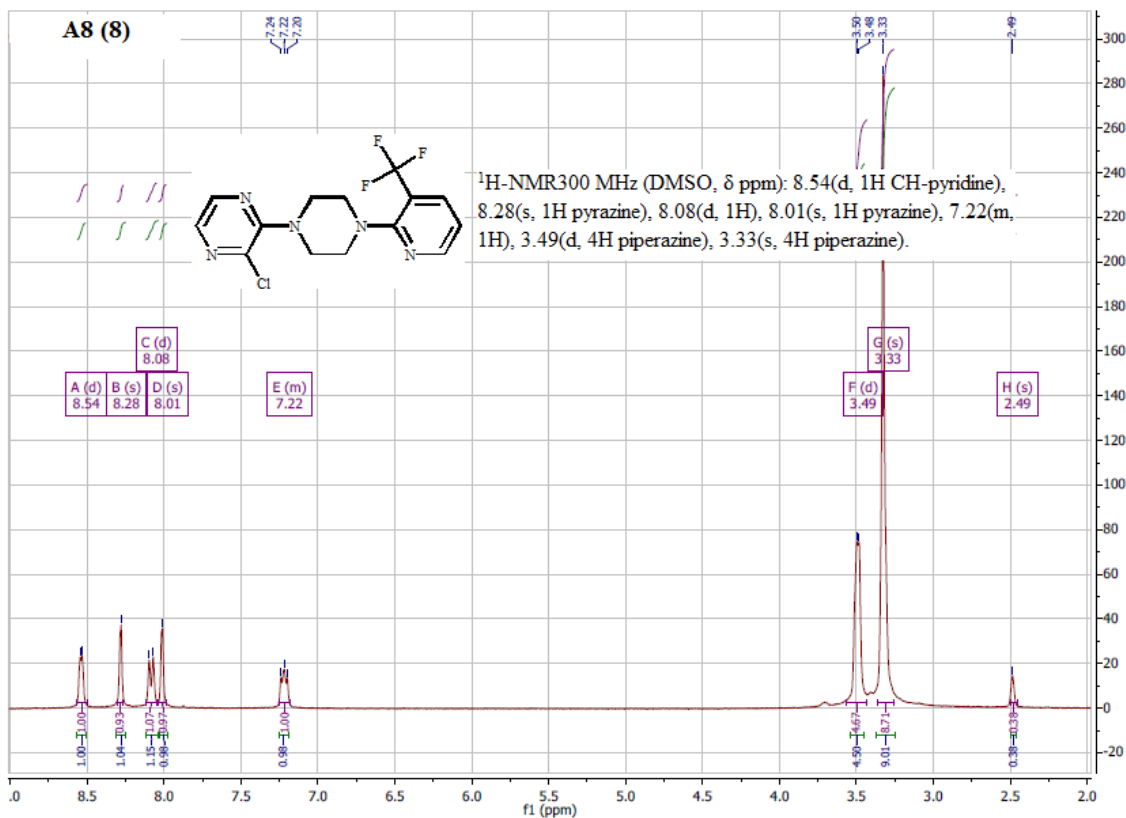
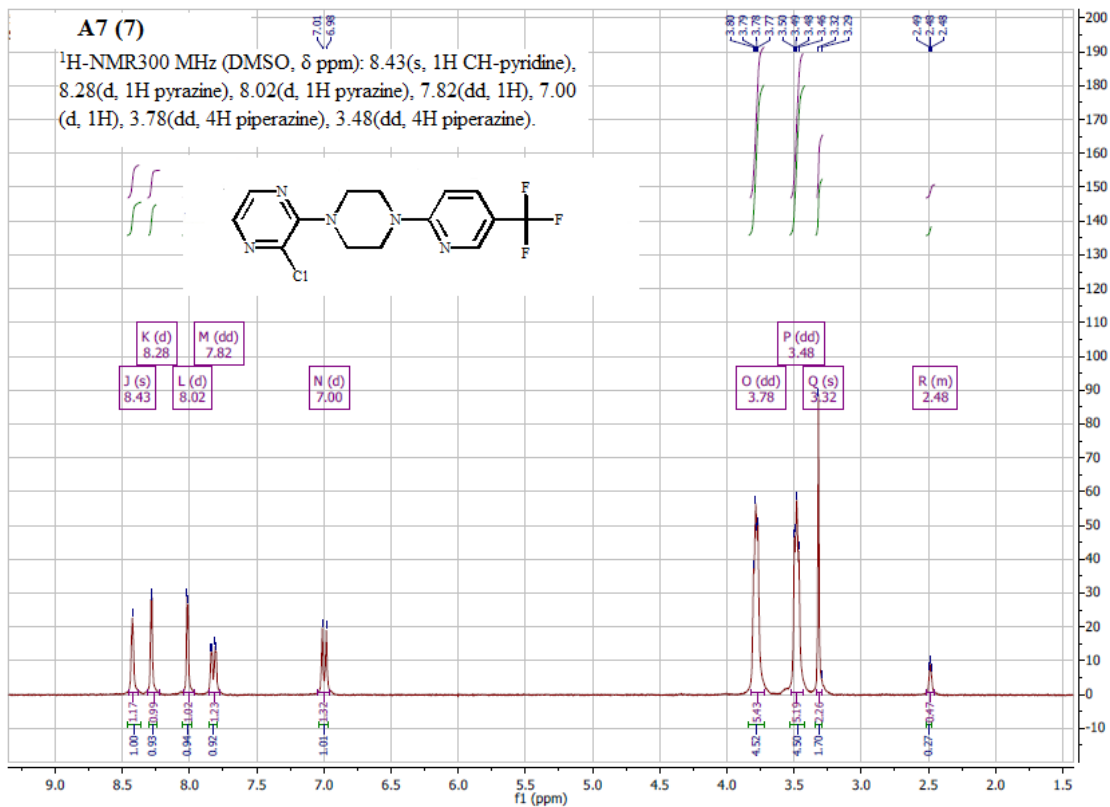
Chapter Six

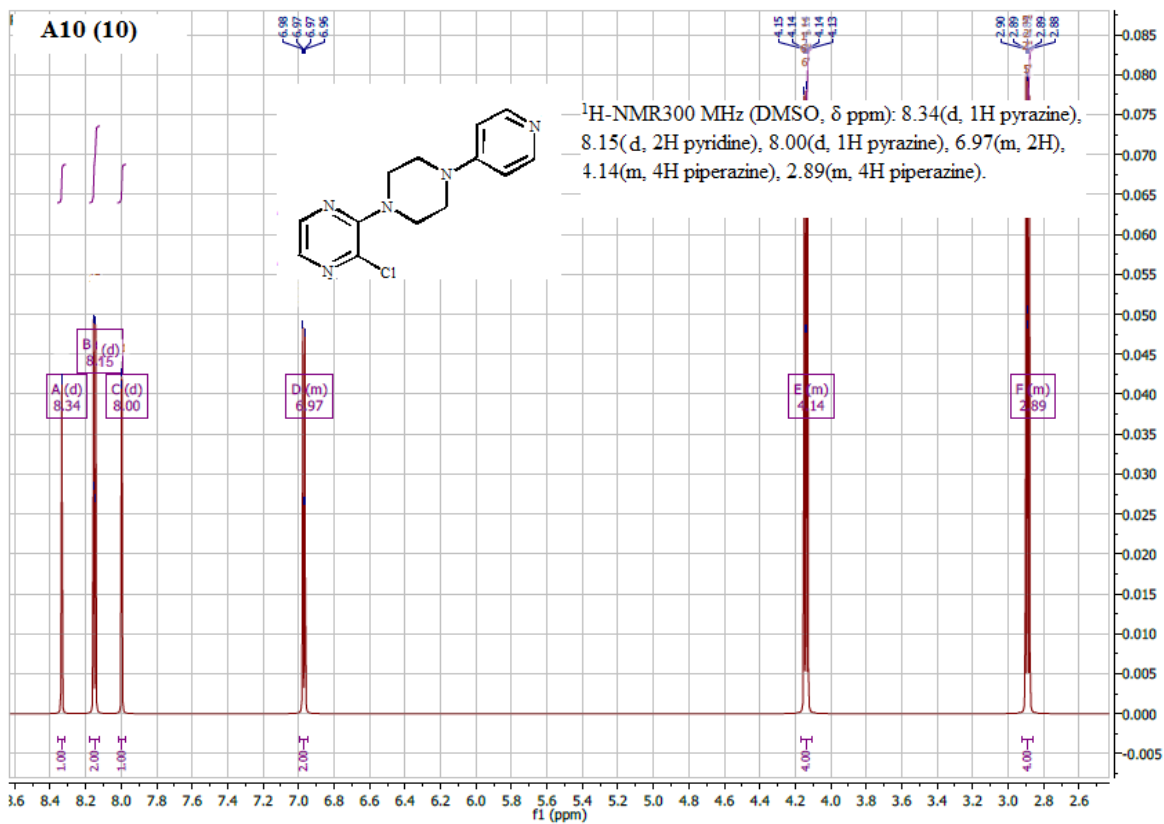
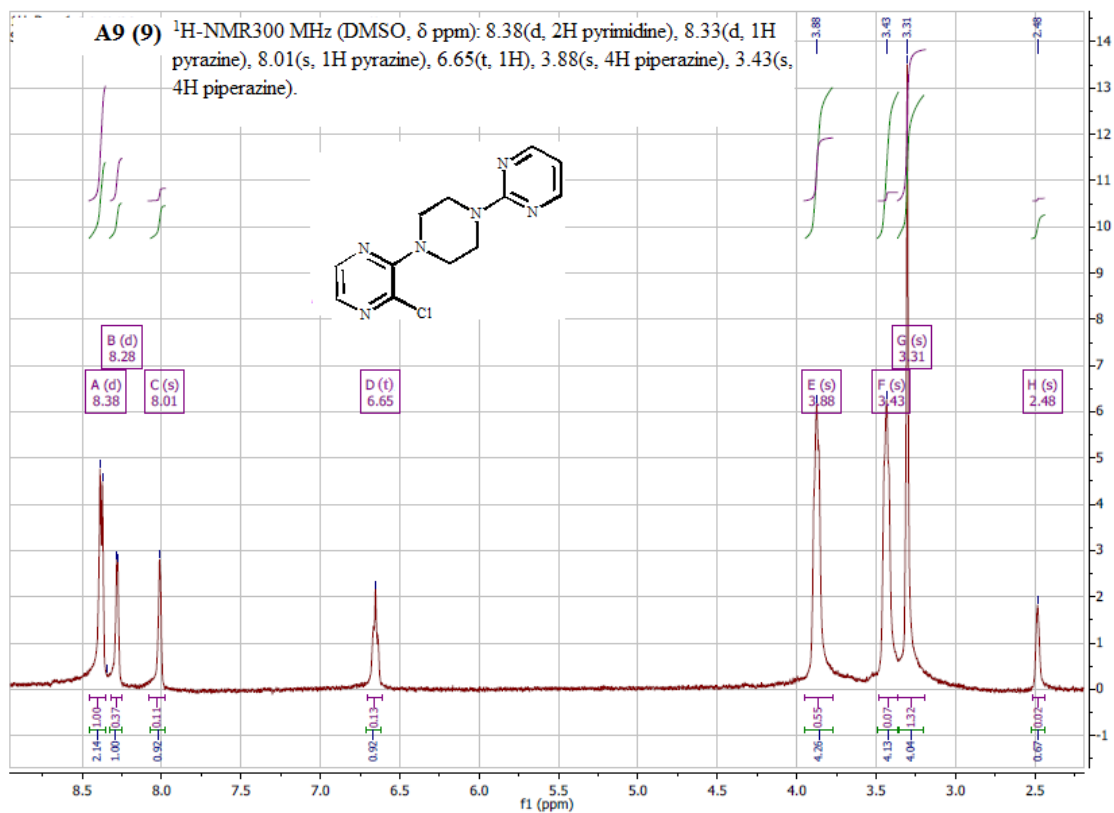
Appendices

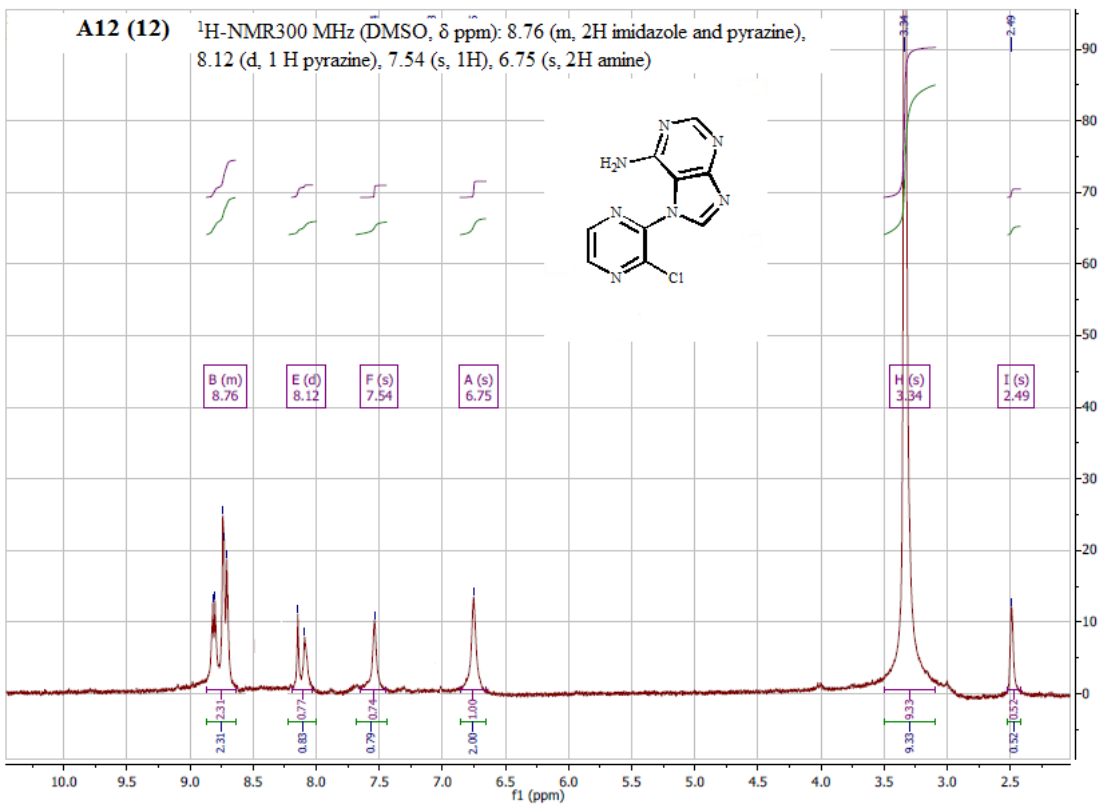
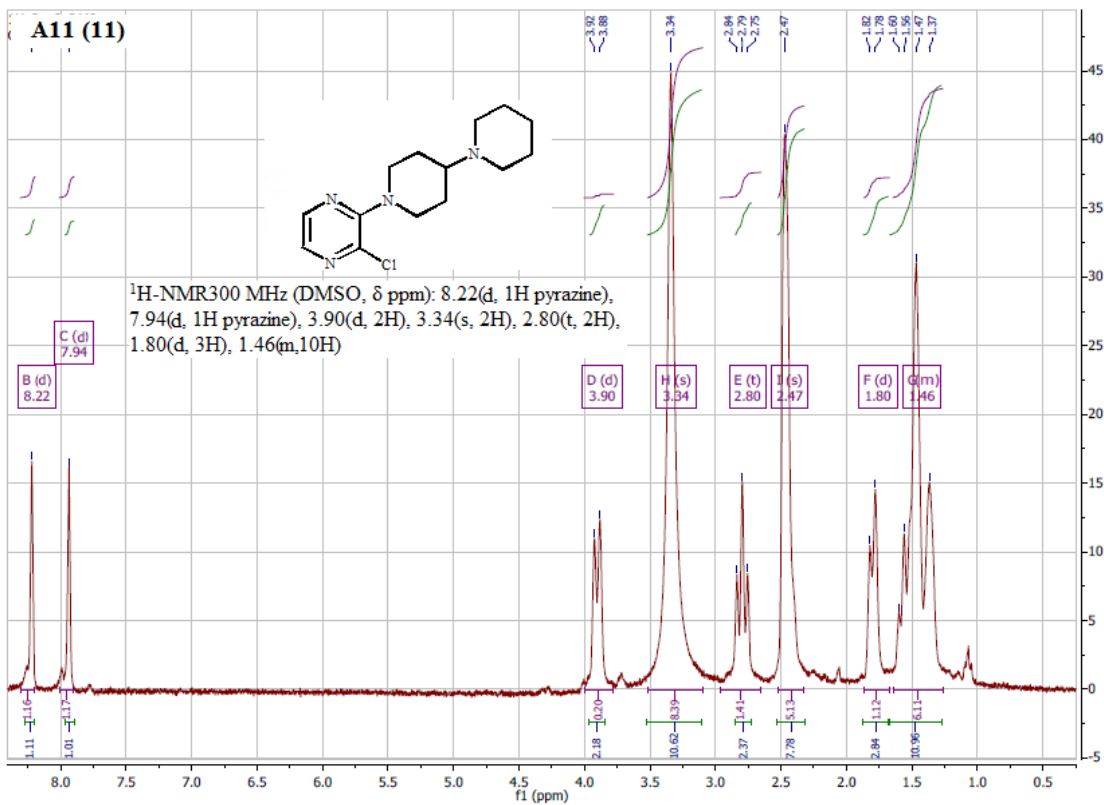


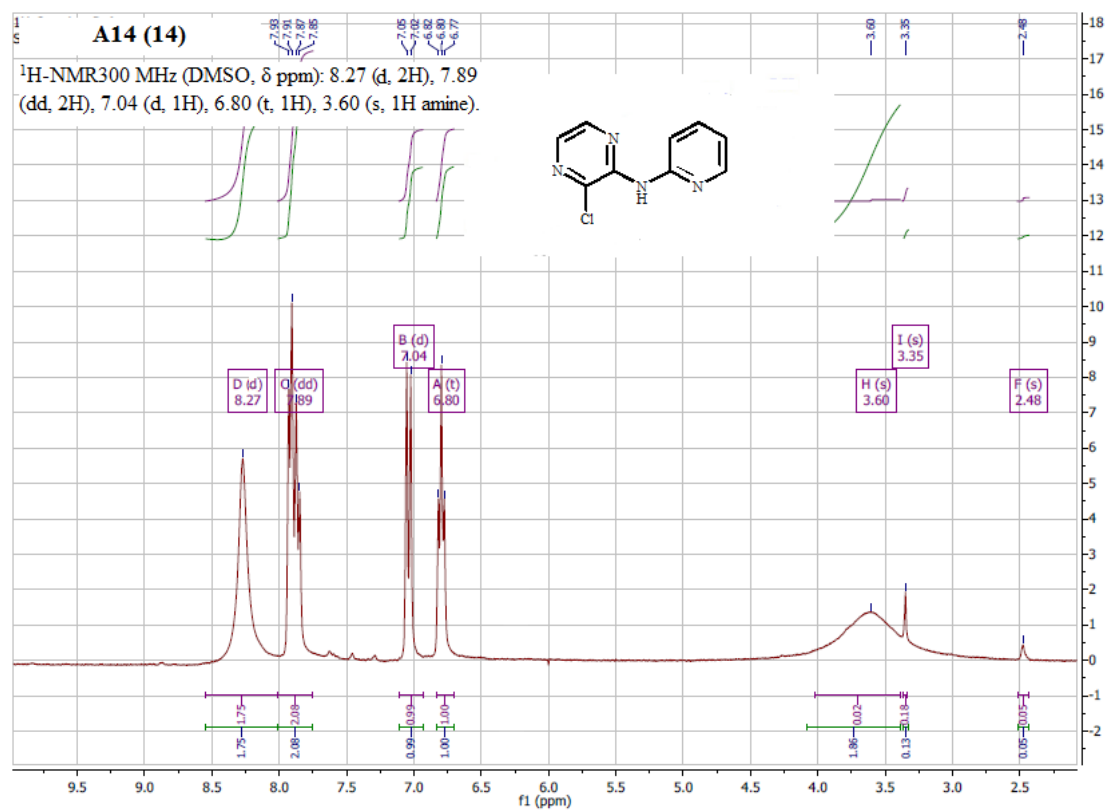
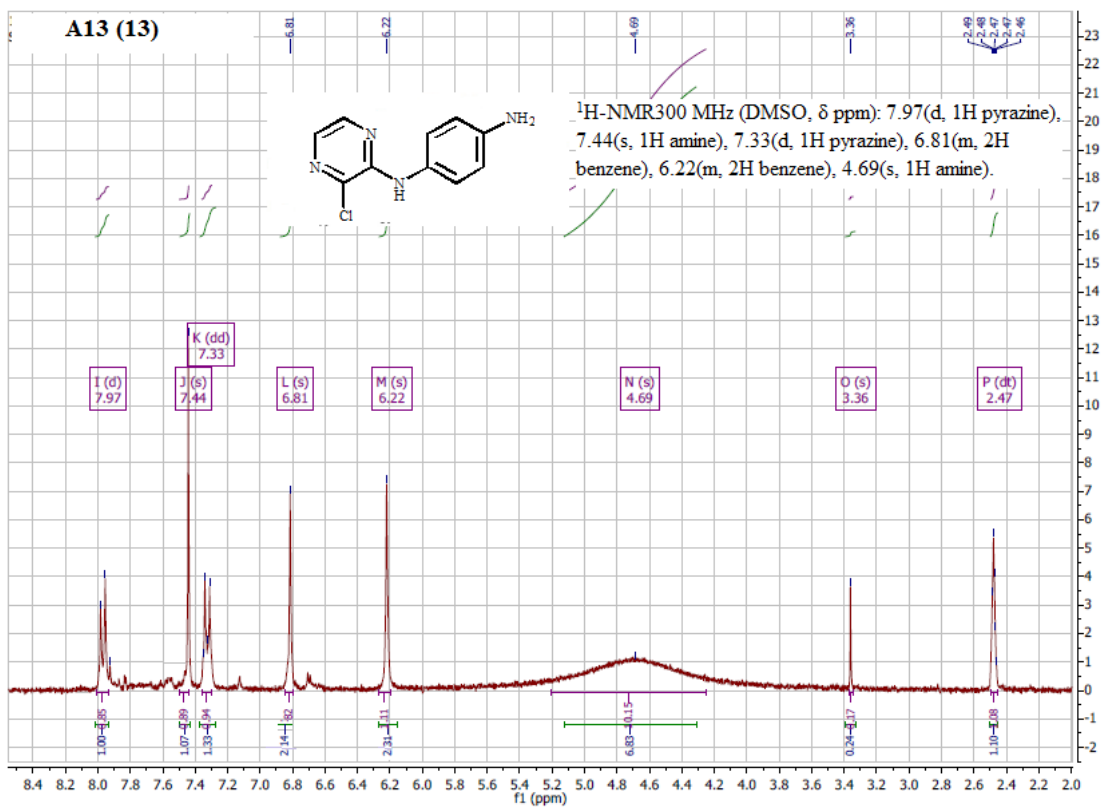


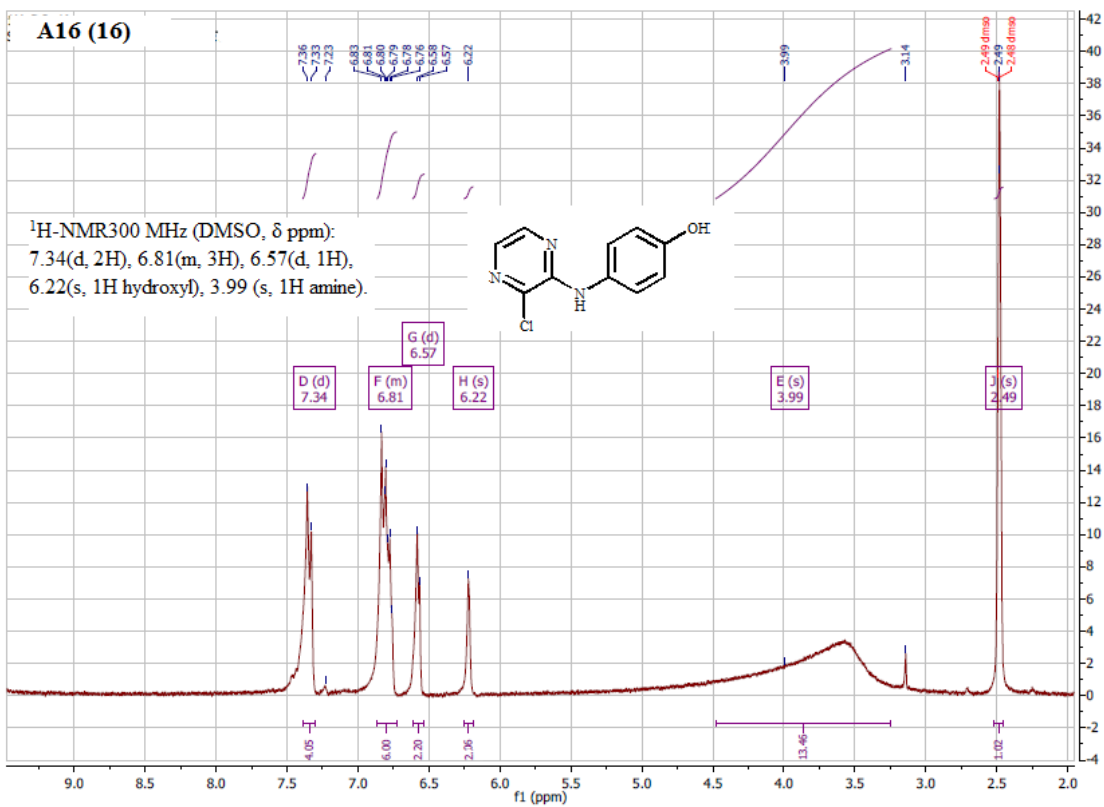
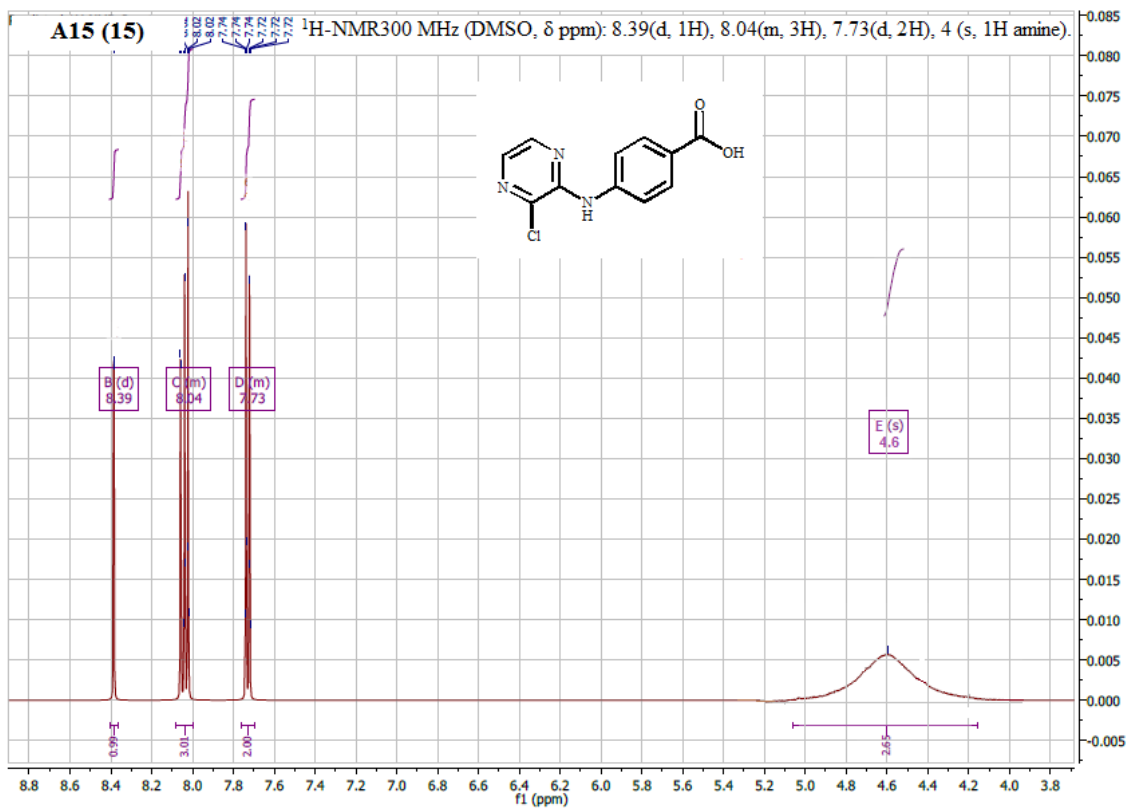


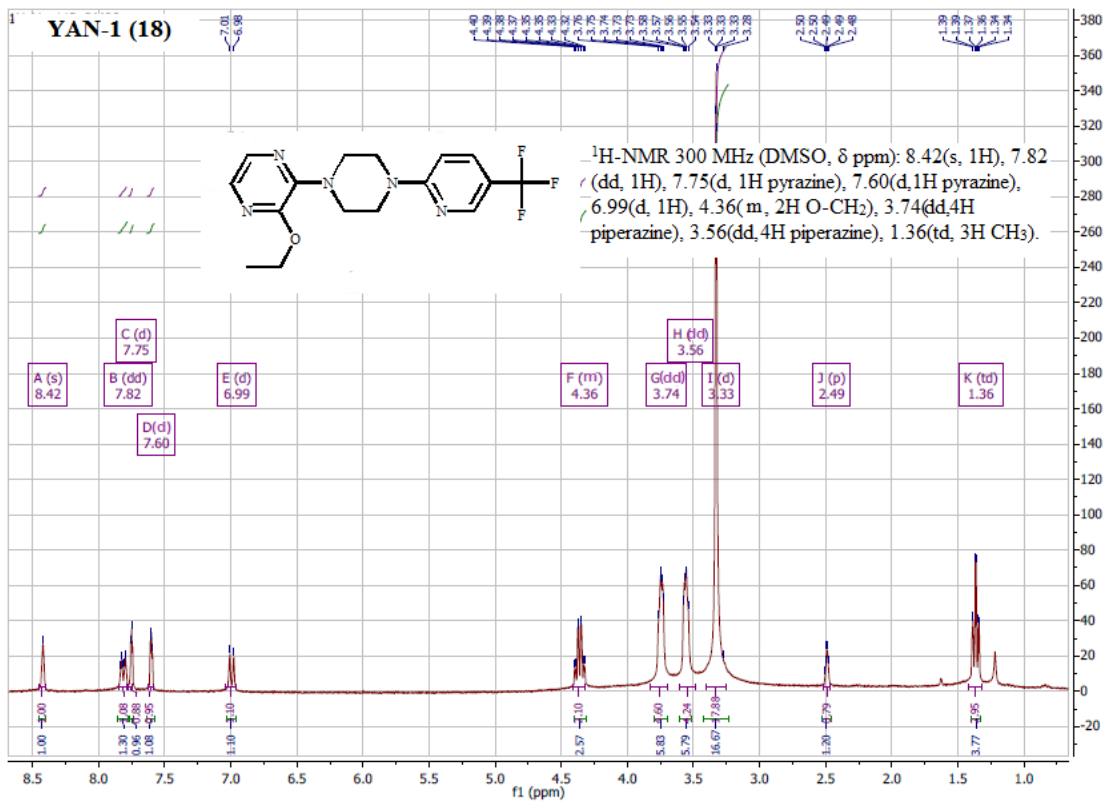
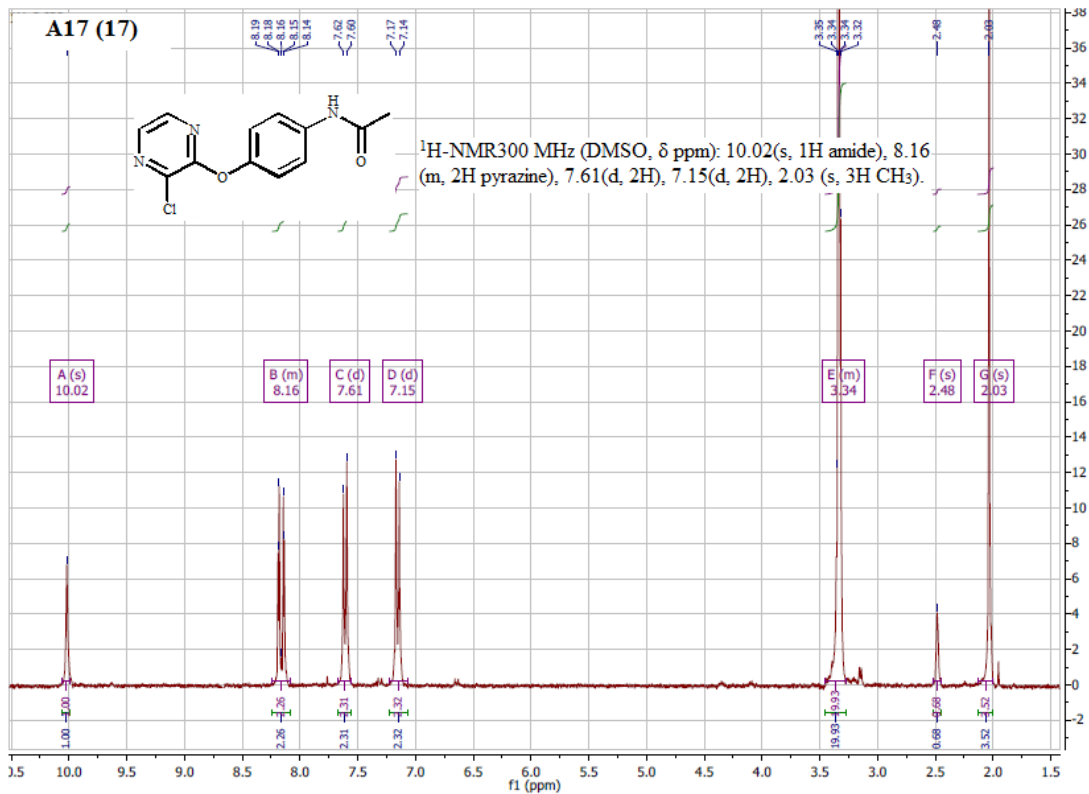


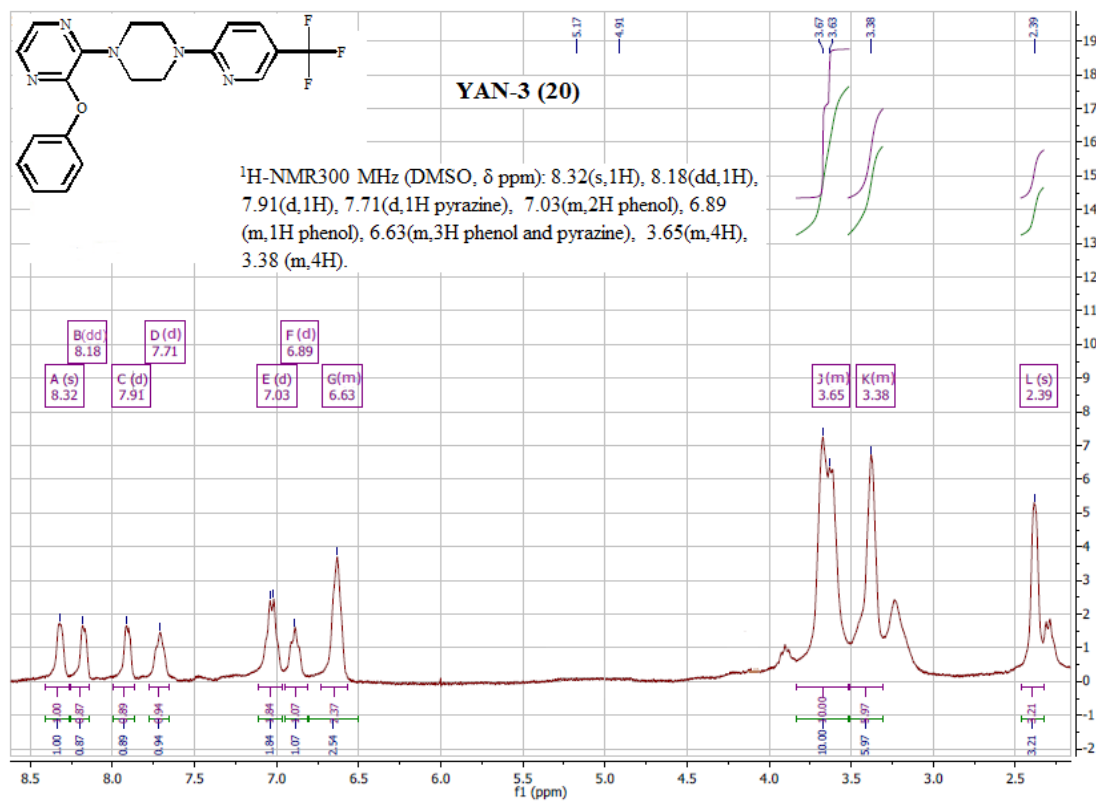
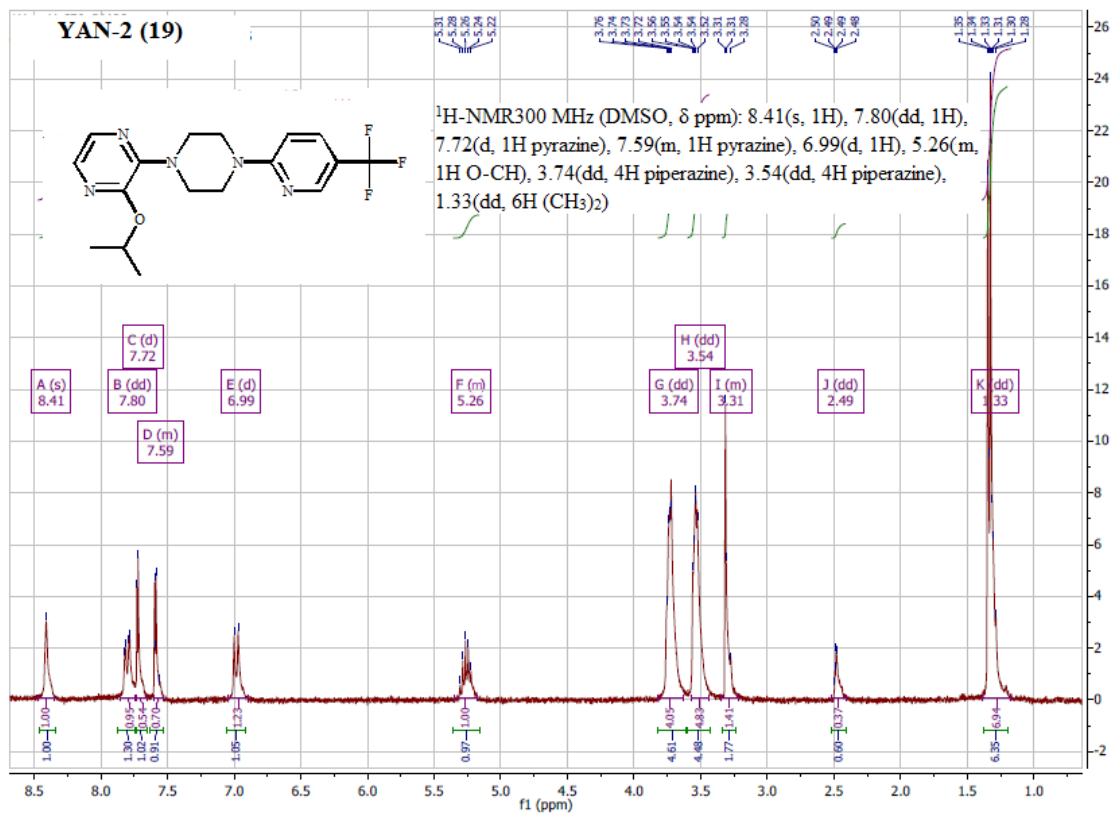


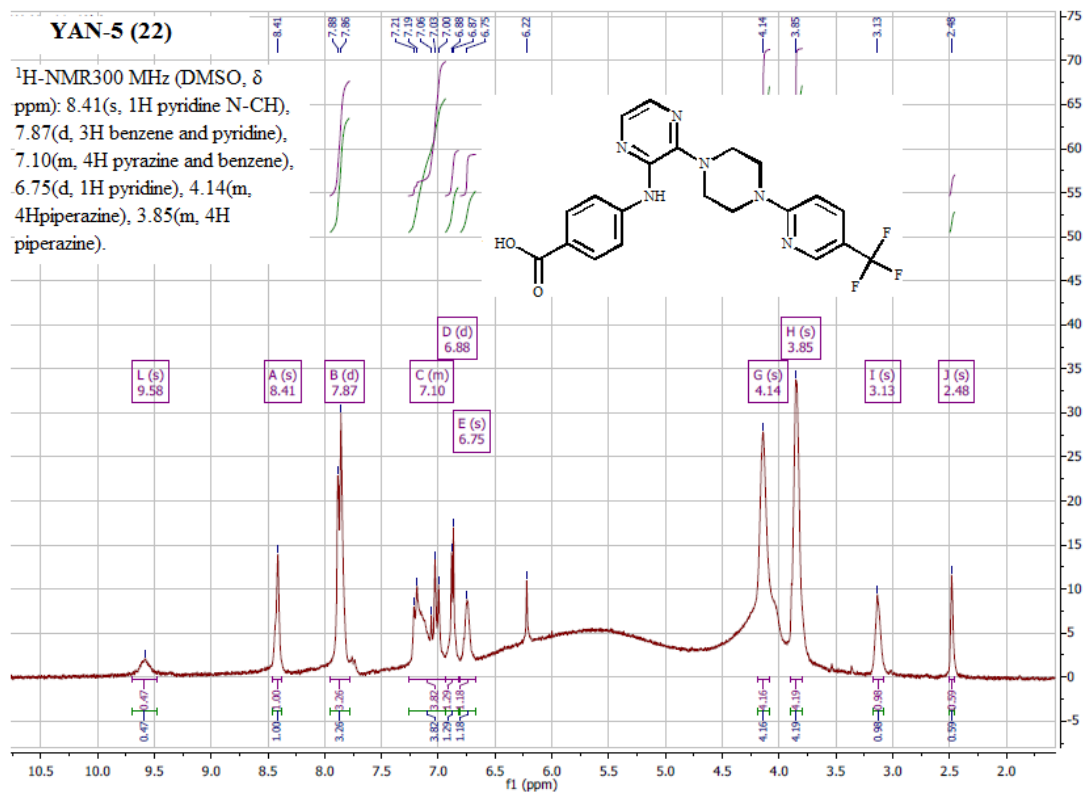
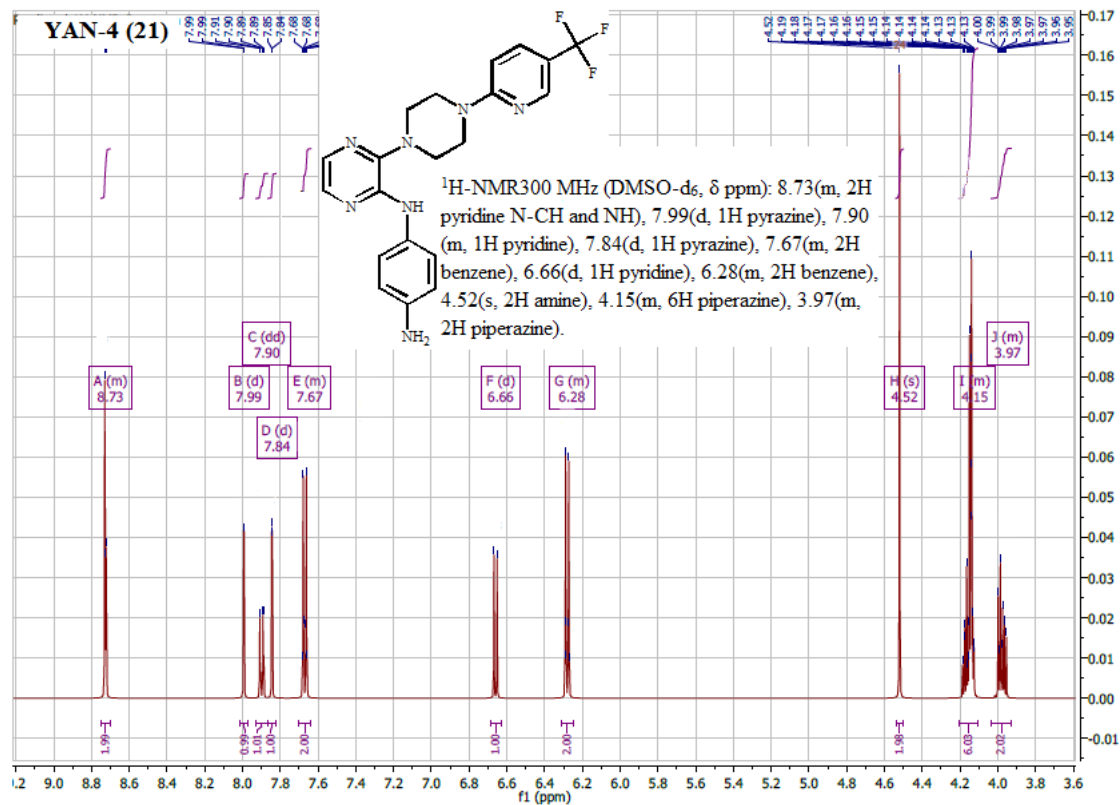


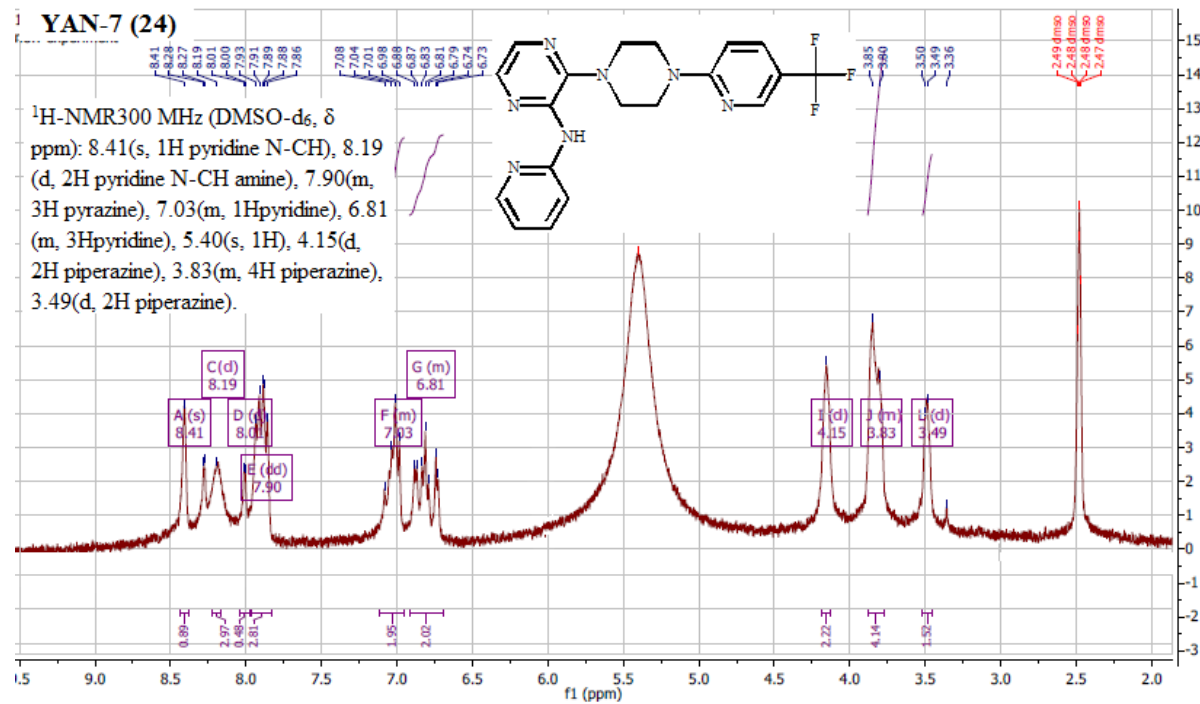
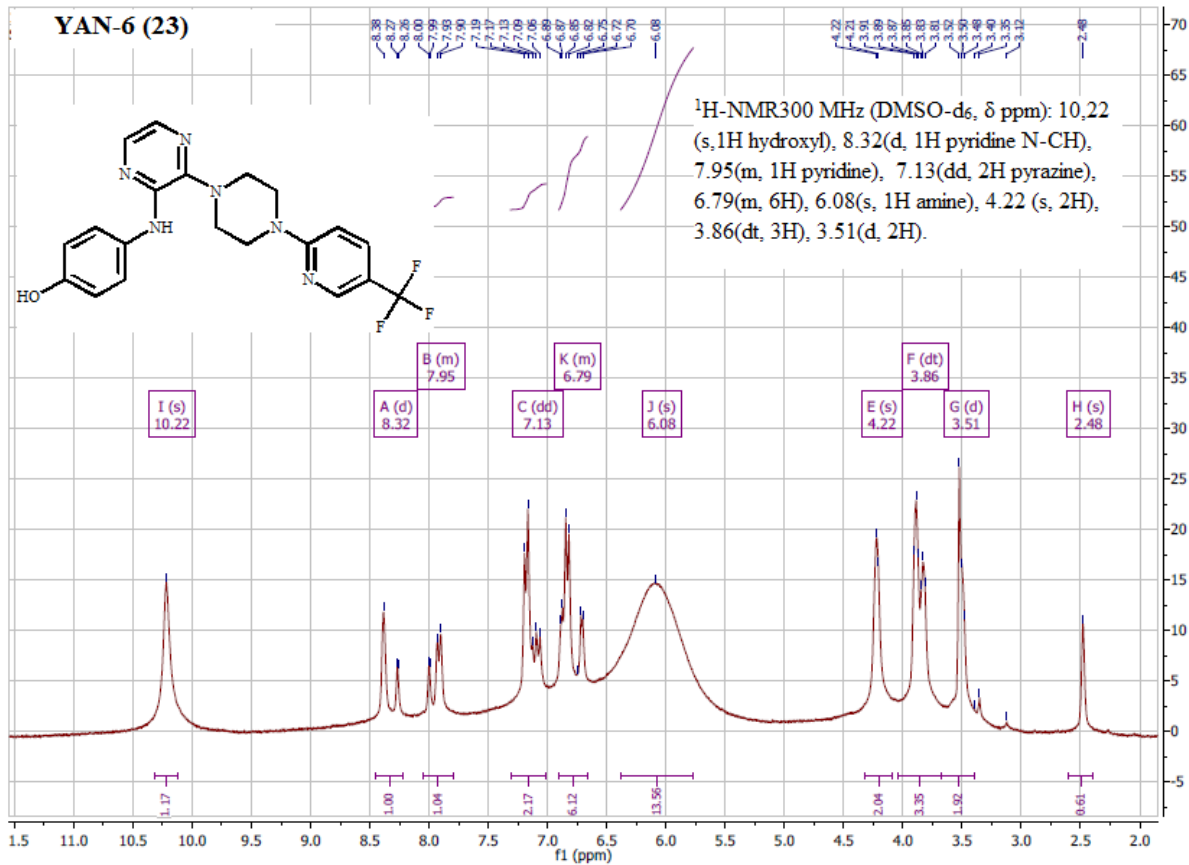


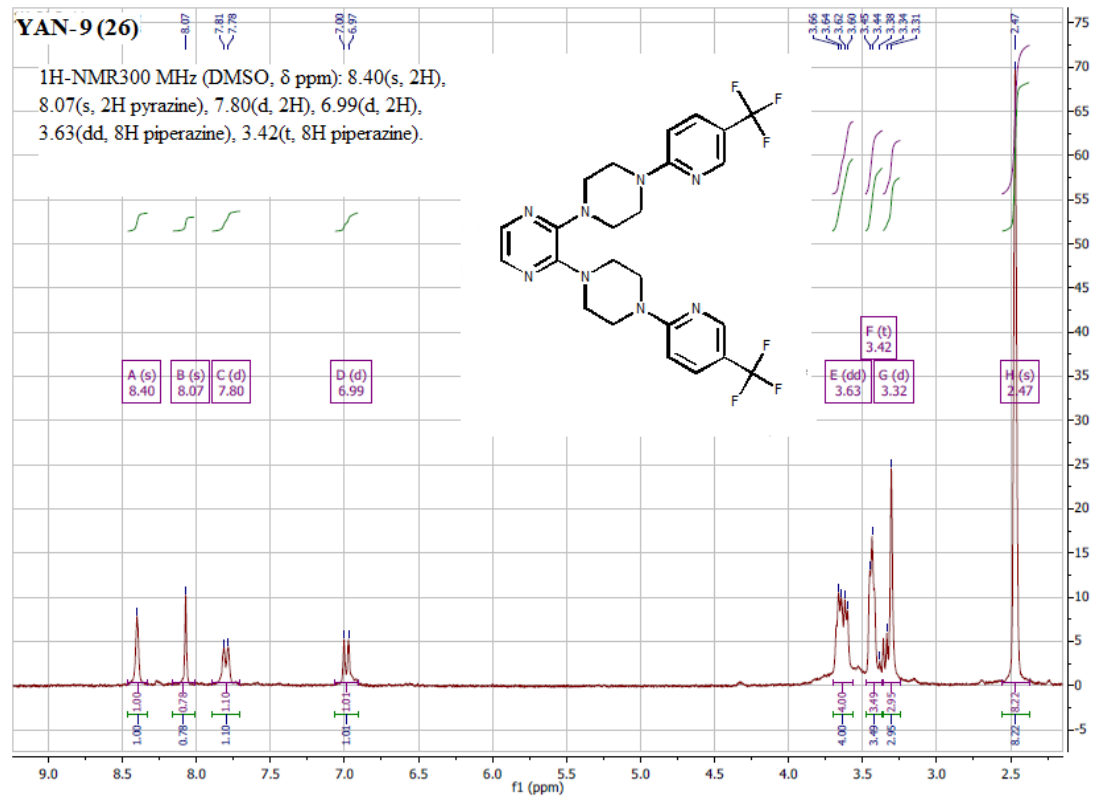
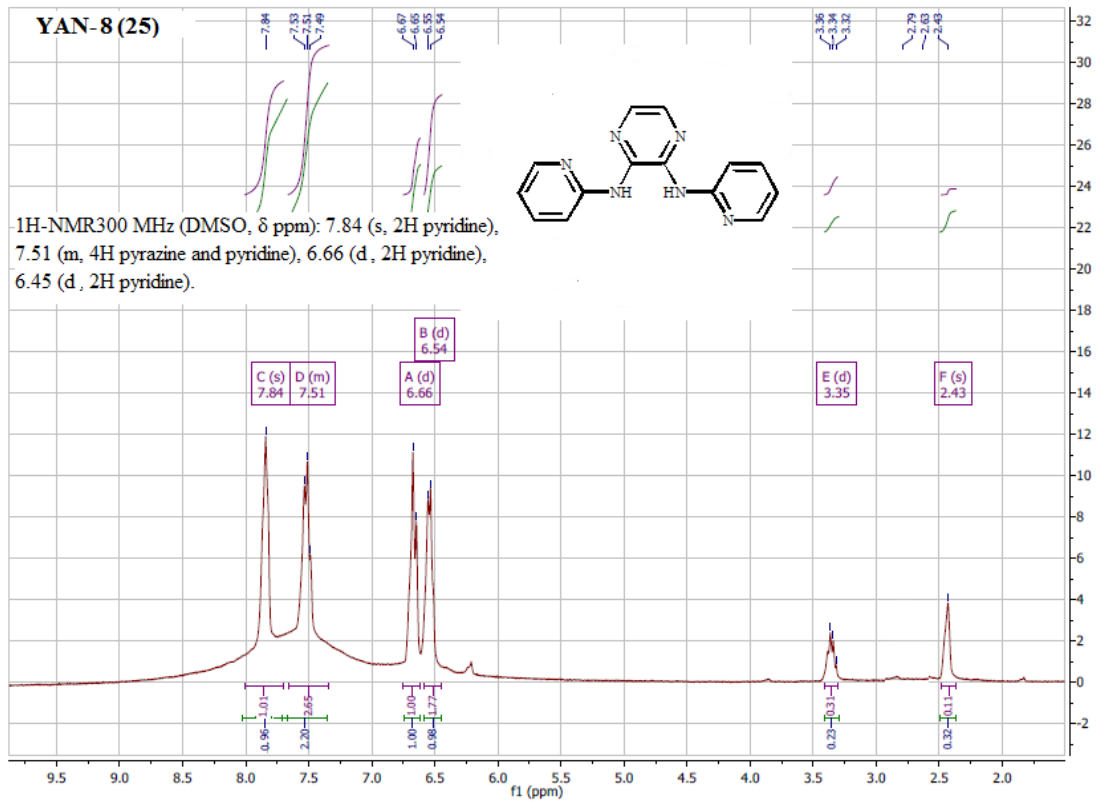


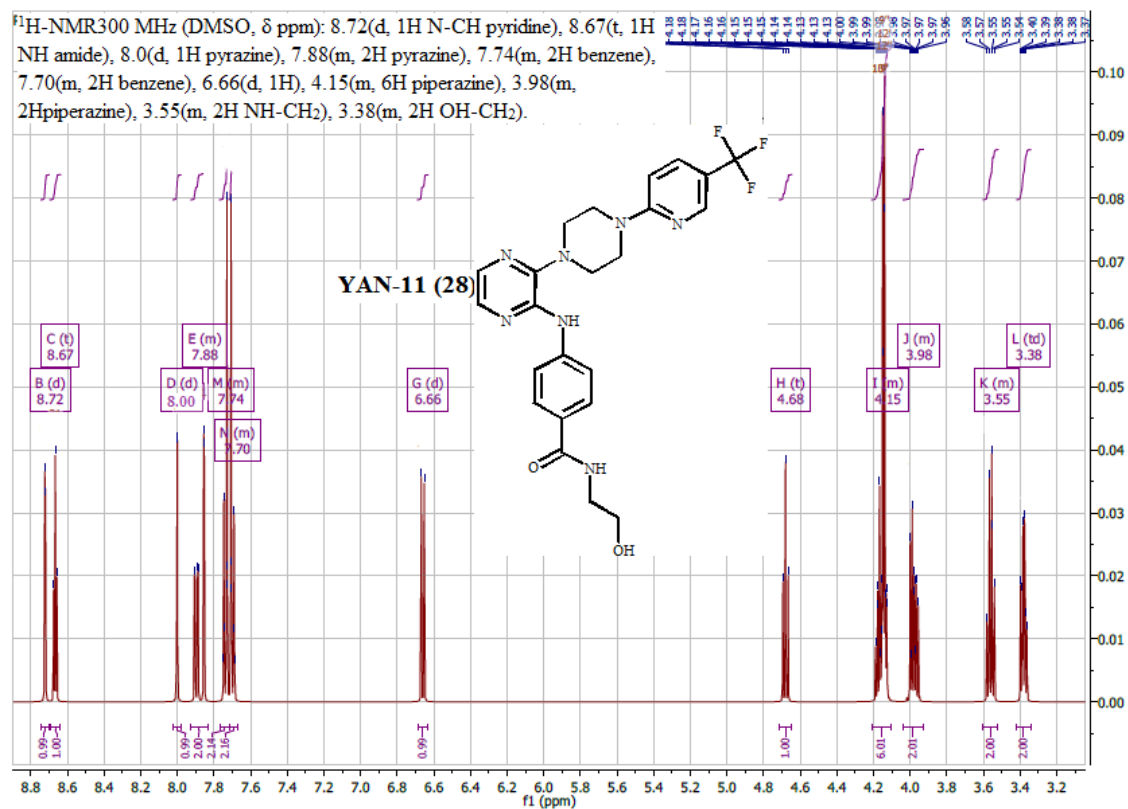
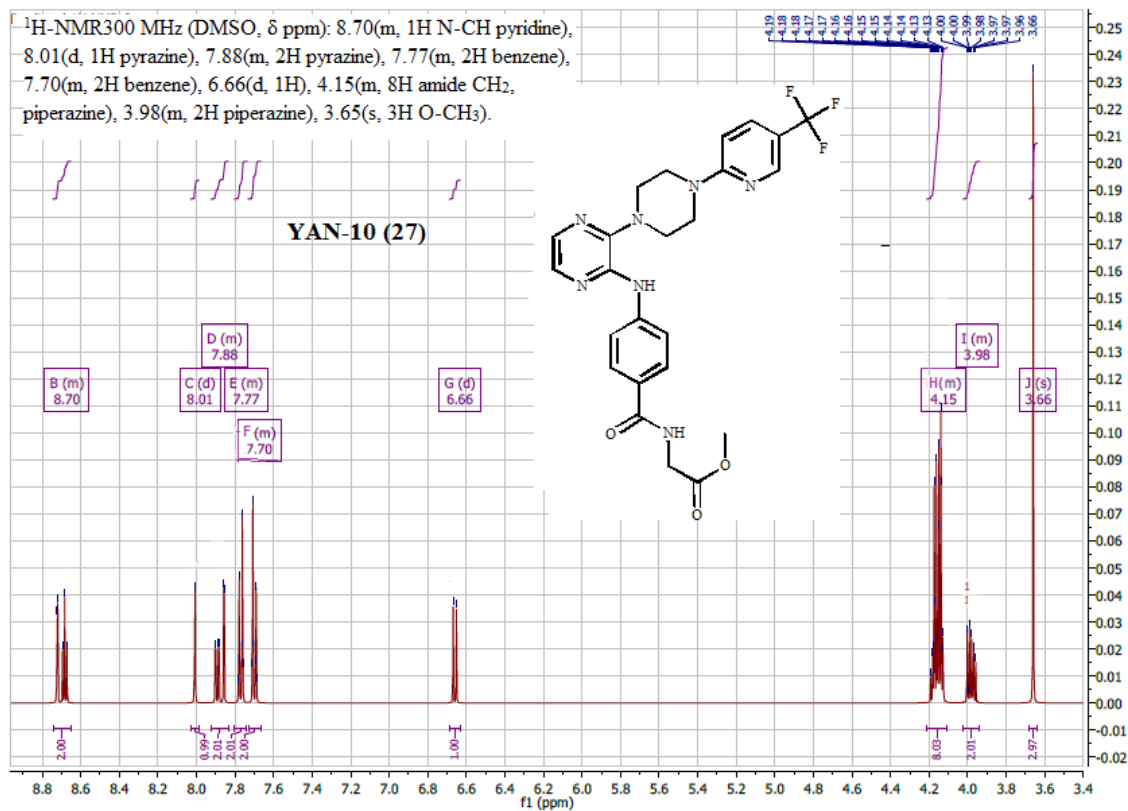


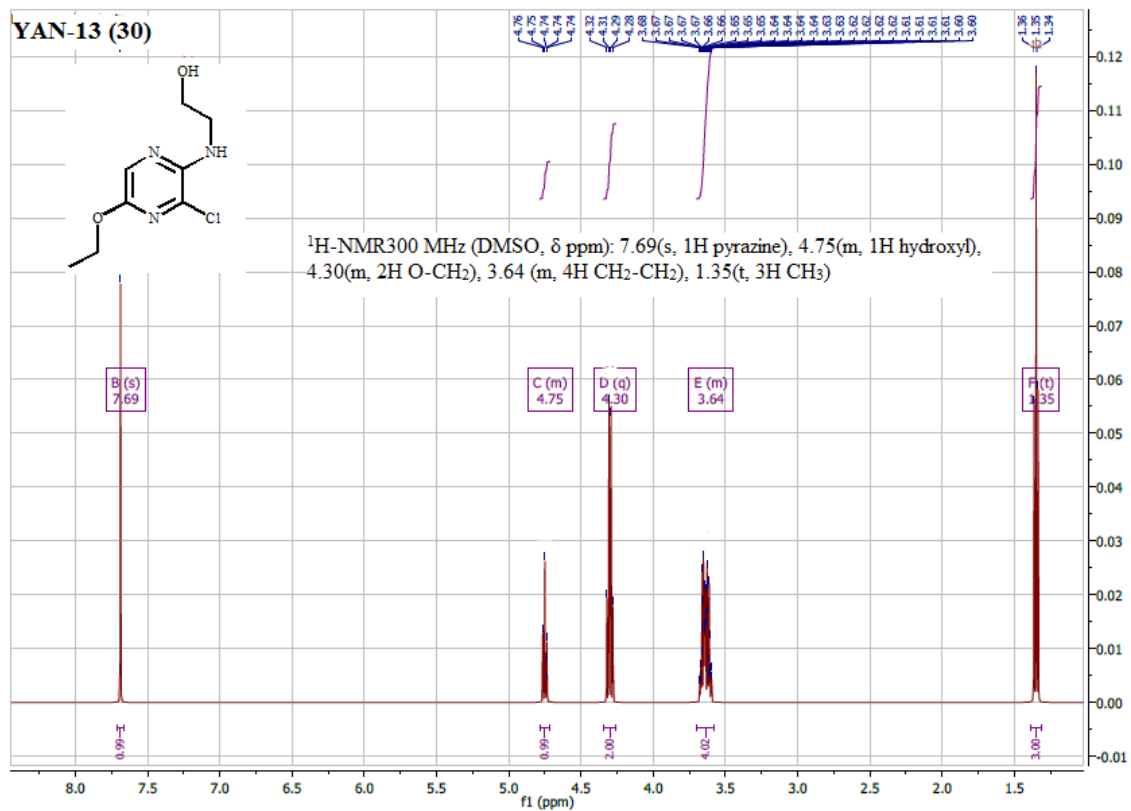
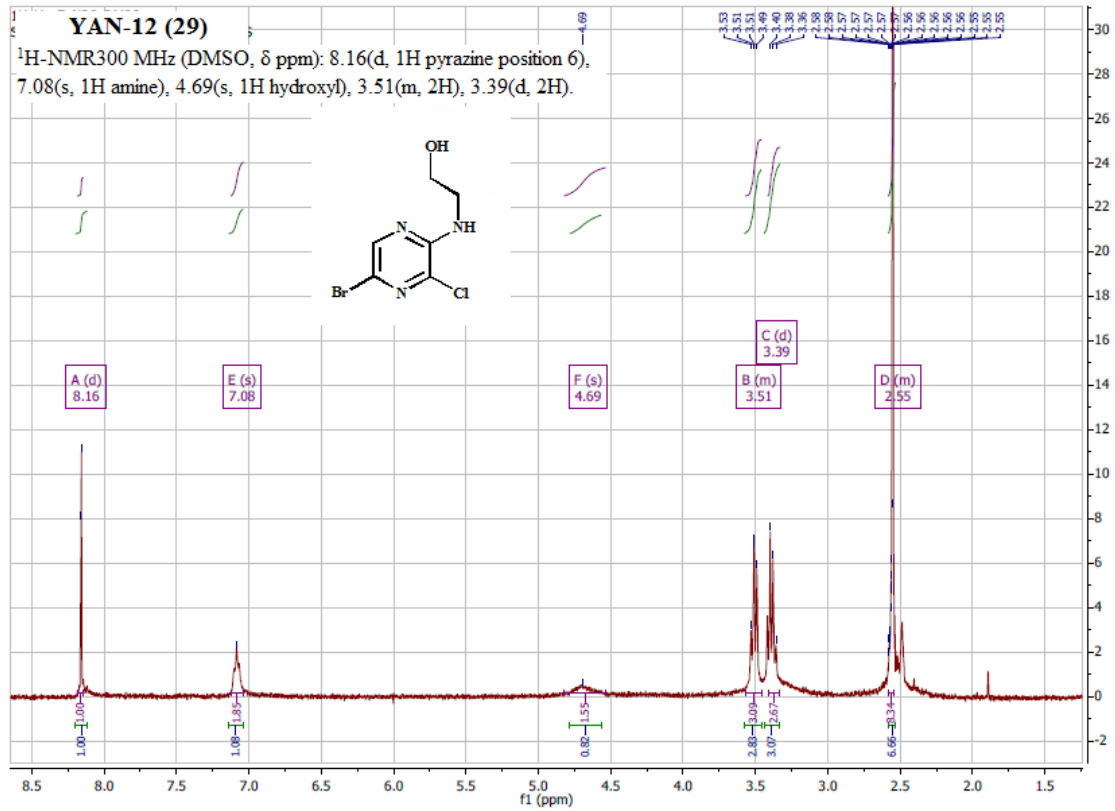


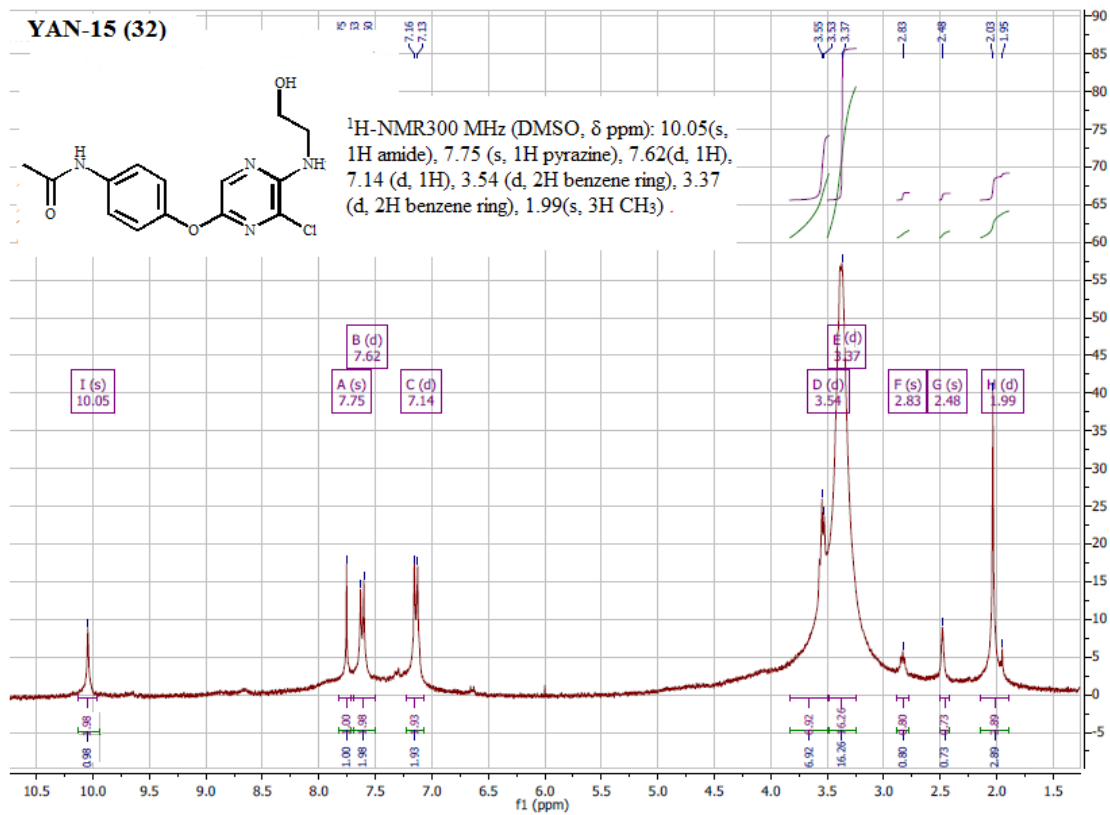
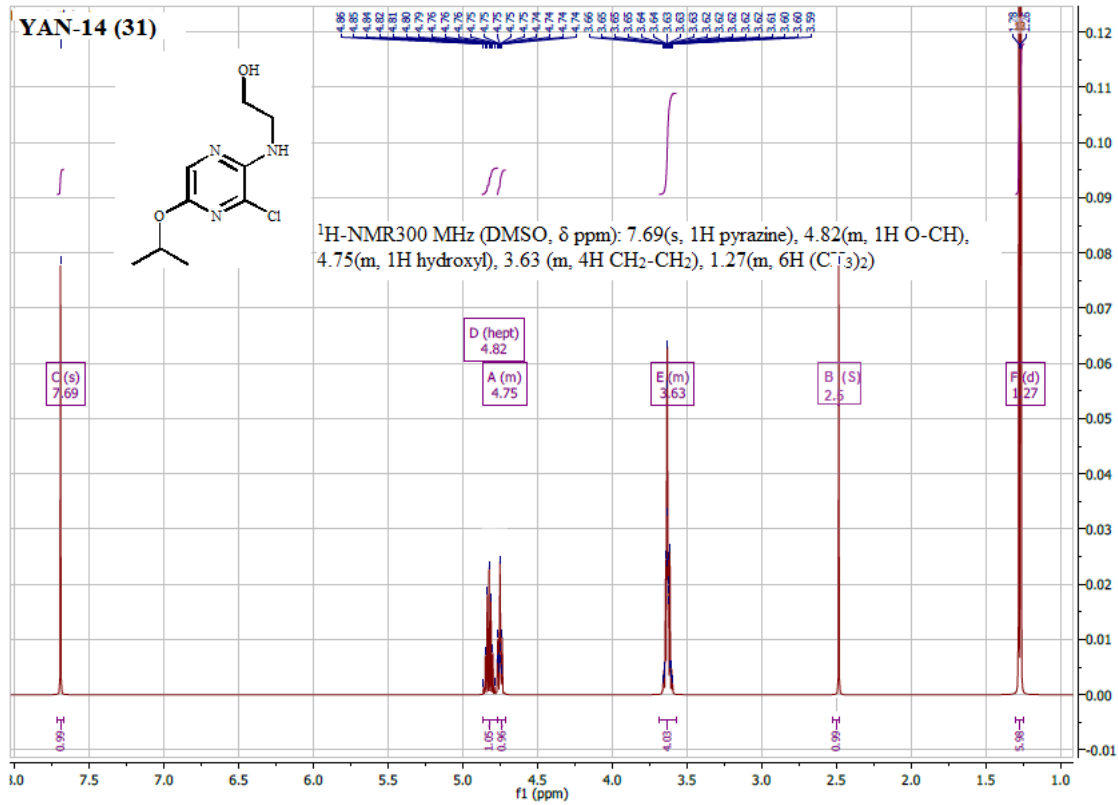










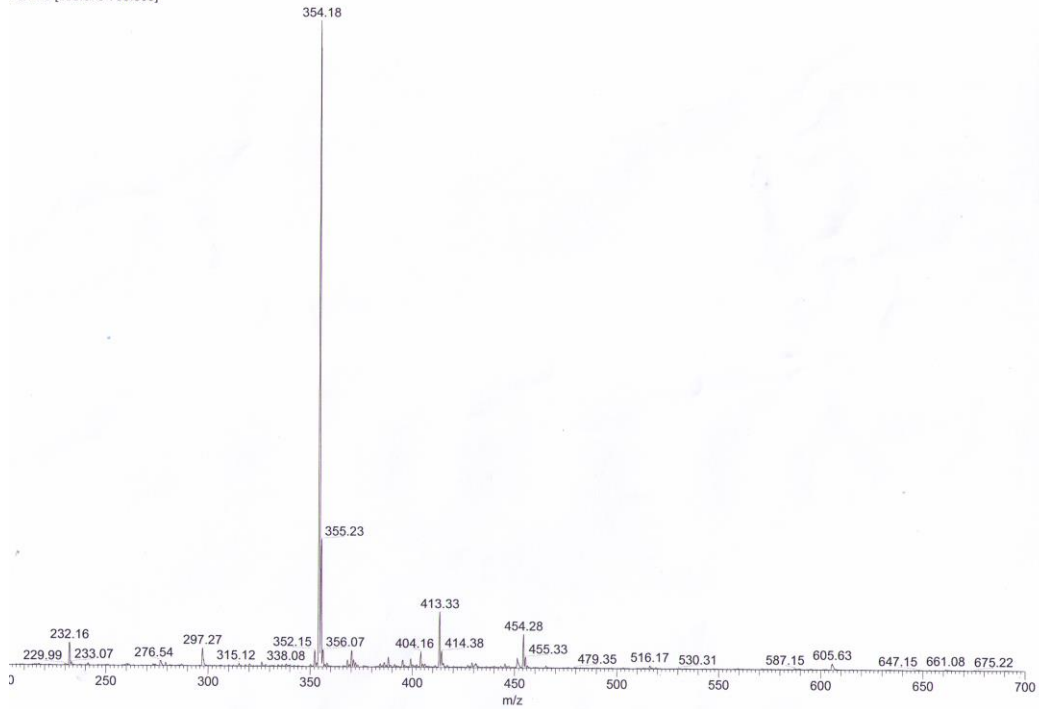


erviceJK-975

03/09/2013 10:50:25

Sawsan Xn-11E

18-78 RT: 0.60-0.72 AV: 11 SB: 17 0.14-0.28 NL: 9.96E7
I Q1MS [198.070-700.000]

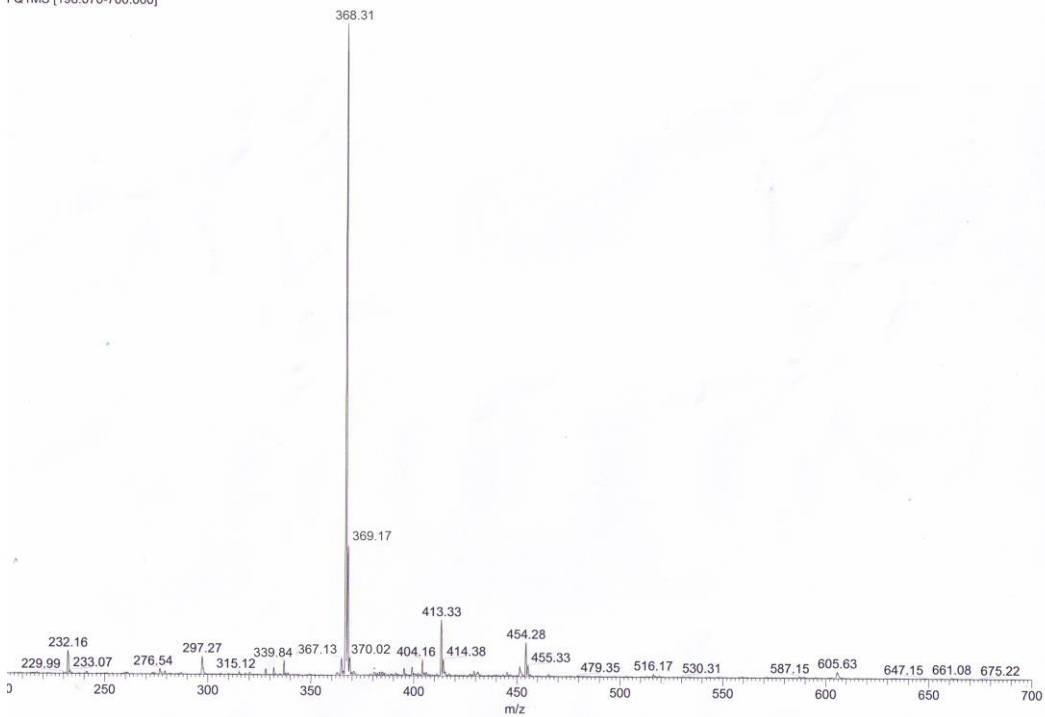


erviceJK-975

03/09/2013 10:37:12

Sawsan Xn-11 iso

18-78 RT: 0.60-0.72 AV: 11 SB: 17 0.14-0.28 NL: 9.96E7
I Q1MS [198.070-700.000]



تصميم, تحضير, وفحص النشاط السمي لمشتقات البيرازين ثنائية التفرع

اعداد: آلاء محمود ربيع فرعون

اشراف : د. يوسف ناجرة

ملخص:

مشتقات البيرازين تمتلك العديد من التأثيرات الدوائية التي تشمل -على سبيل المثال لا الحصر- المضادات الفيروسية، المضادات الحيوية، مضاد الفطريات، مدرات البول، مضادات الاختلاج، مضادات السكري، المسكنات، و مضادات السرطان. نتيجة لذلك، اظهر الباحثون اهتماما في مجال تحضير الادوية القائمة على مشتقات البيرازين هذا و نجحت الكثير من المشتقات التي تم تصنيعها وفحصها في الوصول إلى المجال السريري. وكان احد افرع البحث الواعدة مهتما باستغلال النشاط السمي والمضاد للتكاثر الذي تمارسه مشتقات البيرازين على بعض الخلايا -والذي من الممكن ايعازه لعدد من الآليات احداها تثبيط كينيز البروتين- في تصميم ادوية جديدة مضادة للسرطان.

في هذه الدراسة تم تصميم وتصنيع مجموعة من مشتقات البيرازين الثنائية عبر الاستبدال التسلسلي لذرات الكلور الموجودة في المركب (2,3-dichloropyrazine) بمجموعات اخرى كالأمينات وغيرها. كما تمت تنقية هذه المشتقات باستخدام تقنيات الفصل الكروماتوغرافي وتم التعرف عليها بواسطة التحليل الطيفي ($^1\text{H-NMR}$, $^{13}\text{C-NMR}$, FT-IR, and MS(ESI)).

تم اختبار النشاط البيولوجي (in vitro biological activity) للمشتقة احادية التفرع ((7) (A-7) وثلاثة من نظائرها ثنائية التفرع ((18) (YAN-1), ((19) (YAN-2), ((20) (YAN-3) ضد نوعين مختلفين من خلايا سرطان الدم النخاعي الحاد. تم تحديد سلامة الخلايا باستخدام تقنية (WST-1). اظهرت النتائج الاولية للمشتقات المفحوصة ان المشتقة الاحادية (7) كانت اكثر فعالية من نظائرها الثنائية في تثبيط انتشار وتكاثر نوعي الخلايا المستخدمين , وكان التركيز النصفى اللازم لتثبيط الخلايا المذكورة ((Molm-13 (sh-p53) and Molm-13 (empty vector) 18 و 39 مايكرومولار تباعا.

كما تم توقع النشاط البيولوجي لمجموعة من مشتقات البيرازين احادية وثنائية التفرع باستخدام برنامج (PASS) . بينت النتائج الاولية ان المشتقات الاحادية ((13) (A13), ((14) (A14) والمشتقات الثنائية ((24) (YAN-7), ((25) (YAN-8) اظهرت قيم توقع (Pa values) مرتفعة اثبتت فعالية هذه المشتقات في العمل كمضادات للاورام ومثبطات لمسار اشارات التنبيه. كما ان المشتقات المذكورة سابقا تشاركت في نفس الية العمل وهي تثبيط بروتين الكينيز (protein kinase inhibitors).

علاقة الشكل بالنشاط المستخلصة من نتائج برنامج (PASS) والفحص الاولي للنشاط البيولوجي اثبتت ان نشاط المشتقات المصنعة يتاثر بموقع ونوع التفرع المضاف على حلقة البيرازين. واطهرت المشتقات ثنائية التفرع على الموقعين 2 و3 فعالية افضل من المشتقات ثنائية التفرع على الموقعين 2 و5, بالإضافة الى ذلك, التفرع من النوع الاميني على الموقعين 2 و3 من

حلقة البيرازين كان افضل من الانواع الاخرى من التفرعات فيما يخص الفعالية ضد الاورام. وقد لوحظ ان المجموعات التالية (1-(5-trifluoromethylpyridin-2-yl)-piperazine, 2-aminopyridine) كانت افضل مجموعات تفرع امينية.

من اجل الحصول على نظرة توضيحية لطريقة ارتباط مشتقات البيرازين بالانزيم المطلوب (CDK-2) , تم ربط مجموعة تتكون من 16 مشتقة بالانزيم الاحادي غير النشط باستخدام برنامج (SwissDock) وتمت مقارنة النتائج مع المركب (Aloisine B) والذي يعتبر مثبت معروف لنفس الانزيم.

من ناحية آلية الارتباط احتلت مشتقات البيرازين موقع الارتباط الخاص ب (ATP) وقامت بعمل روابط هيدروجينية مع الهيكل الخاص بالانزيم الواقع ضمن التسلسل المفصلي الذي يربط جزئي الانزيم ببعضهما البعض. كما اظهرت المشتقات قابلية متفاوتة للارتباط بالهدف. وكان للمشتقة ((YAN-8 (25) اعلى قيمة موائمة مع الانزيم عند مقارنتها بالمشتقات الاخرى. علاوة على ذلك، اشارت قيم الموائمة وطاقة الربط الى ان المركب ((YAN-8 (25) يمتلك قابلية اعلى للارتباط مع الانزيم عند مقارنته بالمثبت المعروف Aloisine B.

في النهاية تم التحقق من مدى مشابهة المشتقات المحضرة للأدوية من خلال تطبيق القانون الخماسي. وقد اظهرت النتائج أن كل المشتقات المفحوصة نجحت في موافقة متطلبات القانون الخماسي ما عدا المشتقتين ((YAN-9 (26), ((YAN-10 (27) وذلك لامتلاكهما اوزان ذرية اكبر من 500 دالتون.